HAL
open science

The glutamine-rich N-terminal extension of Drosophila AGO2 mediates antiviral RNA interference in a TRiC/CCT dependent manner

Francesco Bergami

To cite this version:

Francesco Bergami. The glutamine-rich N-terminal extension of Drosophila AGO2 mediates antiviral RNA interference in a TRiC/CCT dependent manner. Virology. Université de Strasbourg, 2017. English. NNT : 2017STRAJ094 . tel-03510339

HAL Id: tel-03510339

https://theses.hal.science/tel-03510339

Submitted on 4 Jan 2022

HAL is a multi-disciplinary open access archive for the deposit and dissemination of scientific research documents, whether they are published or not. The documents may come from teaching and research institutions in France or abroad, or from public or private research centers.

L'archive ouverte pluridisciplinaire **HAL**, est destinée au dépôt et à la diffusion de documents scientifiques de niveau recherche, publiés ou non, émanant des établissements d'enseignement et de recherche français ou étrangers, des laboratoires publics ou privés.

UNIVERSITÉ DE STRASBOURG

ÉCOLE DOCTORALE DES SCIENCES DE LA VIE ET DE LA SANTÉ

UPR 9022

THÈSE présentée par :

Francesco BERGAMI

soutenue le : **06 Novembre 2017**

pour obtenir le grade de : **Docteur de l'université de Strasbourg**

Discipline/ Spécialité : Virologie

The glutamine-rich N-terminal extension of Drosophila AGO2 mediates antiviral RNA interference in a TRiC/CCT dependent manner

THÈSE dirigée par:

M. Jean-Luc IMLER	professeur, université de Strasbourg

RAPPORTEURS :

M. Ronald VAN RIJ	professeur, Radboud University
M. Eric MISKA	professeur, Cambridge university

AUTRES MEMBRES DU JURY :

Mme, Carine MEIGNIN	Docteur, université de Strasbourg

I INTRODUCTION

1. A lot of insects, and even more viruses **6**
1.1 PROTEIN BASED IMMUNITY 12
1.1.1 Inducible antiviral response *14*
1.1.2 Restriction factors *18*
1.2 RNA BASED IMMUNITY 20
1.2.1 The siRNA pathway *26*
1.2.2 The piRNA pathway *38*

2. Stucture-function of AGO proteins **46**
2.1 DOMAIN ORGANIZATION OF AGO PROTEINS 46
2.2 COFACTORS 52

3. Objective of the thesis **58**

II Results

1. A siRNA pathway interactome in *drosophila* S2 cells reveals an enrichment for protein folding machinery. **70**

2. The TRiC/CCT complex interacts with AGO2 and participates in antiviral resistance. **74**

3. The TRiC/CCT complex does not affect expression of the two isoforms of AGO2 ..... **78**

4. The TRiC/CCT complex affects the intracellular distribution of the long form of AGO2. ..... **82**

5. AGO2-S cannot substitute for AGO2-L to control viruses **86**

6. Virus derived siRNA are preferentially sorted onto AGO2-L **90**

7. Dynamics of AGO2 during DCV infection **94**

III Discussion

1. The TRiC/CCT complex dynamically regulates AGO2 antiviral activity **104**

2. The GRR domain is essential for AGO2 efficient antiviral response **105**

3. Phase separated cellular bodies and antiviral RNA silencing **106**

4. A model for the antiviral action of AGO2 in the cellular context **109**

IV Materials and metods
V Supplementary figures
VI Bibliography

I Introduction

The topic of my PhD has been antiviral innate immunity in the insect model organism *D. melanogaster*. The small size, rapid generation and the plethora of genetic tools created in over a century, make flies a very powerful model organism. In the last 30 years, the use of Drosophila for the study of innate immunity greatly contributed to the renewed interest in the field. In this introduction, I explain the relevance of studies on insects and their viruses. I then present the antiviral strategies used by Drosophila and other insects to counter viral infections, which are either protein based (inducible responses, restriction factors) or RNA-based (RNA interference). Finally, I discuss the structure and functional properties of Argonaute proteins in insects, the central components of RNA interference.

1. A lot of insects, and even more viruses

Insects, with over 70% of all listed species, are the largest and most diverse group of animals (Misof et al. 2014). This includes crops and house pests as well as disease vectors.

Climate change and the ever-increasing tropical urbanization promote the spreading of non-native insect species representing a major economic burden for the coming years (Fig. 1A). Invasive insects have an estimated cost of minimum US$70,0 billion per year globally. Insect pests have been reported to reduce agricultural yields by 10–16% before harvest, and a similar amount following harvest (Bradshaw et al. 2016). Climate warming also represents a danger for the expansion of the distributions of many arboviruses (arthorpod born viruses), as documented for bluetongue viruses (BTV), a pathogen of ruminants (Weaver & Reisen 2010).

In addition to the major societal cost deriving from the loss of crops, food stocks and livestock, invasive insects also represent a major threat to human health. With

Fig. 1

A

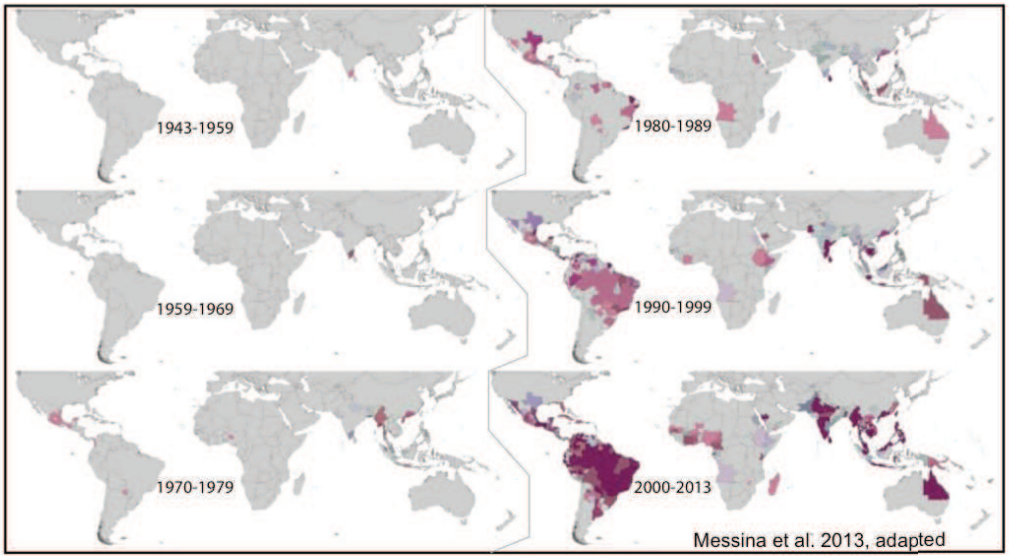
1943-1959
1980-1989
1959-1969
1990-1999
1970-1979
2000-2013
Messina et al. 2013, adapted

B

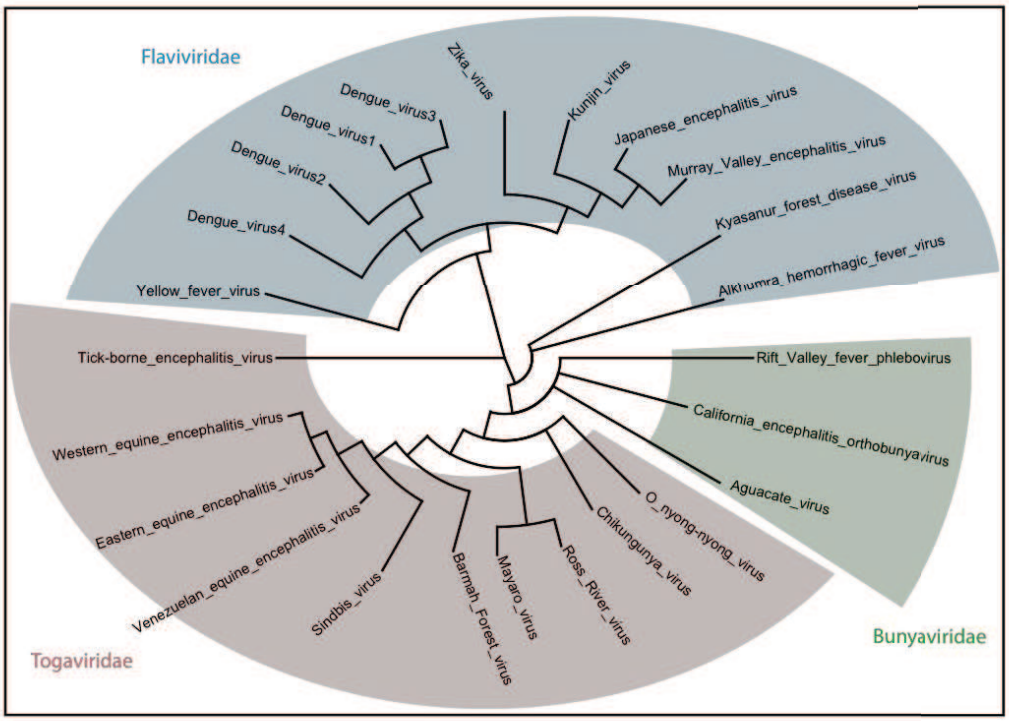
Flaviviridae
Zika_virus
Dengue_virus3
Dengue_virus1
Dengue_virus2
Dengue_virus4
Yellow_fever_virus
Kunjin_virus
Japanese_encephalitis_virus
Murray_Valley_encephalitis_virus
Kyasanur_forest_disease_virus
Alkhumra_hemorrhagic_fever_virus
Tick-borne_encephalitis_virus
Rift_Valley_fever_phlebovirus
California_encephalitis_orthobunyavirus
Aguacate_virus
O_nyong-nyong_virus
Chikungunya_virus
Ross_River_virus
Mayaro_virus
Barmah_Forest_virus
Sindbis_virus
Venezuelan_equine_encephalitis_virus
Eastern_equine_encephalitis_virus
Western_equine_encephalitis_virus
Togaviridae
Bunyaviridae

C

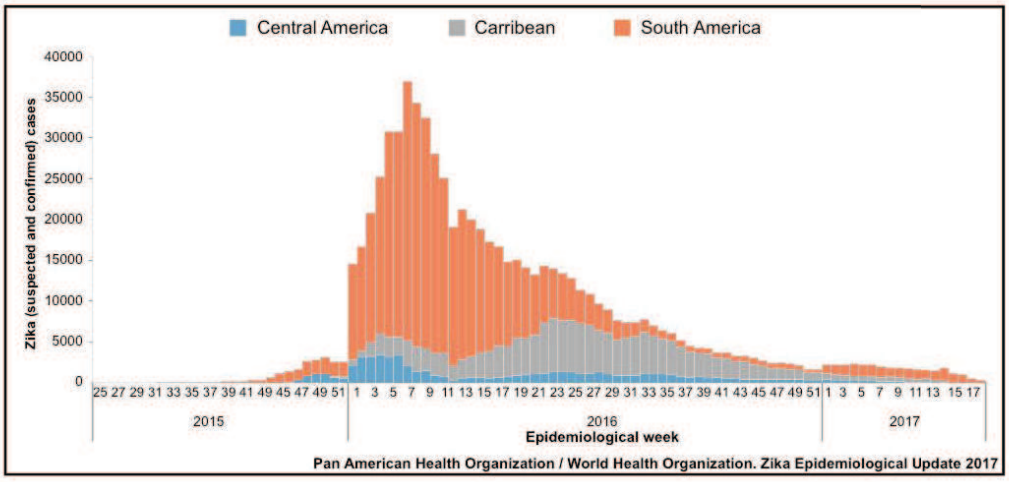
Central America
Carribean
South America
Zika (suspected and confirmed) cases
40000
35000
30000
25000
20000
15000
10000
5000
0
25 27 29 31 33 35 37 39 41 49 45 47 49 51 1 3 5 7 9 11 13 15 17 19 21 23 25 27 29 31 33 35 37 39 41 43 45 47 49 51 1 3 5 7 9 11 13 15 17
2015
2016
2017
Epidemiological week
Pan American Health Organization / World Health Organization. Zika Epidemiological Update 2017

Fig. 1 The threat of Arboviruses

A. Spreading of the four serotypes of Dengue virus from 1943 to 2013. **B.** Philogenetic tree of the most diffused human arboviral pathogens. **C.** Weekly suspected and confirmed cases of infection during the Zika virus outbreak in 2015.

associated health costs exceeding US$6,9 billion per year (2014 estimate) (Bradshaw et al. 2016), the spreading of arboviruses through insects vectors is one of the leading cause of death in the last three centuries (Gubler 1998). Mosquitoes are the most widespread, and therefore, the most concerning disease-spreading insect vector. The expanding habitat of different species of anthropophilic mosquitoes facilitates the spread of arboviruses through an urban cycle (Weaver & Reisen 2010; Messina et al. 2014).

The term arbovirus refers to a non-taxonomical group of viruses (Fig. 1B). Most of them are RNA viruses with double-stranded RNA (dsRNA) genomes or single-stranded RNA (ssRNA) genomes of positive (+) or negative (-) polarity. The majority of arboviruses can be classified in the *Bunyaviridae, Flaviridae, Reoviridae, Rhabdoviridae* and *Togaviridae* families (Gubler 2001). Some of the most globally important arboviruses include Dengue virus (DENV), yellow fever virus (YFV), Chikungunya virus (CHIKV) and, more recently, Zika virus (ZIKV). DENV is almost ubiquitously distributed in the tropical regions, and more recently in Europe, making it the most dangerous human arbovirus. Almost half of the world population (2,5 billion people) is at risk of infection. An estimated 500000 cases of life threatening severe dengue occur every year (World Health Organization 2014). CHIKV is present in Africa, Asia and the Indian subcontinent, and in the last few years the virus spread to new areas causing outbreaks in countries previously unaffected (World Health Organization 2014). Yellow fever was one of the most dangerous diseases linked to the tropical region before the development of an effective vaccine. Even today, there remain every year around 200 000 infections and 30 000 deaths from yellow fever (World Health Organization 2014). During the 2015-16 outbreak of Zika virus in central and south America tens of thousands (Fig. 1C) of cases of infection have been reported (Pan American Health Organization / World

Health Organization. Zika Epidemiological Update 2017). This highlights the potential threat of new or previously considered "under the radar" arboviruses to emerge as health threats.

While being potentially able to cause severe diseases in vertebrates, arboviruses replicate in the mosquito prior to transmission, causing minimal pathologic changes and fitness costs (Lambrechts & Scott 2009). The mosquito becomes persistently infected and can transmit virus with each blood meal suggesting that vector mosquitoes possess the means to efficiently mount an antiviral response able to control the virus. This prompts the necessity of studying the pathways controlling the antiviral immune response in mosquitoes and more generally in arthropods.

Next, I will briefly review the different innate immune pathways of insects with a focus on RNA interference and its main effector molecule Argonaute.

1.1 Protein based immunity

To fight the constant threat of viral infection, living organisms have evolved diverse antiviral resistance pathways. These, in turn, favor the adaptation of viruses to escape antiviral mechanisms. This arms race favors the diversification of host-defense and virus escape mechanisms.

The control of viral replication constitutes a challenge for the host immune system for many reasons. First, unlike other pathogens, viruses are able to replicate, mutate and spread very rapidly, escaping immune surveillance. Their intimate interaction and dependence on various host cellular compartments and machineries makes them difficult targets. Moreover, viruses often encode proteins that attempt to neutralize

immune responses. Therefore, an elaborate immune antiviral arsenal is constantly being selected throughout evolution (Marques & Imler 2016).

1.1.1 Inducible antiviral response

Although RNAi interference represents a broad and efficient antiviral response (see below), viral infection triggers up-regulation of a large number of genes in flies. Some of these Virus-Stimulated Genes (VSGs) have been previously studied in the context of different types of infections, for example, some antimicrobial peptides (AMPs). The analysis of *Drosophila C virus* (DCV) infected Drosophila cells (Dostert et al. 2005) revealed more than 100 induced genes, two thirds of which did not overlap with genes induced by other infections. Several of the virus- induced genes contained Stat binding sites in their promoters, for example virus induced RNA-1 (*vir-1*) and the antimicrobial peptide Listericin/CG9080 (Dostert et al. 2005). DCV infection could induce these genes, but UV-inactivated, non-infectious DCV particles or dsRNA did not, suggesting that active virus replication is required for activation of Jak-Stat signaling (Hedges & Johnson 2008). Mutants for the Jak kinase Hopscotch (*hop*) expressed lower levels of *vir-1* following viral infection. In addition, *hop* mutant flies succumb more rapidly, with higher viral loads, compared to control flies, when infected with DCV (Dostert et al. 2005). It has also been shown that the Jak-Stat pathway participates in the control of Dengue virus infections in Aedes mosquitoes (Souza-Neto et al. 2009; Jupatanakul et al. 2017). The Jak-Stat activation seems to be dependent on the Domeless receptor, which implies the presence of a secreted cytokine-like ligand induced after viral sensing. A recent study reported the involvement of the epigenetic regulator *G9a* in antiviral immunity (Merkling, Bronkhorst, et al. 2015). *G9a* mutant flies show a marked upregulation of the Jak-Stat pathway and hypersensitivity to DCV infection. While this may seem contradictory, the ectopic upregulation of the Jak-Stat pathway followed by DCV

infection cause early mortality in way similar to *G9a* mutants. These results suggest that over activation of the Jak-Stat pathway is detrimental to the survival of the flies and that *G9a* mediates the regulation of Jak-Stat signaling.

A recent trascriptome analysis reported that RNA virus infection induces the heat-shock response (Merkling, Overheul, et al. 2015), which is known to induce chaperone proteins. Knock down and loss of function of the heat-shock response component *Hsf* reduces virus resistance of flies while its overexpression increase the survival following infection.

Among virus-induced genes, *Vago* is particularly interesting because its expression does not depend on the Jak-Stat pathway and seems to depend on the Dicer-2 protein. *Vago* encodes for a 160 amino acids long protein that is able to control DCV replication in the fat body (the main site of DCV replication in the adult fly). The finding that neither AGO2 nor R2D2 was required for *Vago* induction uncouples this sensing function of Dicer-2 from its function in RNA silencing (Deddouche et al. 2008). While the function of *Vago* remains unknown inn flies, where it does not participate in the activation of the Jak-Stat pathway, *Vago* may act as a cytokine activating Domeless in Culex mosquitoes (Paradkar et al. 2012; Paradkar et al. 2014).

The involvement of the immune deficiency (IMD) in viral replication was first highlighted using a Sindbis virus (SINV) replicon expressed from the genome of transgenic flies (Avadhanula et al. 2009). These flies were crossed with mutants of the IMD, Jak-Stat and Toll pathways. An increased replication of the virus was observed in the IMD and Jak-Stat mutants but not in the Toll pathway mutants. An independent study also suggested that the IMD pathway mediates resistance to cricket paralysis virus.

Recently *diedel* (die), a novel virus-induced gene inhibiting the IMD pathway, was identified (Lamiable, et al. 2016). *die* is strongly induced by some viral infections (Coste et al. 2012; Kemp et al. 2013) and can promote host survival by modulating the activation of the IMD pathway and NF-κB signaling. Die belongs to a larger family of proteins that includes homologs found in the genomes of members of three large classes of insect viruses, the Entomopoxvirinae, the Ascoviridae, and the Baculoviridae. The identification of die viral homologs prompts the conclusion that suppression of the IMD pathway is an important evolutionary checkpoint for viruses.

1.1.2 Restriction factors

Restriction factors represent the hosts' first line of defense against viral infections. These proteins are constitutively expressed in the cells prior to the infection and target one or more steps of the viral replication cycle. This makes each restriction factor specific for one family or species of virus.

The first locus reported at which genetic variation affects virus multiplication in flies is *ref(2)P*. A permissive *ref(2)P*^{o} and restrictive *ref(2)P*^{p} alleles were identified (Contamine et al. 1989). Both forms can be co-immunoprecipitated with the N and P proteins from the naturally occurring rhabdovirus Drosophila Melanogaster Sigma Virus (DMelSV) (Wyers et al. 1993), indicating a direct interaction. The interaction of this restriction factor with the *Drosophila* atypical protein kinase C (daPKC), which positively regulates the Toll-signalling pathway and induces the synthesis of AMPs (Avila et al. 2002; Goto et al. 2003), suggest the involvement of the Toll pathway. *Ref(2)P* is the Drosophila ortholog of the mammalian polyubiquitin-binding scaffold protein P62 (sequestosome 1). P62 recognizes autophagic cargos and allows their engulfment into autophagosomes through binding to members of the Atg8/LC3 family (Ktistakis & Tooze 2016). Autophagy has been associated with antiviral activity in flies (Lamiable, Arnold,

et al. 2016; Shelly et al. 2009) and may contribute to the restrictive activity of Ref(2)P against DMelSV.

A naturally occurring polymorphism in a gene called Ge-1 makes Drosophila highly resistant to DMelSV (Cao et al. 2016). Ge-1 is an essential component of P-bodies. Ge-1 is composed of an N-terminal WD40 domain, followed by a long C-terminal extension, important for the localization at P-bodies (Cao et al. 2016). P-bodies have been previously involved in antiviral immunity in insects with both pro- and anti-viral roles (Khong & Jan 2011; Hopkins et al. 2013; Chahar et al. 2013). For example, the dicistrovirus CrPV disrupts P-bodies in Drosophila cells such that viral proteins are available for viral processing (Khong & Jan 2011). Limiting the amount of the decapping enzyme Dcp2, a P-body component, restricts the replication of Rift Valley Fever Virus (RVFV) (Hopkins et al. 2013). Conversely, West Nile Virus co-opts P-bodies components to help its replication, and knocking down the expression of these proteins results in lower viral titers (Chahar et al. 2013).

A natural variant altering susceptibility to DCV was found in the gene *pastrel (pst)*, which encodes an insect specific cytoplasmic protein of unknown function. A genome-wide study revealed a Thr/Ala polymorphism in this C terminal domain, which is strongly associated with increased resistance to DCV, but not to Sigma Virus or Flock House Virus (FHV) (Magwire et al. 2012). The susceptibility of *pst* mutant flies to DCV and a second Dicistrovirus (CrPV), suggests that this restriction factor is specific to this family of virus (Martins et al. 2014).

1.2 RNA based immunity

The identification of the RNA interference mechanism constituted a major discovery in biology. This previously undescribed mechanism brought to light an unappreciated

Fig. 2

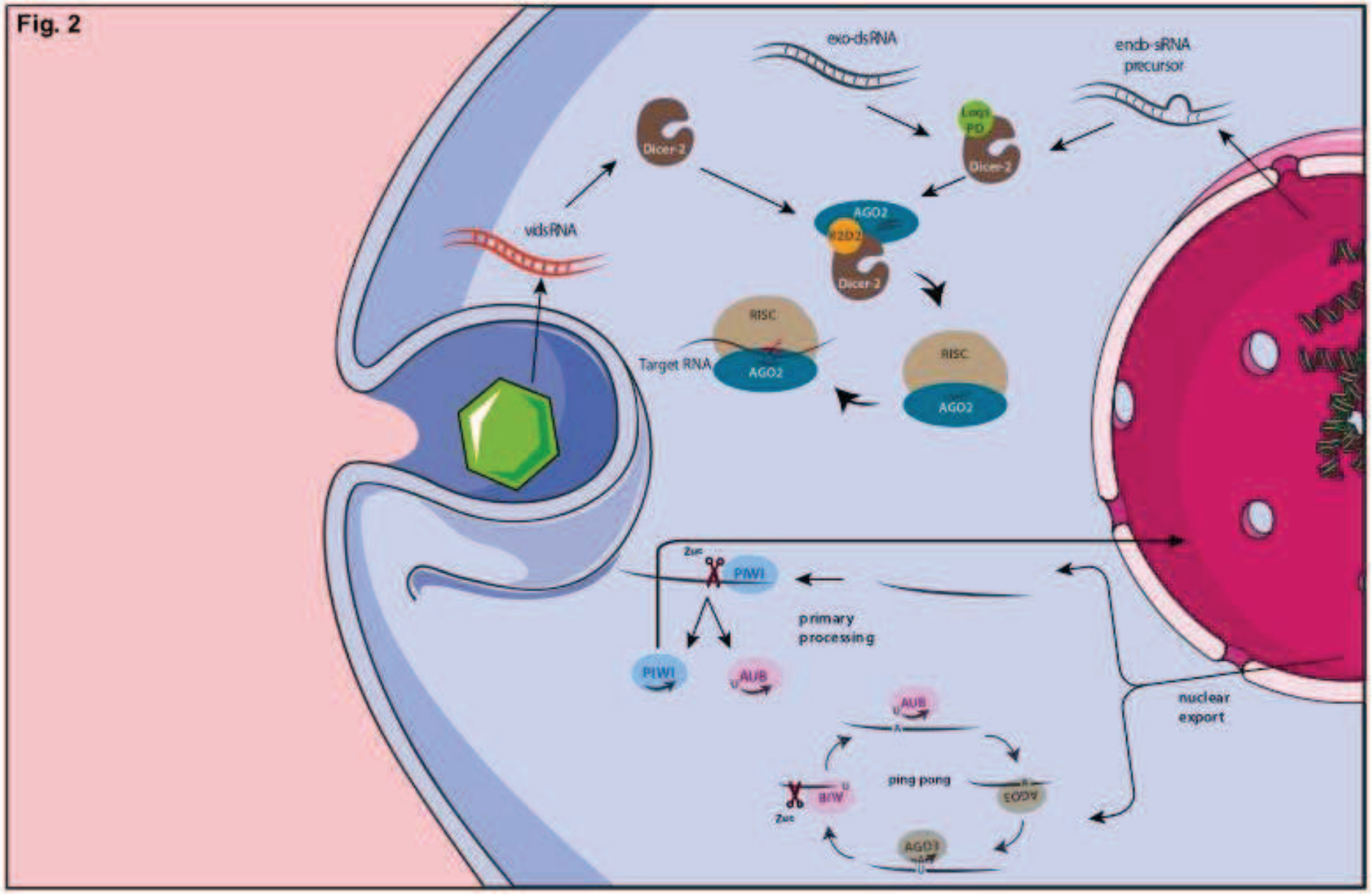
exo-dsRNA
endo-siRNA
precursor
Dicer-2
Loqs
PD
Dicer-2
AGO2
R2D2
Dicer-2
vdsRNA
RISC
Target RNA
AGO2
RISC
AGO2
Zuc
PIWI
primary
processing
PIWI
AUB
AUB
ping pong
Zuc
BRW
EGO/W
AGO3
nuclear
export

Fig. 2 RNA Based immunity

Insect pathways involved in RNA based antiviral immunity.

role of small RNA molecules in different aspects of genome defense, maintenance and gene regulation.

Towards the end of the 1990's, parallel findings in different model organisms (*Arabidopsis thaliana, Nicotiana benthamiana* and the worm *Caenorabitis elegans*) succeeded in explaining this conserved silencing mechanism in a natural context. Experiments in plants showed that viruses can stimulate an RNA silencing response (Voinnet & Baulcombe 1997) and that such a response is maintained by a cellular mechanism that is able to amplify it and spread it through the whole plant (Voinnet & Baulcombe 1997). These findings were strengthened by the identification of viral encoded mechanisms aimed at suppressing it, providing compelling evidence that PTGS represents a natural mechanism for plant protection against viruses. At the same time, a study in *C. elegans* showed that double-stranded RNA is able to induce potent and specific genetic interference (Tabara et al. 1998). The mapping of mutations in two isolated *C. elegans* lines resistant to RNAi, allowed the identification of the first genes (*rde-1*, *rde-4*) involved in this silencing mechanism (Tabara et al. 1999). The protein encoded by the *rde-1* gene was identified as a member of the piwi/argonaute/zwille gene family and it is conserved from plants to vertebrates. Interestingly, an enhanced mobilization of endogenous transposons was observed in some of these RNAi resistant lines. This led to the hypothesis that transposon silencing is one of the natural function for RNAi (Tabara et al. 1999).

RNAi turned out to be a very conserved mechanism amongst different species. This mechanism involves the production of small double stranded RNA duplexes by Dicer proteins. These small RNA are then loaded onto Argonaute proteins that are part of a larger protein complex called the RNA Induced Silencing Complex or "RISC". The loaded small RNA directs RISC in a sequence specific manner to a complementary RNA. Some

Argonaute proteins are able to endonucleotically cleave target RNAs (Slicer competent), inhibiting their expression. Other Argonaute proteins do not posses a catalytical activity but are nevertheless able to recruit different cellular factors (e.g. GW proteins, exonucleases) that interfere with the translation of mRNAs, ultimately resulting in the silencing of the target gene (Hauptmann et al. 2013). Two small RNAs associated mechanisms, namely the siRNA and the PIWI-interacting piRNA pathways, are involved in genome defense against exogenous or endogenous selfish genetic elements in several species. A third small RNA associated mechanism called the microRNA (miRNA) pathway, co-exist with the first two. This miRNA pathway plays an important role in development and in various aspects of cell physiology by fine-tuning gene expression(Filipowicz & Sonenberg 2015).

1.2.1 The siRNA pathway

The RNAi pathway is a major innate antiviral response in insects and one of the best tool vector insects have to restrict arbovirus infections (Gammon & Mello 2015; Ding 2010). The canonical siRNA pathway has been vastly characterized in *D. melanogaster*. It was found that long dsRNAs are diced progressively from the termini into a pool of 21-nucleotide siRNA duplexes by the dsRNA-specific endoribonuclease Dcr-2, an RNase III enzyme, which, together with its cofactor R2D2, then loads the siRNA duplex onto the effector molecule Argonaute(AGO)2. These siRNAs then select by base-pairing their mRNA targets and guide the endoribonucleic cleavage (or slicing) of the target mRNA by AGO2 protein in the middle of the siRNA–RNA duplex. Therefore, siRNAs determine the target specificity of AGO-mediated slicing in RNAi (Kim et al. 2009; Carthew & Sontheimer 2009). A recent study (Iwasaki et al. 2015) identified critical steps that lead to the assembly of the mature RISC using an in-vitro single-molecule approach. Using

eight purified proteins (Ago2, Dcr-2, R2D2, Hsc70, Hsp90, Hop, Droj2 and p23) the authors were able to follow the assembly of a single RISC. A Dcr-2–R2D2-bound siRNA duplex associates with, but rapidly dissociates from, unchaperoned AGO2. The chaperone machinery extends the dwell time of the Dcr-2–R2D2– siRNA complex on AGO2 to facilitate siRNA handover, but this extension requires the recognition of the guide 5'-phosphate by AGO2. In the model proposed by the authors the Hsc70/Hsp90 chaperone machinery has a critical role in supporting a loading-competent state of AGO2, in which the 5' nucleotide-binding a pocket is accessible to the 5'-phosphate of the guide strand of the Dcr-2–R2D2-bound siRNA duplex. Proper anchoring of the 5'-phosphate would trigger loading of the rest of the duplex, leading to successful RISC maturation coupled with closing and stabilization of AGO2.

Many species are equipped with an siRNA pathway as an innate immune system to protect themselves from life-threatening, invasive viruses and/or transposons randomly inserting copies of themselves into the host genome (Ding & Voinnet 2007). These two aspects can be functionally separated. The exogenous (exo-)siRNA pathway consists of a siRNA pathway dedicated to antiviral defense (vsiRNA pathway) that is distinct from the one activated by exogenous dsRNAs. The main difference between these two pathways is the generation of the siRNA duplex, in the vsiRNA pathway the dsRNA substrate can be processed by Dcr-2 alone while the exo-siRNA pathway necessitate of the Dcr-2/Loqs-PD complex (Marques et al. 2013; Marques et al. 2010). The endogenous (endo-)siRNA pathway is active in all somatic cells as a defense against transposable elements insertions and requires both Dcr-2 and Loqs-PD for the biogenesis of the siRNA duplex. These pathways seem to merge downstream of the processing step where vsiRNA, exo-siRNA and endo-siRNA are loaded onto AGO2 by the Dcr-2/R2D2 complex (Fig. 2).

1.2.1.1 The exo-siRNA pathway

Demonstration of the critical role of RNAi as a potent antiviral mechanism in Drosophila is based on three main lines of evidence. First, genetic experiments show that RNAi pathway mutants (*AGO2*-/-, *Dcr-2*-/- and *R2D2*-/-) are hypersensitive to virus infections and succumb faster and with increased viral loads when compared to controls (Wang et al. 2006; Galiana-Arnoux et al. 2006; Van Rij et al. 2006). The second line of evidence is the identification of viral suppressors of RNAi (VSRs) encoded by viruses that counteract this silencing mechanism (Chao et al. 2005; Aliyari et al. 2008; Guo & Ding 2002; van Mierlo et al. 2011), and the third one, is the presence of siRNAs of viral origin (vsiRNAs) in infected cells and flies which can be characterized by high-throughput sequencing (Aliyari et al. 2008; Mueller et al. 2010; Vodovar et al. 2011; Bronkhorst et al. 2012).

The hyper susceptibility of *Dicer-2*, *AGO2* or *R2D2* null mutants flies to a variety of viral infection from both RNA and DNA viruses (CrPV (*Dicistroviridae*), FHV (*Nodaviridae*) and SINV (*Alphaviridae*), IIV-6 (invertebrate iridescent virus 6, *Iridoviridae*)) indicates that the siRNA pathway mediates a broad antiviral defense in flies (Kemp & Imler 2009; Kemp et al. 2013; Bronkhorst et al. 2013). As most immune mechanisms, RNAi exerts an evolutionary pressure on viruses, which in turn have evolved ways to evade this immune response. This creates an evolutionary race between the virus and the host, in which they each need to stay one step ahead of the other in order to survive. The key players of the siRNA pathway are extremely rapid evolving genes; *Dicer-2*, *AGO2* and *R2D2* are among the 3% fastest evolving genes in Drosophila. This fast evolution particularly stands out when compared to the slow evolution of the miRNA pathway genes, *Dicer-1*, *AGO1* and *Loqs* (Obbard et al. 2009). This agrees with the fact that many VSRs have been identified in insect RNA viruses (Chao et al. 2005; Nayak

et al. 2010; van Mierlo et al. 2012). Two of these, B2 from FHV and 1A from DCV interact with dsRNA, preventing the dsRNA recognition and cleavage by Dcr-2. Unlike DCV-1A, which only binds long dsRNAs, FHV-B2 can interact with both long dsRNA and siRNAs. Thus, FHV-B2 can potentially inhibit both the dicing and the loading steps. A third example of VSRs is the protein 1A from CrPV and VP1 from Nora virus (NV) (a natural Drosophila pathogen), which both antagonize AGO2, preventing its proper function (Nayak et al. 2010; van Mierlo et al. 2012). The parallel between these two VSRs is particularly interesting for two reasons; first, they target the same step of the RNAi pathway but with two very different outcomes regarding the course of the infection, NV establishes a non-lethal, persistent infection while CrPV causes lethality. Second, the fact that two distantly related RNA viruses evolved to target the same effector molecule, further highlights the importance of AGO2 antiviral role and helps explaining why this gene is among the fastest evolving genes in Drosophila. More recently, divergent Nora-like virus were reported to naturally infect different drosophilids species (van Mierlo et al. 2014). Strikingly VP1 proteins from different NV are host specific and their activity strictly depends on the ability to bind the host AGO2 protein. For example VP1 of NV isolated from *D. immigrans* binds and inhibit the activity of DimmAGO2 but fails to interact with DmelAGO2. This is a further confirmation that host and virus tend to co-evolve.

The third observation confirming the involvement of the siRNA pathway in antiviral immunity is the presence siRNAs of viral origin that can be detected in infected cells or flies (Wang et al. 2006; Aliyari et al. 2008). These siRNAs are able to confer specific resistance to the viral replication, shown by the fact that flies carrying a transgene directing expression of FHV dsRNA are protected against a challenge by FHV, but not by DCV (Galiana-Arnoux et al. 2006). Also, inoculation of dsRNA corresponding to the

sequence of DCV efficiently protected wild-type flies against DCV infection, but not against SINV (Saleh et al. 2009). Several evidences indicate that these vsiRNAs are the product of Dcr-2 processing a long dsRNA substrate. Deep sequencing of smallRNAs produced in the course of a viral infection in flies and mosquitoes shows a high enrichment in 21 nt long reads as expected of Dcr-2 products. In agreement with this, vsiRNAs cover the entire length of the viral genome with a similar amount of reads coming from the (+) and (-) strand, indicating a long dsRNA as substrate. Lastly, *Dicer-2* mutant flies show a complete loss in the production of vsiRNAs (Aliyari et al. 2008; Mueller et al. 2010; Bronkhorst et al. 2012).

1.2.1.2 The endo-siRNA pathway

Deep sequencing of small RNAs from germline and somatic tissues of Drosophila and of AGO2 immunoprecipitates revealed a population of small RNAs that could be distinguished from miRNAs and piRNAs (Chung et al. 2008; Czech et al. 2008; Kawamura et al. 2008; Okamura, Chung, et al. 2008; Okamura & Lai 2008; Siomi et al. 2008; Wu et al. 2010). Like piRNAs, endo-siRNAs originate from intergenic DNA elements. However, in contrast to piRNA biogenesis, which occurs independently of Dicer proteins, endo-siRNA biogenesis in Drosophila requires Dcr-2 (Vagin et al. 2006; Czech et al. 2008; Ghildiyal & Zamore 2009; Kawamura et al. 2008; Okamura, Balla, et al. 2008). After maturation, endo-siRNAs are loaded onto AGO2 to form the endo-siRISC, which silences transposons and some protein-coding genes (Czech et al. 2008; Ghildiyal & Zamore 2009; Kawamura et al. 2008; Okamura, Balla, et al. 2008).

The *loquacious* (*loqs*) gene gives rise to four isoforms, Loqs-PA, Loqs-PB, Loqs-PC, and Loqs-PD (Förstemann et al. 2007; Jiang et al. 2005; Saito et al. 2005; Hartig et al. 2009). The longest isoform, Loqs-PB, facilitates miRNA processing by Dcr-1 while mutations in Loqs-PD cause a severe reduction in the accumulation of endo-siRNAs, without

impacting the expression level of Dcr-2, indicating its involvement in endo-siRNA processing (Hartig et al. 2009; Marques et al. 2010; Miyoshi et al. 2010; Zhou et al. 2009). R2D2 also associates with Dcr-2 but has been shown to be dispensable for exo-siRNA precursors processing in vitro and for endo-siRNA accumulation (Czech et al. 2008; Ghildiyal & Zamore 2009; Marques et al. 2010; Okamura, Balla, et al. 2008; Zhou et al. 2009; Liu et al. 2003; Liu et al. 2006; Pham et al. 2004; Tomari et al. 2004; Tomari et al. 2007). On the other hand, R2D2 drives Dcr-2 towards dsRNA rather than pre-miRNA *in vitro* (Cenik et al. 2011). endo-siRNAs which, like exo-siRNA, are 2'-O-methylated at the 3' end once loaded onto AGO2, are resistant to β-elimination, unlike miRNA, which are not modified at their 3' end. siRNA become sensitive to β-elimination in R2D2 mutants (Ghildiyal & Zamore 2009). Indeed, endo-siRNAs are misdirected to AGO1 in cells lacking R2D2 (Ameres et al. 2011; Marques et al. 2010; Okamura et al. 2011). Loqs and R2D2 act sequentially in exo-/endo-siRNA processing and loading, respectively (Marques et al. 2010). In the context of viral infections, processing of viral dsRNA is completely independent from Loqs-PD (Marques et al. 2013). These observations support the idea that R2D2 plays a crucial role in endo-siRNA sorting and loading. More recently, the group of M. Siomi reported observations that help understanding the role of R2D2 in endo-siRNA loading onto AGO2 (Nishida et al. 2013). These authors showed that Dcr-2 and R2D2 colocalize in cytoplasmic foci that they named D2 bodies, and presented evidence that in R2D2-depleted cells endo-siRNAs, but not exo-siRNAs, were misdirected to AGO1. These results suggest that R2D2 mediates endo-siRNA sorting by localizing Dcr-2, and presumably endo-siRNA duplexes, to D2 bodies, with which AGO2 but not AGO1 transiently localizes(Nishida et al. 2013). R2D2 is required to avoid endo-siRNA misdirection to Ago1, which is capable of loading incompletely complementary miRNA duplexes and endo-siRNA duplexes.

1.2.2 The piRNA pathway

PIWI interacting RNAs (piRNAs) were originally discovered during small RNA profiling studies of *D. melanogaster* development (Aravin et al. 2001; Aravin et al. 2003) and were initially termed repeat-associated small interfering RNAs (rasiRNAs) because most of these small-RNA species corresponded to intergenic repetitive elements. piRNAs are slightly longer (24–31 nt) than miRNAs and siRNAs, possess 2'-O-methyl modification sites at the 3' terminus, and are processed from single-stranded precursor transcripts expressed from regions termed piRNA clusters via a Dicer-independent mechanism (Vagin et al. 2006; Siomi et al. 2011). piRNA clusters contain a large number and variety of transposon and the produced piRNAs mainly regulate the expression and mobilization of transposons. Because transposons have a high risk of damaging the cellular genome, the piRNA-mediated regulation is essential for preserving normal gametogenesis and reproduction.

PIWI proteins are conserved in a wide range of eukaryotes, from sponges to humans, and they are expressed mainly in the gonads (Grimson et al. 2008; Siomi et al. 2011). The prototype of PIWI proteins is encoded by the *Drosophila piwi* (P-element-induced wimpy testes) gene, which was originally identified as an essential gene for germline development (Thomson & Lin 2009; Cox et al. 1998). Drosophila contains three distinct PIWI genes: *AGO3*, *aubergine* (*aub*), and *piwi*. Piwi and aub are required for both male and female fertility, whereas AGO3 is essential for female fertility (Cox et al. 1998; Lin & Spradling 1997). Derepression of transposons is observed in each of these PIWI mutant ovaries, indicating that all three PIWI proteins have nonredundant roles in gonad development and transposon silencing. Aub and AGO3 cleave their target transposon transcripts in the cytoplasm, whereas Piwi can regulate its target transposons at the transcriptional level in the nucleus (Vagin et al. 2006; Kalmykova et al. 2005; Vagin et al.

2004; Sabin et al. 2013; Brennecke et al. 2007; Gunawardane et al. 2007). Two major pathways generate piRNAs: the primary processing pathway and the ping-pong cycle that amplifies secondary piRNAs. Primary piRNAs have a bias toward having uridine (U) at their 5' nucleic acid (1U bias), whereas secondary piRNAs show 10-nt complementarity with primary piRNAs at their 5' ends and possess a sense bias with adenosine at the tenth nucleotide (10A bias).

In *Drosophila* ovaries, the primary pathway operates in both germline and surrounding somatic cells. Long primary transcripts from the piRNA clusters are exported to the cytoplasm. Within this process, the precursors are further trimmed to the mature piRNA size by the activity of a 3'–5' exonuclease. The DmHen1/Pimet methyltransferase then 2'-O-methylates the 3' ends of piRNAs to produce mature Piwi–piRNA complexes or Piwi–piRISCs (Saito et al. 2007; Horwich et al. 2007). Piwi–piRNA complexes are then imported into the nucleus to transcriptionally regulate target genes (Sienski et al. 2012).

Aub together with AGO3 initiate the ping-pong cycle in the cytoplasm to produce secondary piRNAs. The ping-pong pathway takes place at an electron-dense perinuclear structure known as the nuage because both PIWI proteins and other factors involved in piRNA biogenesis accumulate in the structure (Lim & Kai 2007). Ping-pong amplification is unique because it couples piRNA biogenesis to target silencing. In fly germ cells, Aub, associated with a cluster-derived primary piRNA, detects and, through its slicer activity, cuts active transposon transcripts. These cleavage events produce the 5' ends of new piRNAs that are in sense orientation to transposons. Following loading into Ago3 and maturation through either trimming by an unknown nuclease or Zucchini- (Zuc) dependent 3' end formation, Ago3-piRNA complexes in turn recognize and cleave cluster

transcripts to generate more antisense piRNAs with sequences identical (or near-identical) to the original primary small RNA triggers (Czech & Hannon 2016).

Recent work from the groups of P. Zamore and J. Brennecke revealed deeper levels of interplay between the primary and secondary piRNAs biogenesis pathways and further clarified the involvement of Zucchini (Zuc). The de novo primary piRNA pathway starts with piRNA intermediates released from piRNA cluster transcripts in an Aub- and AGO3-independent manner. Zuc slices them consecutively every ~26 nt, aided by Armitage (Armi) and other factors in the primary pathway (e.g., Minotaur and Gasz). Those primary piRNAs are loaded into Piwi and Aub, but not Ago3. Cleavage by AGO3 or Aub produces piRNA intermediates with a 5' monophosphate. The 3' cleavage products are loaded onto Aub and AGO3, followed by Zuc-dependent cleavage ~26 nt from their 5' ends. This cleavage produces the 3' ends of the "Ping-Pong partner" secondary piRNA and the 5' ends of long RNAs that become substrates for Zuc, which processively cleaves the RNA to generate phased piRNAs loaded into Piwi and, to a lesser extent, Aub (Mohn et al. 2015; Han et al. 2015).

Although the canonical function of the piRNA pathway is to silence transposons, thus protecting genome integrity, de novo production of piRNAs derived from viruses has been reported in insect cell lines. These viral piRNAs (vpiRNAs) are produced independently of the siRNA pathway activity and may represent an additional line of defense against arboviruses infection in mosquitoes (Brackney et al. 2010; Vodovar et al. 2012; Hess et al. 2011; Goic et al. 2016; Leger et al. 2013; Miesen et al. 2016; Miesen et al. 2015). vpiRNAs were first reported in Drosophila Ovarian Somatic Sheet (OSS) cells persistently infected by a number of different RNA viruses (Wu et al. 2010). Because OSS cells lack the enzymes necessary to the ping-pong amplification pathway, these vpiRNAs possessed only a 1U signature typical of primary piRNAs. However, mutant adult flies

for key components of the piRNA pathway (*Zuc, Piwi, Aub*, and *AGO3*) are no more susceptible than wild-type flies to virus infection and vpiRNAs are not produced in response to the infection (Petit et al. 2016). In summary, piRNAs do not appear to participate in antiviral immunity in drosophila, and their contribution to the control of arboviruses in mosquitoes remains to be confirmed *in vivo.*

2. Stucture-function of AGO proteins

2.1 Domain organization of AGO proteins

The Argonaute protein family was first identified in plants, its members are defined by the presence of PAZ (Piwi-Argonaute-Zwille) and PIWI domains (Bohmert et al. 1998). The global structure and domain organization of Argonaute proteins are remarkably conserved in arechea, bacteria and eukaryotes (Willkomm et al. 2015). Prokaryotic Argonautes have been shown to use either RNA or DNA as guide to silence target DNA (Olovnikov et al. 2013).

The eukaryotic Argonaute proteins can be separated into AGO clade proteins (similar to the *Arabidopsis thaliana* AGO1) and PIWI clade proteins (similar to the *Drosophila* PIWI). AGO proteins represent the effector of the miRNA and the siRNA pathway, thus acting as post-transcriptional regulators. PIWI proteins are mainly expressed in germline cells, where these proteins bind to piRNAs and function in the silencing of transposable elements (Meister 2013). The structure of Argonaute proteins is comprised of an amino-terminal (N) domain, a PAZ domain, a MID domain and a PIWI domain. The crystal of human AGO2 (MacRae 2008) reveals a structure composed of two lobes each containing two of the four domains forming the protein, MID-PIWI and N-PAZ (Fig. 3A). The two lobes act as walls to a central channel that accommodate the single stranded RNA guide, similar to the DNA guide of prokaryotic Argonautes (Song 2004). The 5' of the RNA guide is tightly associated with the MID domain, with a number of hydrogen bonds coordinating the correct positioning of the 5' end. Nucleotides 2 to 6 of the guide RNA are widened out, with Watson-Crick faces exposed to the solvent, supporting the seed-pairing model (MacRae 2008). The N domain is necessary for an efficient strand selection following the loading of the small-RNA duplex (Kwak & Tomari 2012). This domain acts like a wedge, driving the duplex unwinding and giving the RISC complex the ability to find its complementary target. The PAZ domain anchors the 3′ end of the small RNA by bending

Fig. 3

A

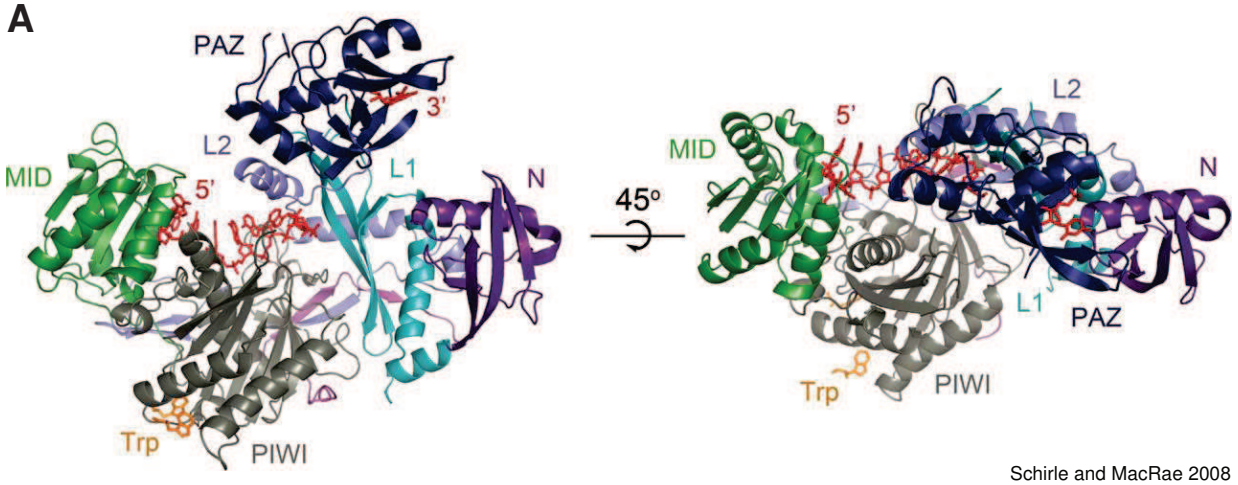

Schirle and MacRae 2008

B

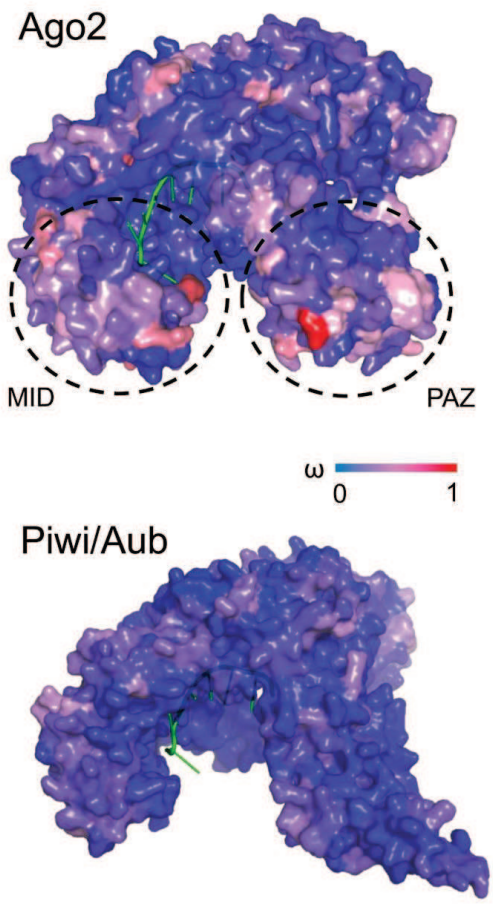

Lewis et al. 2016

C

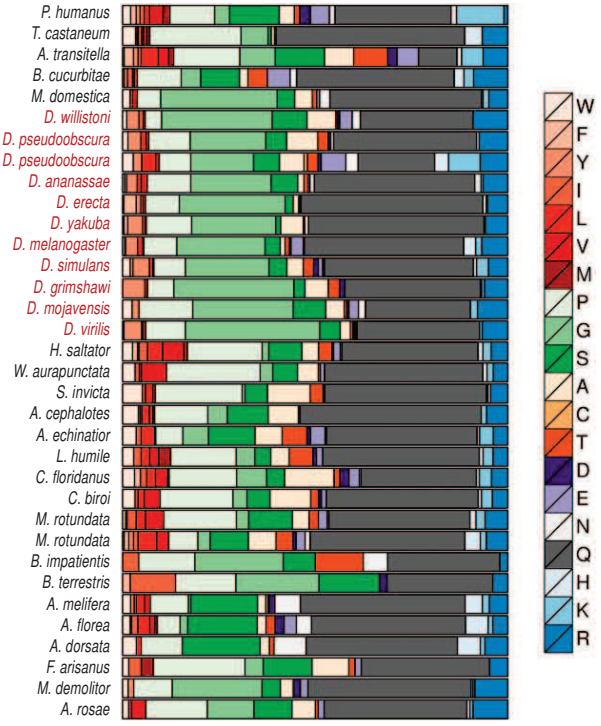

Palmer et al. 2016, adapted

Fig. 3 Structure-Function of AGO2

A. Crystal Structure of Human AGO2. **B.** Mapping of the most (blue) to least (red) conserved residues of AGO2 proteins in different insect species. **C.** Amino acid composition of the GRR region of AGO2 in 34 different insect species.

it into a specific binding pocket (Jinek & Doudna 2009). The PIWI domain adopts a fold similar to that of RNaseH (Jinek & Doudna 2009), which is in line with the "slicer" activity of Argonaute proteins. Two tryptophan-binding pockets have been identified on the side of the PIWI domain facing the solvent. The distance between these pockets closely matches the distance of the tryptophan residues present in GW proteins pointing to the PIWI domain as a possible binding site (MacRae 2008).

A recent study of Argonautes proteins in 86 different dipteran species showed that the paralog genes originated from duplications of AGO2 and AGO3 experienced a sustained increase in evolutionary rate, possibly driven by the acquisition of new functions (Lewis et al. 2016). The mapping of the rapidly evolving residues on a structural model of AGO2 and AGO3 identifies hotspots of adaptive evolution in the residues localized at the entrance of the RNA binding pocket of AGO2 but not AGO3. Given the location of these hotspots, away from the small-RNA guide, a rapid evolution could reflect differences in target binding and cleavage (Fig. 3B). As an alternative, selection could be driven by VSRs which are encoded by many viruses to inhibit AGO2 target clevage (van Mierlo et al. 2012; van Mierlo et al. 2014; Wang et al. 2006).

Conversely to these highly conserved domains, the N-terminal portion of Argonaute proteins tends to be very disordered and divergent between different species (Hain et al. 2010; Obbard et al. 2006). Indeed, this region is characterized by a low complexity, highly repetitive structure. This is particularly marked in the *AGO2* gene products of arthropod species where the N-terminal region contains a strikingly high number of glutamine-rich repeats (GRR) (Hain et al. 2010). Although the overall amino acid composition of this GRR domain is conserved (Fig. 3C), the number of repeats and the structure is highly divergent even between closely related species like *D. melanogaster* and *D. simulans* (159 and 101 glutamine residues, respectively) (Hain et al. 2010; Palmer

& Obbard 2016). Natural occurring variations in the length and repeat pattern of the GRR domain is associated with some difference in resistance to DCV infection (Palmer & Obbard 2016), nonetheless, this effect is small compared to *pst* (Magwire et al. 2012). *In vitro* data showed that an AGO2 molecule fully missing the GRR domain is still perfectly functional concerning RISC assembly and target cleavage (Liu et al. 2009). This is coherent with the observation that one of the two isofroms of AGO2 in *D. melanogaster* completely lacks the GRR domain.

2.2 Cofactors

Human AGO2 identifies miRNA targets by scanning potential target using one-dimensional diffusion along the RNA. When it finds a target fully complementary to the miRNA, AGO remains stably associated (Chandradoss et al. 2015). Despite being such a powerful molecule AGO2 still require additional components in order to mediate an efficient silencing of its target. Argonaute proteins activity is tied to its assembly into the RISC complex. Significant progress has been made in the identification of Argonaute proteins cofactors (Iwasaki et al. 2010; Iwasaki et al. 2015; Lee, et al. 2009; Harris et al. 2011; Gibbings et al. 2009).

For target mRNA repression, AGO proteins involved in miRNA-guided silencing, directly interact with GW182. GW182, in turn interacts with cytoplasmic poly(A)-binding protein (PABPC) and other cytoplasmic complexes to mediate the deadenylation and decapping of target mRNA, followed by its degradation (Jonas & Izaurralde 2015).

Multivesicular bodies (MVBs) have been shown to recruit active miRISCs associated with target mRNAs into GW-bodies that are physically associated with MVBs. If MVBs do not form, there is an accumulation of early endosome-associated miRISCs accompanied

Fig. 4

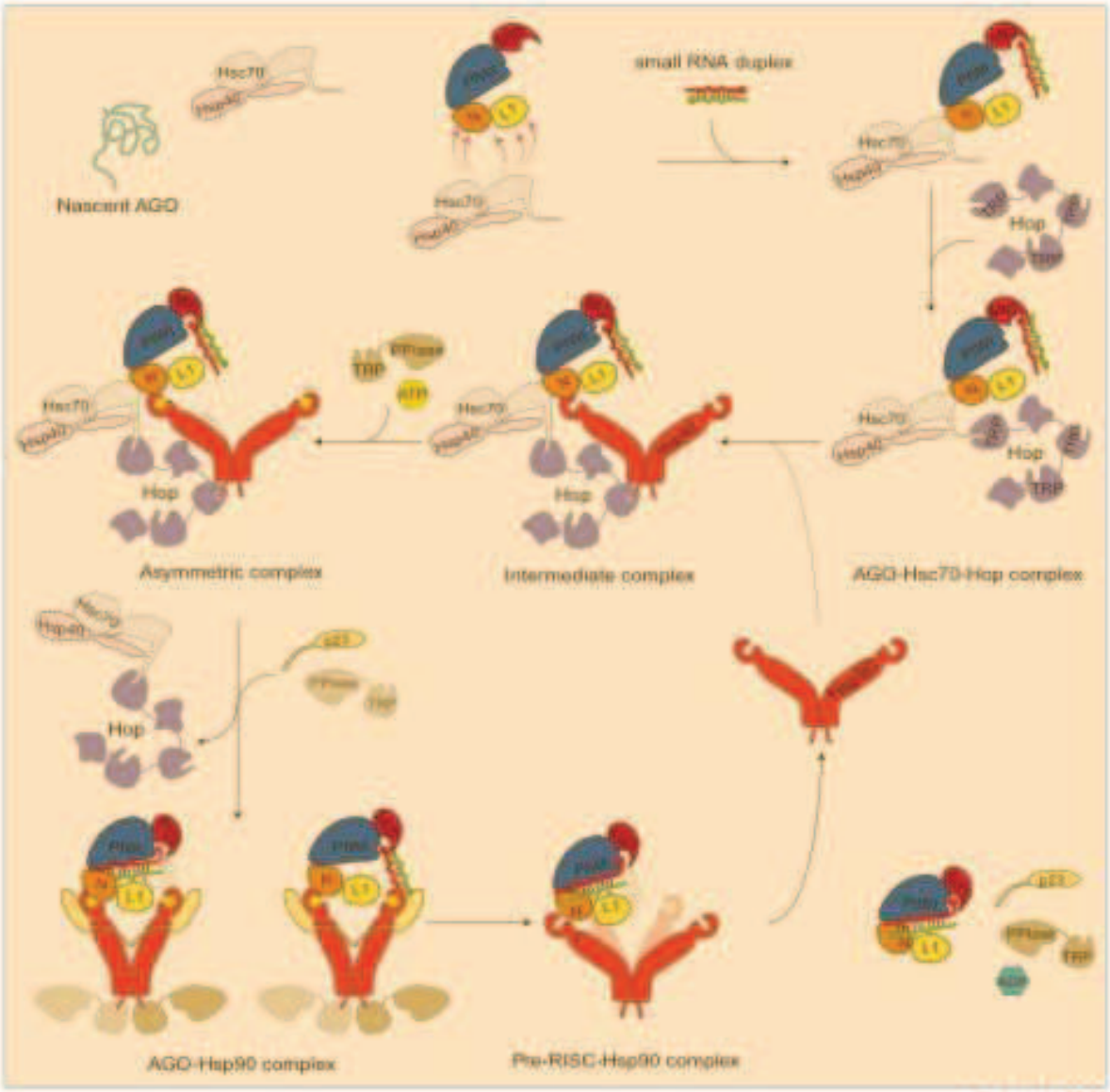

Nakanishi 2016

Fig. 4 Chaperonin proteins & AGO2

Schematic representation of the involvement of chaperonin proteins in the loading of AGO2 with a smallRNA duplex. This model was built using data from yeast, *C. elegans,* mammals and insects.

by a decrease in active GW-body-associated miRISCs (Lee, et al. 2009; Harris et al. 2011; Gibbings et al. 2009).

The loading of the smallRNA duplex onto an Argonaute molecule is a crucial step. Characterization of the structural feature of Drosophila AGO1 and AGO2 during the loading step showed a dependency on ATP (Kawamata et al. 2009). The model accompanying these findings suggests that, given the remarkable flexibility of the AGO structure, ATP might be used to trigger dynamic conformational opening of Ago proteins to accept RNA duplexes. This model is supported by the fact that Hsc70/Hsp90chaperone machinery is essential of an efficient loading of AGO proteins (Iwasaki et al. 2010). A recent review (Fig. 4) compiled a detailed model of the small RNA loading step encompassing data from *Drosophila* as well as mice, plants and C. elegans (Nakanishi 2016).

Fig. 5

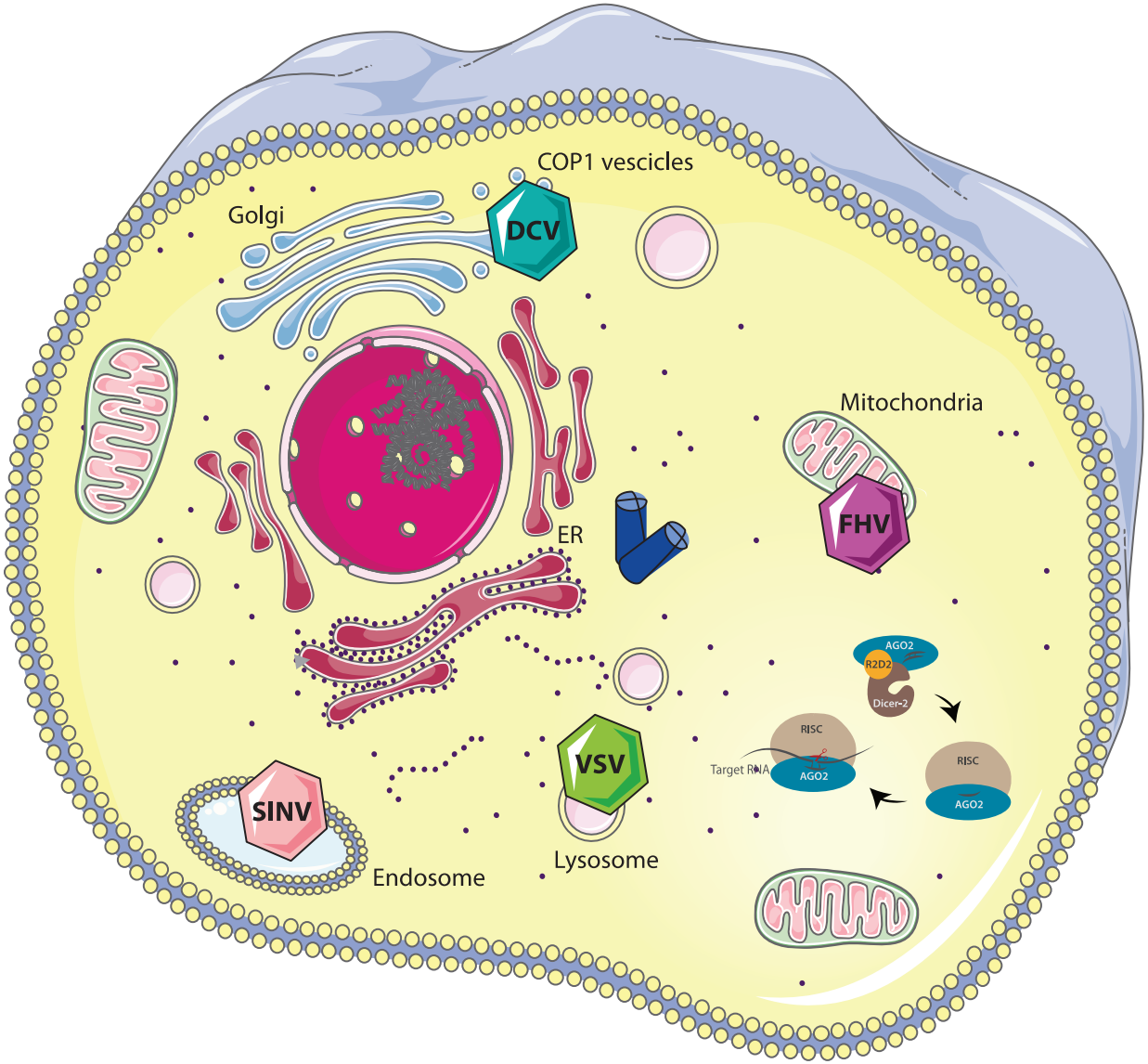
COP1 vescicles
Golgi
DCV
Mitochondria
FHV
ER
AGO2
R2D2
Dicer-2
RISC
Target RNA
AGO2
RISC
AGO2
VSV
SINV
Endosome
Lysosome

Fig. 5

Schematic representation of the cellular compartment in which DCV, VSV, FHV and SINV replicate.

3. Objective of the thesis

Although the three key components (AGO2, Dcr-2 and R2D2) of the antiviral siRNA pathway in *Drosophila* are well defined, many questions concerning their function and interaction networks remain unanswered. The Dcr-2 dependant inducible antiviral response that is operating in parallel to RNAi, suggests the existence of important and unknown antiviral Dcr-2 partners that do not necessary participate in classical RNAi. Another question remaining unanswered in the field of antiviral RNAi is how Dcr-2 is able to sense and process viral products when viruses replicate in secluded viral factories separated from the cytoplasm (Fig. 5).Most of the mechanistic details, describing how the siRNA pathway targets the viral genome, are either the result of indirect observations, or are inferred by *in vitro* experiments. Defining new molecular partners of AGO2, Dcr-2 and R2D2 in an infectious context *in vivo* may reveal how *Drosophila* cells deal with viral infection. Indeed, the identification of protein complexes assembling around these three molecules upon viral stimulation would permit the identification of new potential antiviral sensors and/or effectors. The RNAi response to different viruses does not seem to be always the same. For example, DCV and SINV but not other viruses induce the antiviral protein *vago*. Thus, a comparison of the siRNA interactome after a challenge with different viruses could be informative. Finally, the identification of an endo-/exo-siRNA pathway protein niche would help defining the molecular nodes governing these different pathways.

To identify the proteins interacting with Dcr-2, R2D2 and AGO2, we used a biotin-tag affinity purification system, which allows high efficiency recovery of molecules expressed at physiological levels in Drosophila cells, using the high affinity of streptavidin for biotin (Fukuyama et al. 2012). Dicer-2, R2D2 and AGO2 were tagged at their N- or C-terminal ends with a 15 amino-acid sequence, and stably expressed in a

Fig. 6

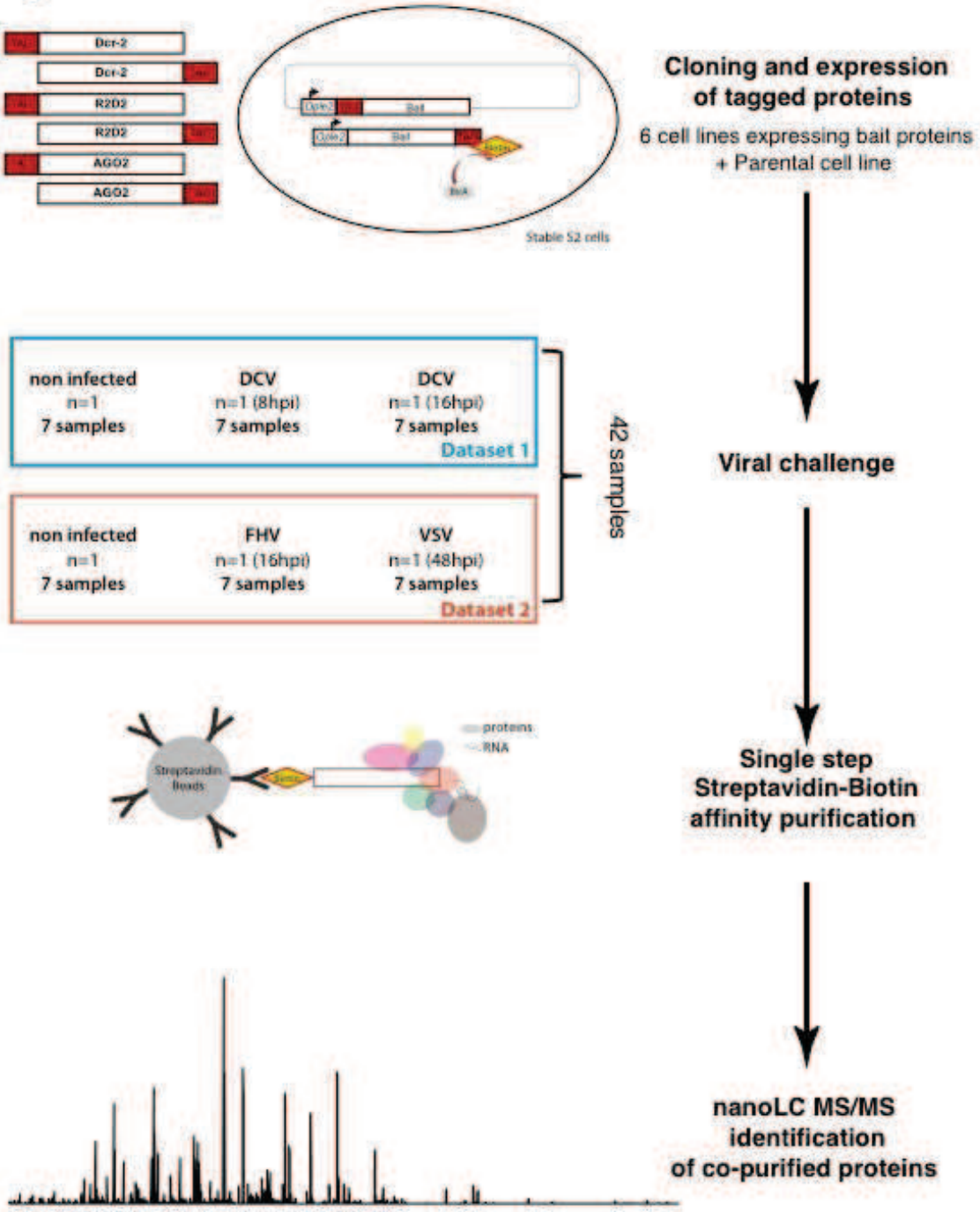
Dcr-2
Dcr-2
R2D2
R2D2
AGO2
AGO2
Stable S2 cells
Cloning and expression
of tagged proteins
6 cell lines expressing bait proteins
+ Parental cell line
non infected
n=1
7 samples
DCV
n=1 (8hpi)
7 samples
DCV
n=1 (16hpi)
7 samples
Dataset 1
non infected
n=1
7 samples
FHV
n=1 (16hpi)
7 samples
VSV
n=1 (48hpi)
7 samples
Dataset 2
42 samples
Viral challenge
Streptavidin
Beads
proteins
RNA
Single step
Streptavidin-Biotin
affinity purification
nanoLC MS/MS
identification
of co-purified proteins

Fig. 6 Strategy used to define the siRNA pathway interactome

The bait proteins Dcr-2, AGO2 and R2D2 were tagged at their amino- or carboxy-terminal extremities with a 15 amino-acid biotinylation target sequence. S2 cells epressing the bacterial biotin ligase BirA were stably transfected with the corresponding expression constructs. Cells were then either mock infected or infected with DCV (8h and 16h), FHV (16h) or VSV (48h). Cell lysates were affinity purified in a single step on streptavidin beads, digested with trypsin, and analyzed by nanoLC MS/MS on a FT ICR mass spectrometer.

hemocyte-like Drosophila S2 cell line expressing the bacterial biotin-ligase BirA, which mediates biotinylation (Fig. 5). Expression of the tagged bait proteins is controlled by the baculovirus OpIE2 immediate early promoter, which is moderately active in Drosophila cells. BirA expressing cell lines transfected with the six expression plasmids (three proteins, tagged at their N- or C-terminal extremities) were selected for stable expression of the proteins of interest at a moderate level. A targeted RNAi screen was then performed to assess the contribution of the identified proteins to the control of viral replication (Fig. 6). This functional proteomic approach revealed an association of AGO2 with the TriC/CCT chaperonin complex, which has been the topic of my PhD thesis.

Fig. 7

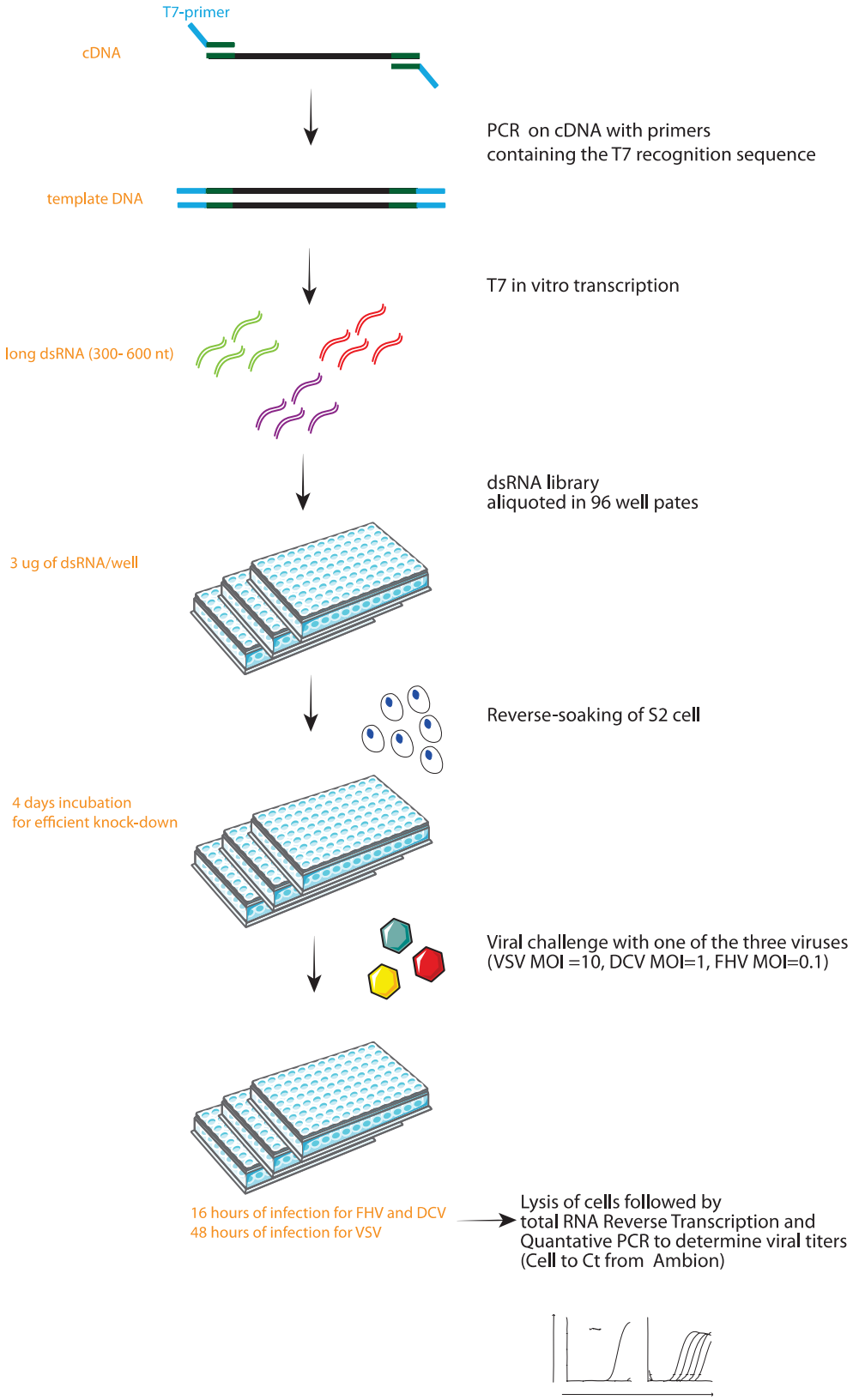
T7-primer
cDNA
PCR on cDNA with primers
containing the T7 recognition sequence
template DNA
T7 in vitro transcription
long dsRNA (300- 600 nt)
dsRNA library
aliquoted in 96 well pates
3 ug of dsRNA/well
Reverse-soaking of S2 cell
4 days incubation
for efficient knock-down
Viral challenge with one of the three viruses
(VSV MOI =10, DCV MOI=1, FHV MOI=0.1)
16 hours of infection for FHV and DCV
48 hours of infection for VSV
Lysis of cells followed by
total RNA Reverse Transcription and
Quantative PCR to determine viral titers
(Cell to Ct from Ambion)

Fig. 7 General RNAi-screening strategy

Gene specific primers harboring the T7 promoter sequence were designed using the E-RNAi algorithm and used to generate a library of dsRNAs. The dsRNA library was used to reverse soak S2 cells, which were then infected with DCV, FHV or VSV. Viral replication was assessed by RT-QPCR 16 hours post infection for FHV and DCV, or 48 hours for VSV.

II Results

1. A siRNA pathway interactome in *Drosophila* S2 cells reveals an enrichment for protein folding machinery.

Stable cell lines expressing N- or C-terminal AVI-tagged Dicer-2, R2D2 and AGO2 were constructed and validated. These six cell lines, plus one control line expressing only the bacterial *BirA* gene, encoding a biotin ligase (Fukuyama et al 2014), were used in two independent sets of experiments. In the first one, they were either mock treated or infected by Drosophila C virus (DCV) (8h or 16hpi). In the second one, they were mock treated or infected with Flockhouse virus (FHV) (16hpi) or Vesicular stomatitis virus (VSV) (48hpi). These three viruses belong to different families: *Dicistroviridae* (DCV), *Rhabdoviridae* (VSV), and *Nodaviridae* (FHV). A total of 42 samples were obtained (7 cell lines x 6 conditions). Biotinylated bait proteins were recovered by single step affinity purification on Streptavidin coupled beads and analyzed by mass spectrometry. Overall, we identified 103 interacting proteins covering a broad range of molecular functions. The comparison of the interactomes in the different conditions has been described elsewhere (Mazjoub, PhD thesis, 2013 UniStra). Below, we focus on the global list of interactants that were identified. As expected, Dcr-2 was pulled-down with R2D2 and vice versa. AGO2 was also pulled down with R2D2. The most represented molecular functions are related to translation with a number of ribosomal proteins, but also factors involved in protein folding (Fig. 1A). In the latter category, we recovered heat-shock proteins known to be induced by some viral infections (e.g. Hsp70) (Merkling, Overheul, et al. 2015), but also heat-shock cognate proteins, which regulate the function of AGO2 and antiviral RNAi (e.g. Hsc70-3,4) (Iwasaki et al. 2010; Dorner et al. 2006). Strikingly, our analysis also revealed the presence of six of the eight subunits of the TRiC/CCT chaperonin complex (CCT1, CCT7, CCT6, CCT3, CCT2, CCT4), which mediates folding of large multi-domain proteins (Rüßmann et al. 2012).

Fig. 1

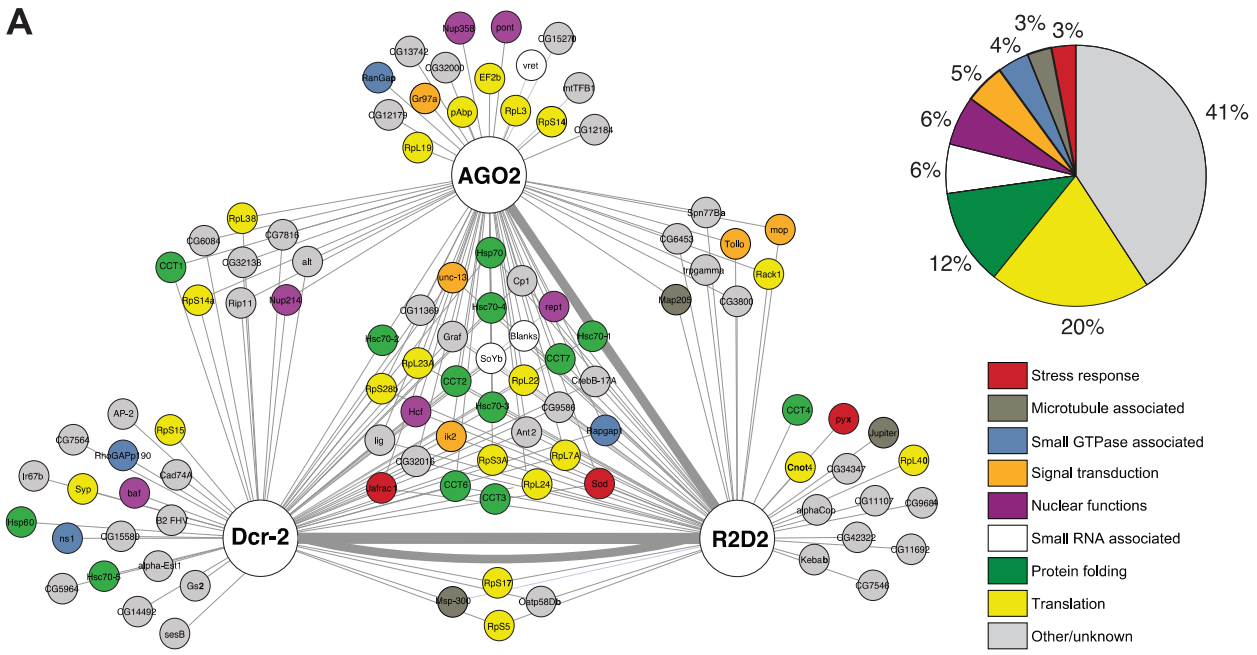
A
AGO2
Dcr-2
R2D2
41%
20%
12%
6%
6%
5%
4%
3%
3%
Stress response
Microtubule associated
Small GTPase associated
Signal transduction
Nuclear functions
Small RNA associated
Protein folding
Translation
Other/unknown

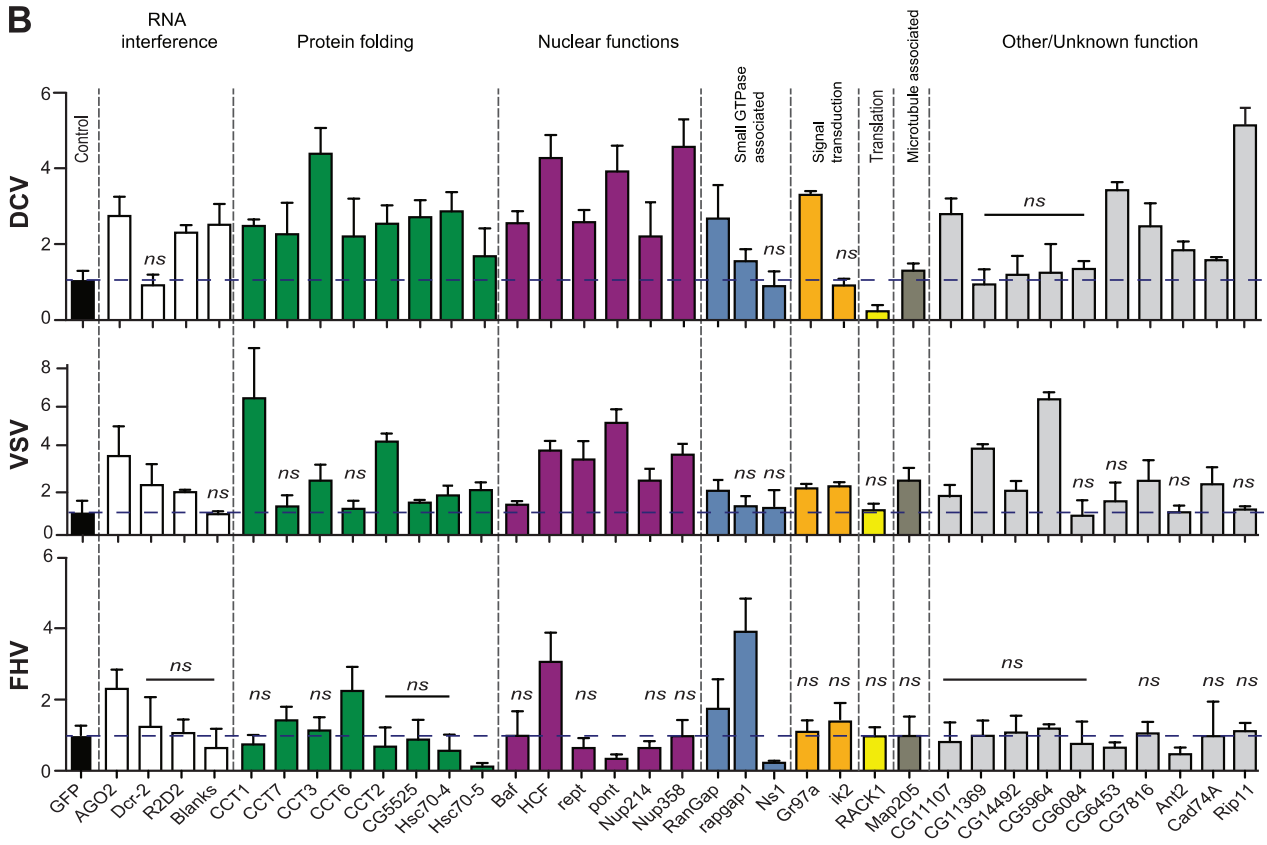
B
RNA interference
Protein folding
Nuclear functions
Small GTPase associated
Signal transduction
Translation
Microtubule associated
Other/Unknown function
Control
DCV
VSV
FHV
ns
GFP
AGO2
Dcr-2
R2D2
Blanks
CCT1
CCT7
CCT3
CCT6
CCT2
CG5525
Hsc70-4
Hsc70-5
Baf
HCF
rept
pont
Nup214
Nup358
RanGap
rapgap1
Ns1
Gr97a
ik2
RACK1
Map205
CG11107
CG11369
CG14492
CG5964
CG6084
CG6453
CG7816
Ant2
Cad74A
Rip11

Fig. 1. Definition of an interactome for the antiviral siRNA pathway

A. Schematic representation of the interactants identified. The bait proteins Dcr-2, R2D2 and AGO2 are represented as enlarged circles. Each protein is color-coded based on molecular functions. **B.** Hits from the targeted RNAi screen showing a 2-fold change in viral RNA for at least one virus and having shown no viability or proliferation defects upon knockdown. ns: non significant. Bars with no *ns* sign means that the difference is statistically significant (P value < 0.05).

We next tested the relevance of these interactions with a targeted RNAi screen in the context of viral infections. Upon knock down, 15 genes significantly affected the viability of the cells, which prevented further characterization. Of the remaining 88 genes, 17 showed a proliferation index below 50%, indicating an impact on cell fitness and were not further analyzed. The remaining 71 genes, for which the dsRNA treatment had no effect on cell viability or proliferation, were tested for their effect on replication of DCV, FHV and VSV. 16 hours (DCV and FHV) or 48 hours (VSV) post infection, cells were lysed and viral RNA accumulation was assessed by RT-QPCR. Silencing of 34 genes led to an increase or a decrease of two folds or more in the replication of at least one of the three tested viruses (Fig. 1B). Among the 34 hits, we found genes previously shown to be involved in either antiviral immunity or RNAi in *Drosophila*, including *pontin* and *reptin*, also known as RuvBL1 and RuvBL2 (Yasunaga et al. 2014), *Blanks* (Gerbasi et al. 2011), *Hsc70-4* (Iwasaki et al. 2010; Iwasaki et al. 2015; Dorner et al. 2006). Of note, silencing any of the six components of the TRiC/CCT complex identified by mass spectrometry led to increased viral replication of at least one of the three virus tested. Altogether, these results suggest that the TRiC/CCT complex interacts with core components of the siRNA pathway and that this interaction is relevant for antiviral RNA interference. We therefore decided to investigate further the role of the TRiC/CCT complex.

2. The TRiC/CCT complex interacts with AGO2 and participates in antiviral resistance.

The TRiC/CCT complex is a type II chaperone formed by two stacked hetero-octameric rings (Fig. 2A). It has been estimated that as much as 10% of cytosolic proteins rely on this complex for a correct folding (Lopez et al. 2015). To confirm the interaction observed by mass spectrometry, we overexpressed tagged versions of AGO2,

Fig. 2

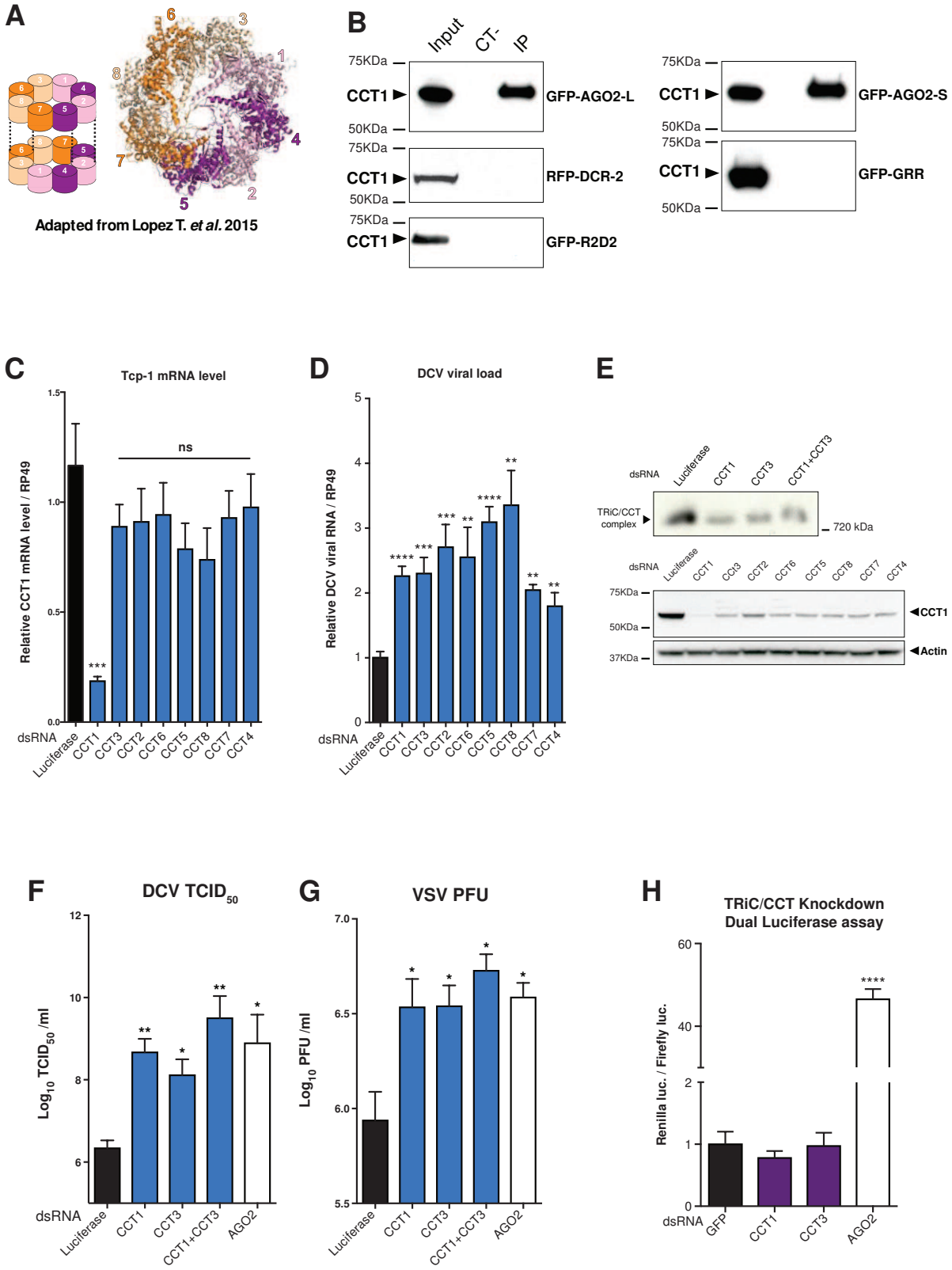
A
Adapted from Lopez T. et al. 2015
B
Input
CT-
IP
75KDa
50KDa
CCT1
GFP-AGO2-L
RFP-DCR-2
GFP-R2D2
GFP-AGO2-S
GFP-GRR
C
Tcp-1 mRNA level
Relative CCT1 mRNA level / RP49
ns
dsRNA
Luciferase
CCT1
CCT3
CCT2
CCT6
CCT5
CCT8
CCT7
CCT4
D
DCV viral load
Relative DCV viral RNA / RP49
E
TRiC/CCT complex
720 kDa
37KDa
Actin
F
DCV TCID50
Log10 TCID50 /ml
CCT1+CCT3
AGO2
G
VSV PFU
Log10 PFU /ml
H
TRiC/CCT Knockdown
Dual Luciferase assay
Renilla luc. / Firefly luc.
GFP

Fig. 2 the TRiC/CCT complex and AGO2 restrict viral infection in S2 cells

A. Schematic representation of the structure and subunit organization TRiC/CCT complex (From (Lopez et al. 2015)). **B.** Immunoprecipitation of tagged AGO2-L, AGO2-S, GRR, Dcr-2 or R2D2 followed by immunoblot analysis with antibodies against CCT1. Uncoupled saturated agarose beads were used as negative control (central lane). **C.** Expression of CCT1 as determined by qRT-PCR in cells silenced for the indicated genes. **D.** Relative abundance of DCV RNA monitored by qRT-PCR in cells treated with control dsRNA or dsRNAs targeting the TRiC/CCT complex subunits. **E. (top)** Native PAGE followed by immunoblot against the CCT1 subunit showing the abundance of the TRiC/CCT complex in its native conformation. **(bottom)** Immunoblot against CCT1 showing the abundance of the protein following the knockdown of each single subunit of the TRiC/CCT complex. **F, G.** Viral titers of DCV ($TCID_{50}$) and VSV (Plaque assay), respectively, in cells silenced for the indicated genes. **H.** Luciferase activity in cells treated with a dsRNA targeting luciferase and silenced for the indicated genes (*P value<0.05; **P value<0.01; ***P value<0.001; ****P value< 0.0001). Graphs in panels C, D, F-H are the result of two (C, D, H) or three (F, G) independent experiments, each containing at least two biological replicates. Blots are the result of at least two independent experiments.

Dcr-2 and R2D2 in S2 cells. We did not detect intercation of CCT1 with Dcr-2 or R2D2 but immunoprecipitation followed by western blot against the CCT1 subunit of the TRiC/CCT complex confirmed that CCT1 interacts with both isoforms of AGO2 (Fig. 2B, see below). We next silenced the expression of the eight subunits of the TRiC/CCT complex (Fig. 2C) and analyzed the impact on DCV, a natural Drosophila pathogen (Fig.2D). All subunits affected the replication of DCV without any indication of a compensatory effect, in agreement with a previous report (Kitamura et al. 2006). Indeed, silencing two of the eight subunits disrupted the assembly of the TRiC/CCT complex, as revealed by western blot following native gel electrophoresis (Fig. 2E, top). As a result, silencing any of the eight subunits resulted in a decreased amount of CCT1 in S2 cells (Fig. 2E, bottom). Monitoring of infectious titer for DCV confirmed that the TRiC/CCT complex opposes viral replication, like AGO2 (Fig. 2F). This effect was not virus-specific because the infectious titer for VSV, a (-) strand RNA virus with markedly different dynamics of replication than DCV in flies, was also significantly increased upon silencing CCT1 or CCT3 (Fig. 2G). Surprisingly however, silencing of CCT1 (or CCT3) did not result in de-repression of a luciferase reporter gene in cells treated with a long dsRNA targeting this gene, unlike silencing of AGO2 (Fig. 2H).

3. The TRiC/CCT complex does not affect expression of the two isoforms of AGO2

We next analyzed if the TRiC/CCT complex affected the expression or stability of AGO2. Immunoblot analysis of S2 cell extracts revealed two bands of 132 kDa and 90 kDa corresponding to the two isoforms of AGO2 previously described (Hain et al. 2010) (Fig. 3A) (hereafter referred to as AGO2-L and AGO2-S).

The interaction of AGO2 with a chaperonin complex suggests that the TRiC/CCT complex plays a role in the folding of this large multidomain protein. Thus the increased

Fig. 3

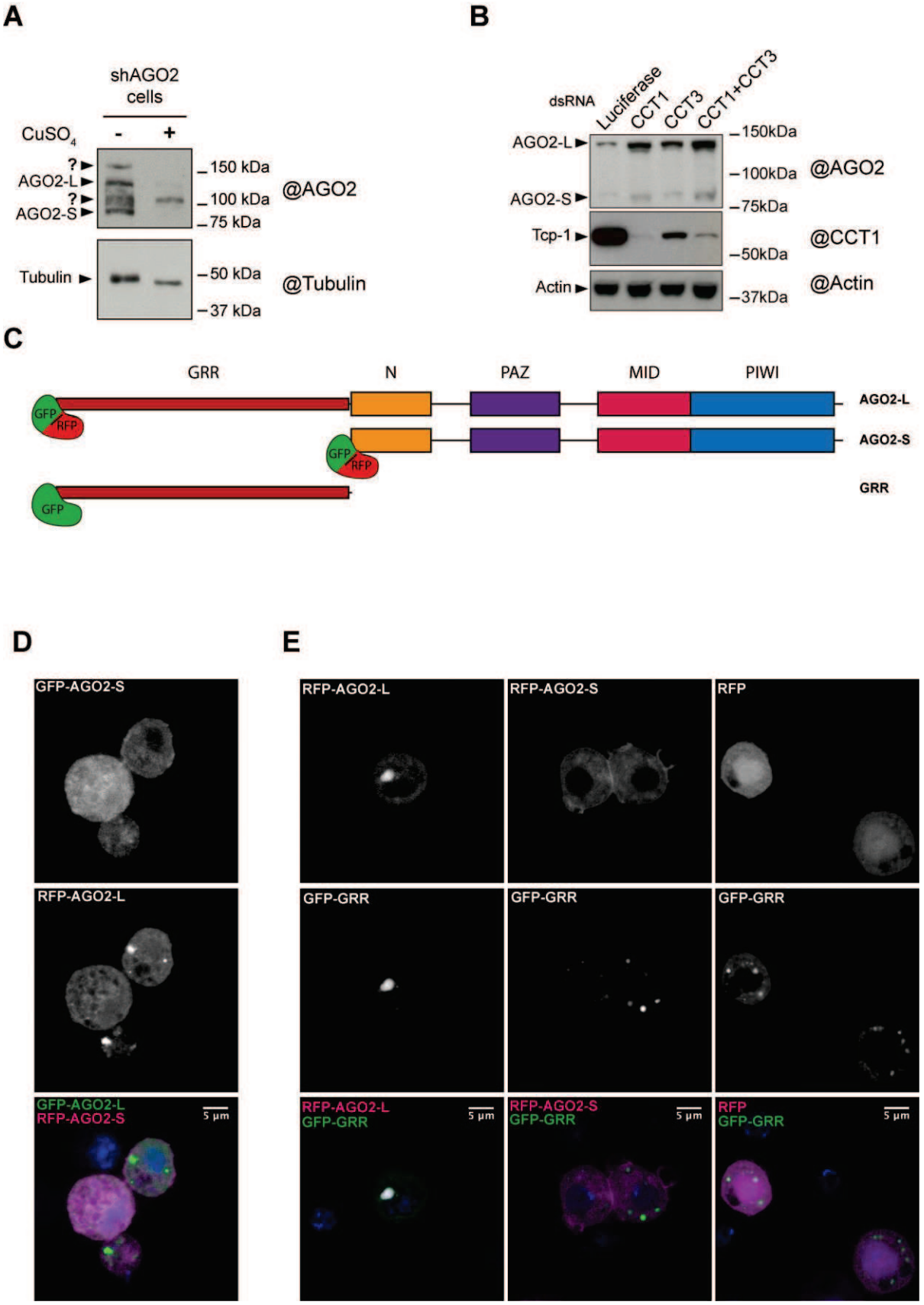
A
shAGO2 cells
CuSO4
-
+
?
AGO2-L
?
AGO2-S
150 kDa
100 kDa
75 kDa
@AGO2
Tubulin
50 kDa
37 kDa
@Tubulin
B
dsRNA
Luciferase
CCT1
CCT3
CCT1+CCT3
AGO2-L
AGO2-S
150kDa
100kDa
75kDa
@AGO2
Tcp-1
50kDa
@CCT1
Actin
37kDa
@Actin
C
GRR
N
PAZ
MID
PIWI
GFP
RFP
AGO2-L
AGO2-S
GRR
D
GFP-AGO2-S
RFP-AGO2-L
GFP-AGO2-L
RFP-AGO2-S
5 µm
E
RFP-AGO2-L
RFP-AGO2-S
RFP
GFP-GRR
GFP-GRR
GFP-GRR
RFP-AGO2-L
GFP-GRR
RFP-AGO2-S
GFP-GRR
RFP
GFP-GRR

Fig. 3 S2 cells express two isoforms of AGO2, whose stability is not affected by the TRiC/CCT complex

A. Immunoblot against AGO2 showing the two isoforms present in S2 cells. A stable cell line expressing an shRNA targeting AGO2 under the control of a copper inducible promoter has been used to validate the specificity of the bands. Anti-Tubulin antibody was used as loading control. The two bands marked with "?" are not consistently detected and do not correspond to the predicted size of the AGO2 isoforms. **B.** Immunoblot against AGO2 in S2 cells treated with control dsRNA, CCT1 dsRNA, CCT3 dsRNA or both at the same time. Anti-Actin antibody was used as loading control. **C.** Schematic representation of the GFP/RFP tagged recombinant AGO2 contructs. **D.** Representative pictures of S2 cells transiently transfected with GFP-AGO2-L and RFP-AGO2-S. Blots are the result of one (B) or three (A) independent experiments.

viral replication observed in TRiC/CCT silenced cells could result from altered folding and degradation of AGO2. However, silencing of two different subunits of the TRiC/CCT complex did not affect any of the isoforms (Fig. 3B). The interaction of AGO2 with this chaperone complex suggests a role in folding of this large multidomain protein. Of note, the TRiC/CCT complex also participates in the folding of proteins that possess polyglutamine regions, thus preventing their aggregation (Kitamura et al. 2006). The N-terminal region of AGO2, although not corresponding to a polyglutamine stretch sensu stricto, contains many glutamine-rich repeats (GRRs) (Hain et al. 2010; Palmer & Obbard 2016). This prompted us to see if inhibition of the TRiC/CCT complex resulted in altered localization of AGO2 in cells. To monitor the intracellular distribution of the long and short isoforms of AGO2, we constructed GFP or RFP tagged versions of the proteins (Fig. 3C). Genetic complementation of AGO2 mutant flies revealed that the N-terminal fusion did not affect the function of AGO2 (Fig. S2A).

Confocal microscopy revealed some difference between the AGO2-L and AGO2-S in transiently transfected S2 cells (Figure 3D). Indeed, while both proteins exhibited a diffuse cytosolic localization, AGO2-L also formed some foci that did not colocalize with *bona fide* markers for P bodies or stress granules (Fig. S3A). Expression of the N-terminal region of AGO2-L containing the GRR region led to the formation of large cytoplasmic granules (Fig. 3E).

4. The TRiC/CCT complex affects the intracellular distribution of the long form of AGO2.

To further study the differences between AGO2-L and AGO2-S, we established stable cell lines expressing GFP tagged versions of the two proteins. Upon knock down of CCT1 or CCT3, we observed an increase in the number of cells containing granules of AGO2-L

Fig. 4

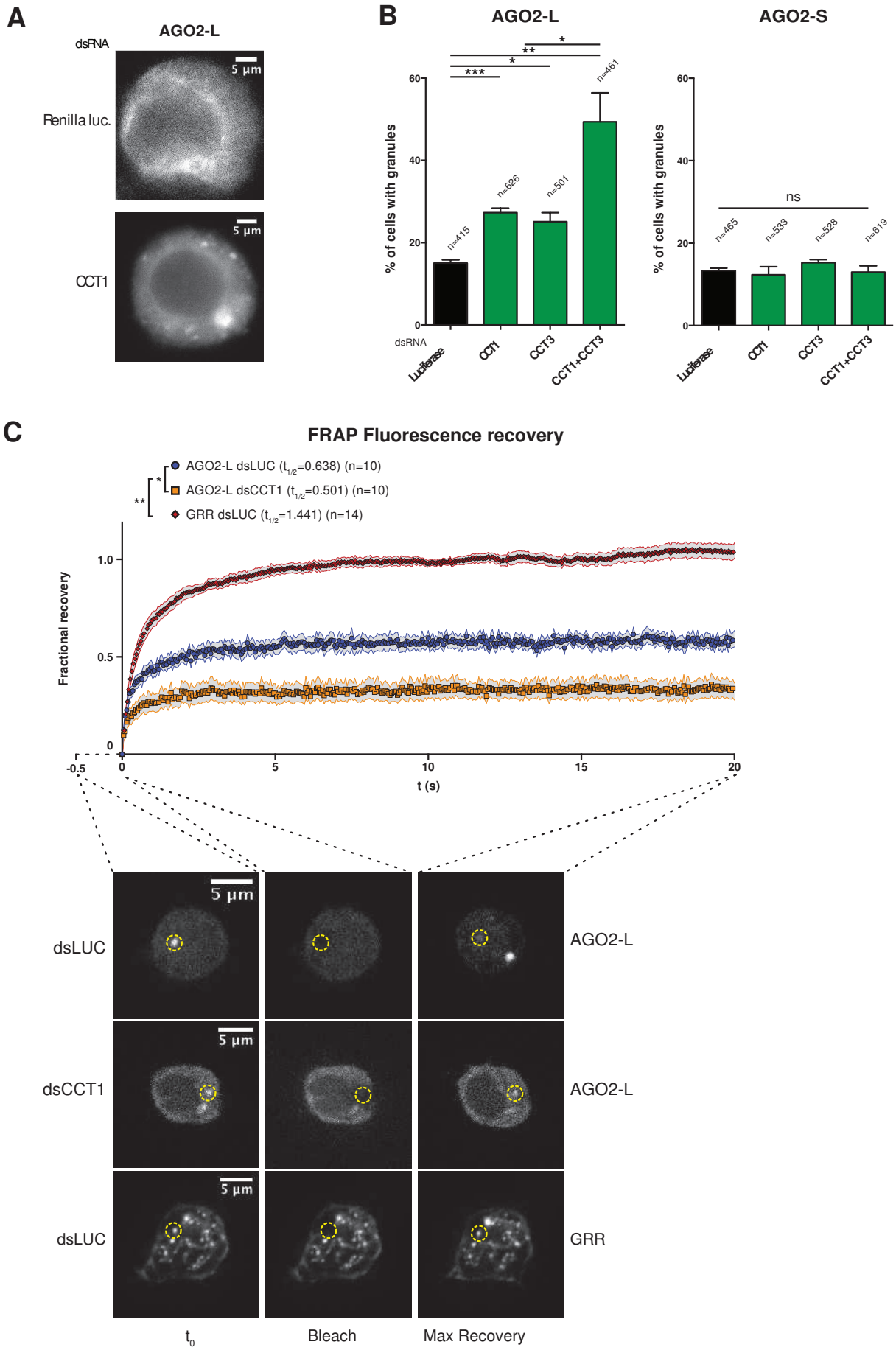
A
AGO2-L
dsRNA
Renilla luc.
CCT1
5 µm
B
AGO2-L
AGO2-S
% of cells with granules
n=415
n=626
n=501
n=461
n=465
n=533
n=528
n=619
ns
dsRNA
Luciferase
CCT1
CCT3
CCT1+CCT3
C
FRAP Fluorescence recovery
AGO2-L dsLUC (t1/2=0.638) (n=10)
AGO2-L dsCCT1 (t1/2=0.501) (n=10)
GRR dsLUC (t1/2=1.441) (n=14)
Fractional recovery
t (s)
dsLUC
dsCCT1
AGO2-L
GRR
t0
Bleach
Max Recovery

Fig. 4 The TRiC/CCT complex controls the dynamics of AGO2-L granules

A. Representative images of S2 cells stably expressing GFP-AGO2-L in control or CCT1-silenced conditions. **B.** Bar chart showing the percentage of cells containing granules in stably transfected cells expressing either GFP-AGO2-L or GFP-AGO2-S. Cells were treated with control dsRNA, CCT1 dsRNA, CCT3 dsRNA or both at the same time. **C. (top)** Plot showing the fractional fluorescence recovery of bleached GFP-AGO2-L granules in cells treated with either control dsRNA or dsRNA targeting CCT1. The value "1" represent the fluorescence intensity prior to photobleaching. **(bottom)** Pictures representative of the different conditions before (t_0), immediately after photobleaching (Bleach), and after maximum recovery of fluorescence (Max Recovery). (*P value < 0.05; **P value < 0.01; ***P value < 0.001). Graphs in panels B and C are the result of three (F, G) independent experiments.

(Fig. 4A, B). Conversely, in cells expressing AGO2-S, no difference was observed between samples treated with dsRNA targeting either CCT1 or CCT3 and control dsRNA (Fig. 4B). However, we noticed that treatment of these cells with dsRNA triggered the appearance of granules containing AGO2-S in about 15% of the cells. These results suggest that the TRiC/CCT complex prevents GRR-mediated aggregation of AGO2-L.

To gain further insight on the granules formed by AGO2-L, we used FRAP (Fluorescence Recovery After Photobleaching). Isolated granules were bleached and imaged until maximum fluorescence was recovered (Fig. 4C, S3B, C). We observed that granules formed by AGO2-L recovered with a $t_{1/2}$ of 0.683 s. This was significantly faster than the recovery of granules composed of the GRR domain alone ($t_{1/2}$=1.441 s), indicating that the AGO2-L granules are not mere protein aggregates, but correspond to dynamic structures. Additionally, silencing of CCT1 resulted in faster fluorescence recovery ($t_{1/2}$=0.501 s) of the AGO2-L granules. We conclude that these granules are dynamic and not mere aggregates of misfolded proteins. Furthermore, the TRiC/CCT complex controls the dynamics of these granules, which may impact the antiviral function of AGO2.

5. AGO2-S cannot substitute for AGO2-L to control viruses

The results presented above suggest that AGO2-L and AGO2-S are functionally distinct. To clarify this point, we used stable cells lines expressing an shRNA targeting the PIWI domain of AGO2 (TRiP.HMS00108) under the control of a copper-inducible metallothionine promoter (Fig. 5A). We then generated recombinant GFP-tagged AGO2 constructs (L and S forms) containing point mutations in the site targeted by the shRNA (AGO2 shR) to rescue the AGO2 depletion (Fig. 5A). Both AGO2-L and AGO2-S rescue silencing of a luciferase reporter gene in cells treated with a luciferase long dsRNA (Fig.

Fig. 5

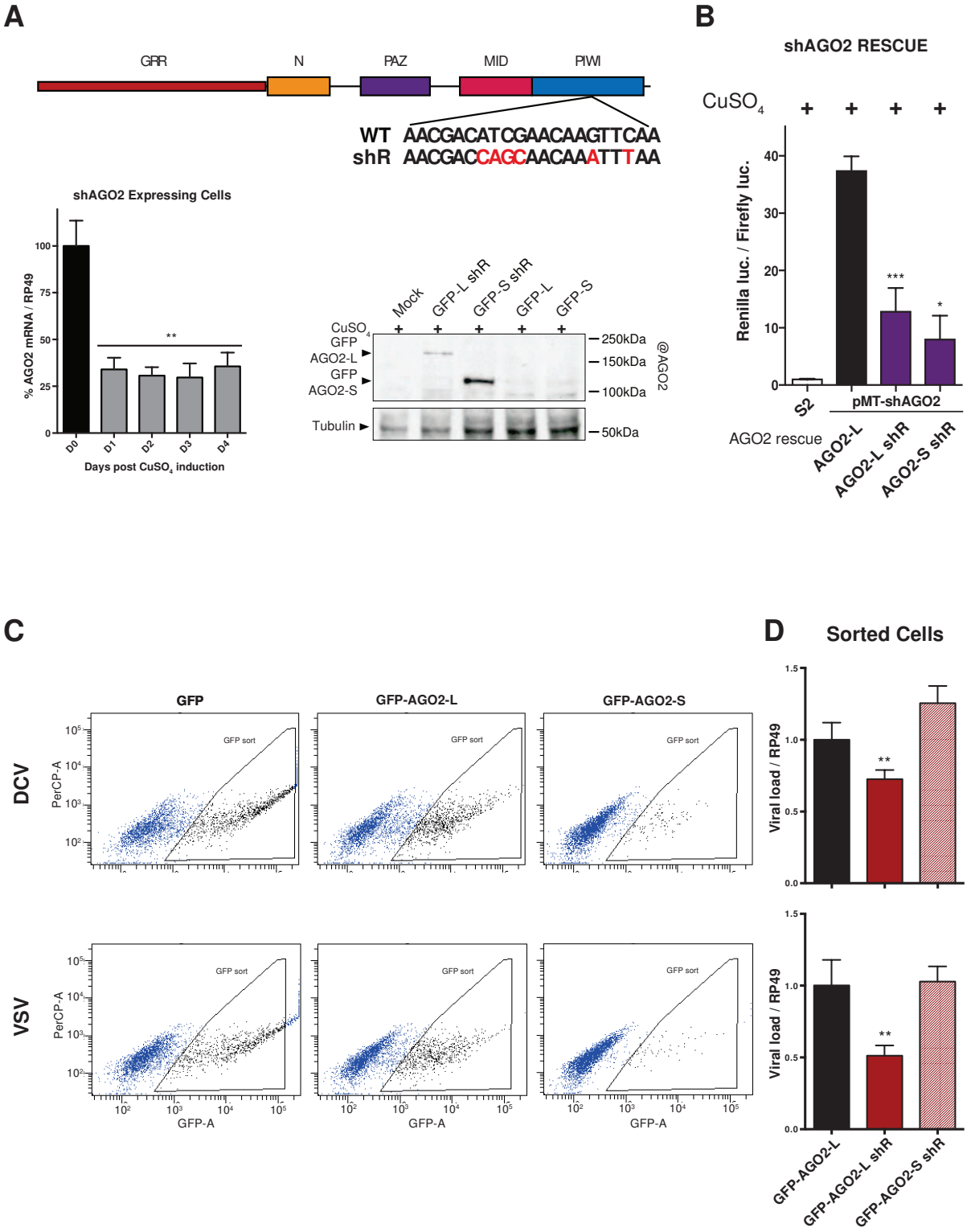
A
GRR
N
PAZ
MID
PIWI
WT AACGACATCGAACAAGTTCAA
shR AACGACCAGCAACAAATTTAA
shAGO2 Expressing Cells
% AGO2 mRNA / RP49
Days post CuSO4 induction
D0
D1
D2
D3
D4
Mock
GFP-L shR
GFP-S shR
GFP-L
GFP-S
CuSO4
GFP
AGO2-L
GFP
AGO2-S
Tubulin
250kDa
150kDa
100kDa
50kDa
@AGO2
B
shAGO2 RESCUE
CuSO4
Renilla luc. / Firefly luc.
S2
pMT-shAGO2
AGO2 rescue
AGO2-L
AGO2-L shR
AGO2-S shR
C
GFP
GFP-AGO2-L
GFP-AGO2-S
DCV
VSV
PerCP-A
GFP-A
GFP sort
D
Sorted Cells
Viral load / RP49
GFP-AGO2-L
GFP-AGO2-L shR
GFP-AGO2-S shR

Fig. 5 The N-terminal GRR is necessary for the antiviral activity of AGO2.

A. (top) Schematic representation of AGO2, highlighting the region in the PIWI domain targeted by the shRNA and the point mutations (in red) made to create the shRNA-resistant (shR) constructs. **(bottom)** Validation of the knockdown of AGO2 in stable cells expressing the shRNA under the control of a copper inducible metallothionein promoter (left) and rescue of the shR mutants by immunoblot against AGO2 (right). **B.** Luciferase activity in cells treated with a dsRNA targeting luciferase and co-transfected with a luciferase vector, a vector silencing AGO2 (pMT-shAGO2) and the indicated AGO2 rescue expression plasmids. S2 cells in the presence of copper were used as a positive control for the silencing. GFP-AGO2-L non-resistant to the shRNA was used as negative control. **C.** Dot plot showing the gating used to sort GFP-positive S2 cells by flow cytometry. **D.** Viral RNA load as determined by qRT-PCR on sorted cells infected with either DCV (top) or VSV (bottom). (*P value < 0.05; **P value < 0.01; ***P value < 0.001). Graphs in panels A, B and D are the result of two (A, D) or three (B) independent experiments, each containing at least two biological replicates.

5B). We next tested the ability of both isoforms to silence viral replication. Transfected cells were sorted for GFP expression and viral replication was monitored by qRT-PCR (Fig. 5C,D). AGO2-L, complemented cells contained significantly less DCV or VSV RNA than non-complemented cells or cells complemented with AGO2-S. We conclude that the GRR domain plays an important role in the antiviral function of AGO2 although it is not required for long dsRNA-mediated RNAi. This is consistent with the observation that the TRiC/CCT complex is not required for silencing a luciferase reporter gene by long dsRNA (Fig. 2H).

6. Virus derived siRNA are preferentially sorted onto AGO2-L

We next sought to understand what differentiates AGO2-L from AGO2-S in the context of viral infection. We infected the stable cell lines expressing GFP-AGO2-L or GFP-AGO2-S with DCV, lysed the cells and performed immunoprecipitation using the GFP tag. The protein fraction of the immunoprecipitation was run on a standard SDS-PAGE followed by western blot using anti-GFP and anti-R2D2 antibodies (Fig. 6A). Surprisingly, we observed that R2D2 co-immunoprecipitated with AGO2-S, but not AGO2-L, although a faint band could be detected in one of the four experiments. In addition the interaction between AGO2-S and R2D2 is strongly decreased upon viral infection (Fig. 6A, bottom), even though the total amount of R2D2 is not modified. This suggests that R2D2 is displaced upon viral infection.

We next extracted the small RNAs associated with the immunoprecipitated AGO2 proteins. They were purified and ran on a highly resolutive denaturing polyacrylamide gel and analyzed by northern blot, using probes originating from DCV or endogenous siRNA loci (esi-2) (Fig. 6B, C). Strikingly, DCV derived siRNAs were found associating only with AGO2-L (Fig. 6B, right). No DCV signal was detected in non-infected cells, thus

Fig. 6

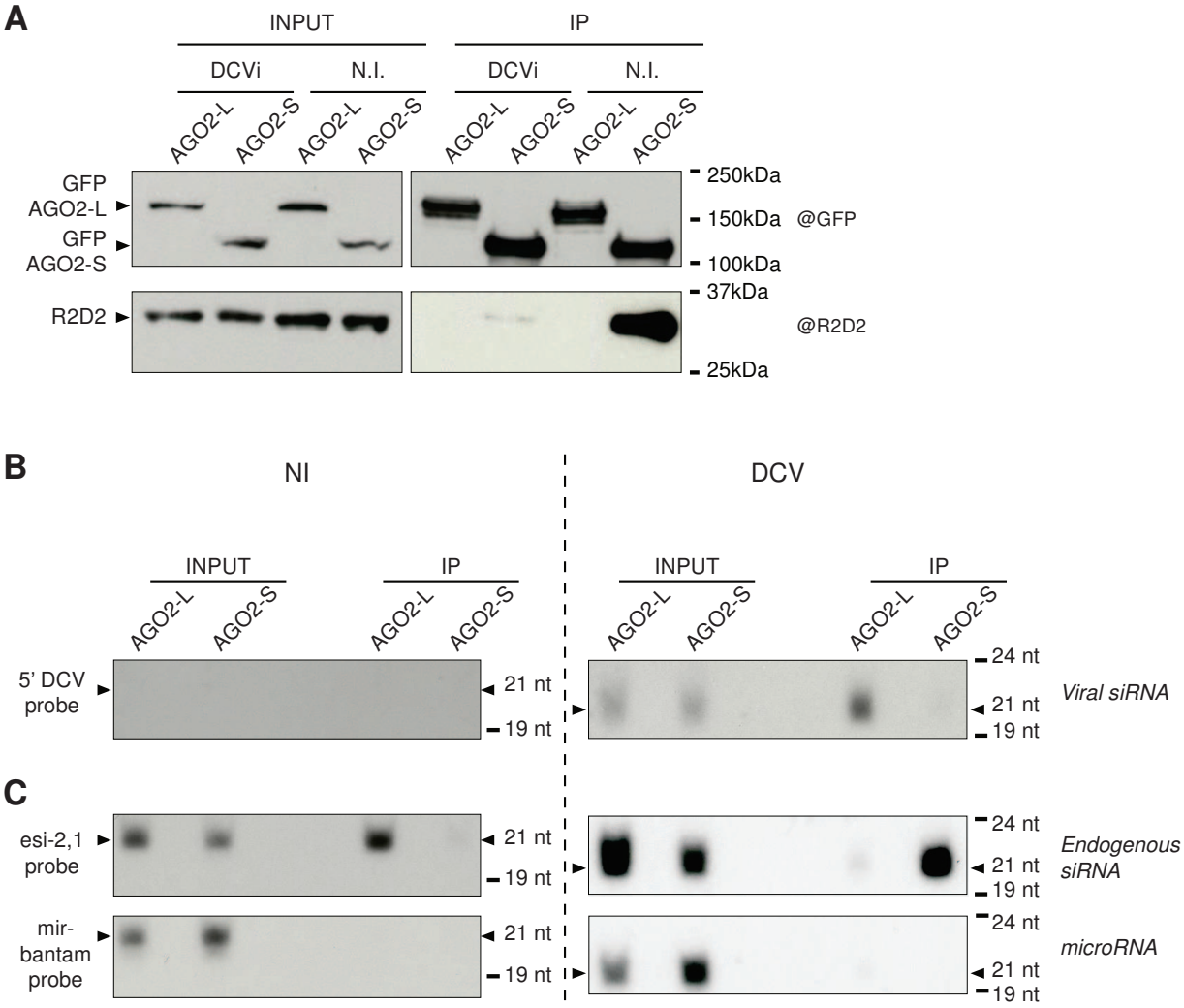
A
INPUT
IP
DCVi
N.I.
DCVi
N.I.
AGO2-L
AGO2-S
AGO2-L
AGO2-S
AGO2-L
AGO2-S
AGO2-L
AGO2-S
GFP AGO2-L
GFP AGO2-S
R2D2
250kDa
150kDa
100kDa
37kDa
25kDa
@GFP
@R2D2
B
NI
DCV
INPUT
IP
AGO2-L
AGO2-S
AGO2-L
AGO2-S
5' DCV probe
21 nt
19 nt
24 nt
Viral siRNA
C
esi-2,1 probe
Endogenous siRNA
mir-bantam probe
microRNA

Fig. 6 The two isoforms of AGO2 differ for their interaction with R2D2 and small RNAs

A. Immunoblot of the protein fraction of the AGO2-L and AGO2-S immunoprecipitates. The membrane was probed with either anti-GFP antibody (top) or anti-R2D2 antibody (bottom). **B.** Northern-blot of the small RNAs isolated from AGO2-L and AGO2-S immunoprecipitates from either non-infected cells or cells infected with DCV. The membrane was incubated with probes targeting the first 500 bases of the DCV genome. **C.** The same membrane was stripped and re-probed with an oligo probe targeting the endo-siRNA esi-2,1. The blots are representative of at least two independent experiments.

validating the specificity of the probes (Fig. 6B, left). On the other hand, endo-siRNAs associated mainly with AGO2-L in non-infected cells, but were predominantly detected in the AGO2-S immunoprecipitate upon viral infection (Fig. 6C). This confirms that the AGO2-L isoform plays a central role in antiviral RNAi and is preferentially loaded with virus derived siRNA in the context of an infection.

7. Dynamics of AGO2 during DCV infection

We next monitored the distribution of GFP-AGO2-L in S2 cells infected with DCV (Fig. 7). In cells treated with control dsRNA, we observed the rapid and transient formation of large GFP-AGO2-L aggregates upon DCV infection (Fig. 7A). These granules were detected as early as 2h post infection, which correspond to the onset of DCV replication and occupied the perinuclear space, where DCV replicates on Golgi-derived membranes (Cherry et al. 2006). FHV-B2-GFP fusion protein, which binds with high affinity to dsRNA, colocalized with AGO2-L in these transient aggregates (Fig. 8). This suggests that AGO2-L is recruited to the site of viral replication where dsRNA replication intermediates are produced. Silencing CCT1 had no effect on the formation of the aggregates. Strikingly however, the aggregates were stabilized during the length of the experiment when CCT 1 was silenced (Fig.7A, B). AGO2-S also formed aggregates upon viral infection but the difference between non-infected and DCV-infected cells was not significant as in the case of AGO2-L (Fig. S4A). However, the virus-induced formation of AGO2-S granules was more pronounced when CCT1 was silenced.

In order to understand what differentiates the aggregates formed by AGO2-L from the ones formed by AGO2-S we used FRAP. Fluorescence recovery in the large perinuclear aggregates occurred more rapidly for AGO2-L ($t_{1/2}$=1.558 s) compared to AGO2-S ($t_{1/2}$=2.555 s), suggesting that the GRR domain facilitates the dynamic relocalization of

Fig. 7

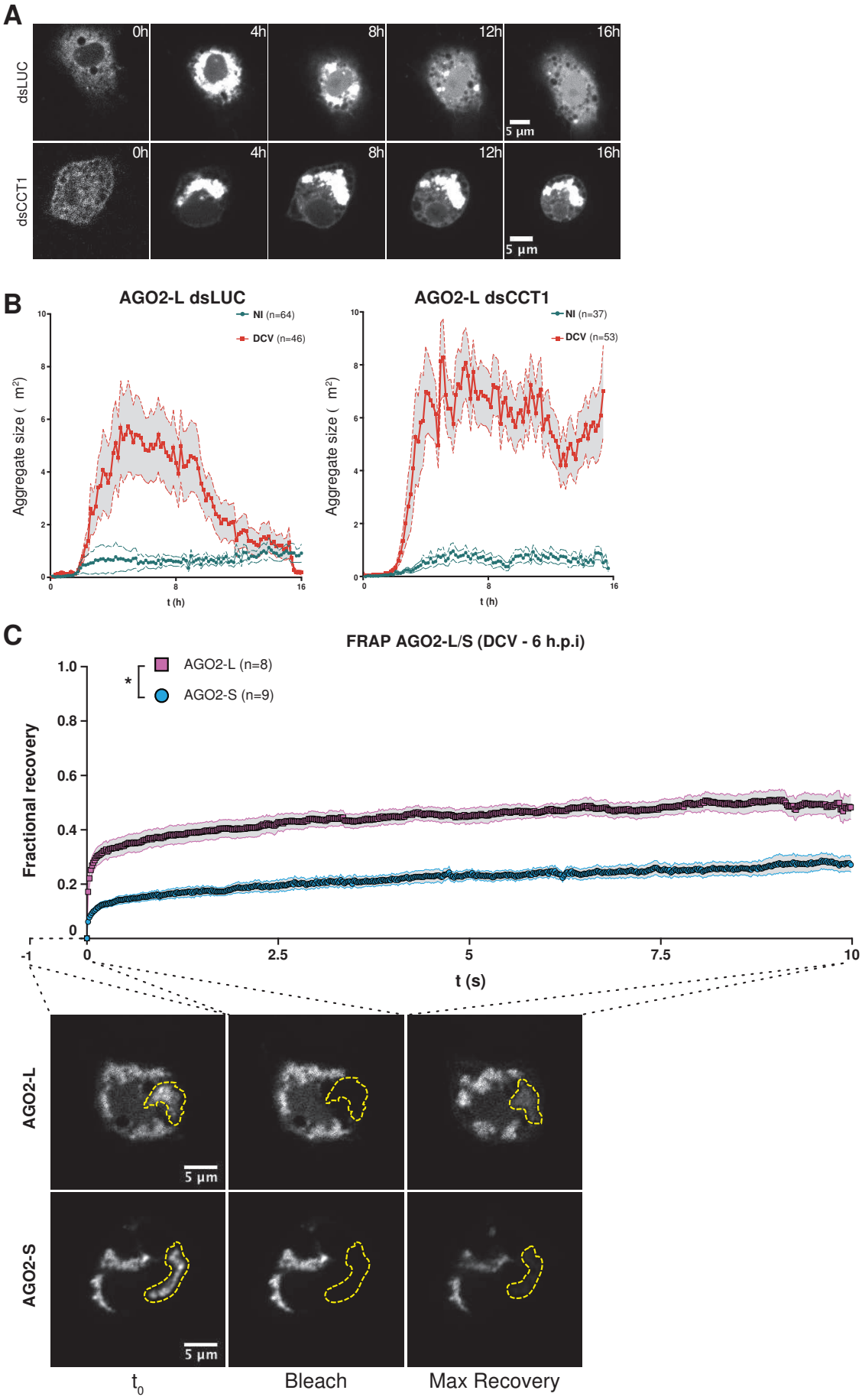
A
dsLUC
dsCCT1
0h
4h
8h
12h
16h
5 µm
B
AGO2-L dsLUC
AGO2-L dsCCT1
NI (n=64)
DCV (n=46)
NI (n=37)
DCV (n=53)
Aggregate size (m2)
t (h)
C
FRAP AGO2-L/S (DCV - 6 h.p.i)
AGO2-L (n=8)
AGO2-S (n=9)
*
Fractional recovery
t (s)
AGO2-L
AGO2-S
t0
Bleach
Max Recovery

Fig. 7 Viral infection induces formation of transient AGO2 perinuclear aggregates

S2 cells treated with either control dsRNA or dsRNA targeting CCT1 were transfected with RFP-tagged AGO2-L or AGO2-S. The cells were then mock-treated or infected with DCV and imaged at 100x magnification for 16 hours with 10 minutes time points. **A.** Representative pictures of a single DCV infected cell imaged over 16 hours (0, 4, 8, 12, 16 hours time points) treated with either control (top) or CCT1 (bottom) dsRNA. **B.** Size tracking of the aggregates formed by AGO2-L in cells mock-treated or infected with DCV. Control (left) or CCT1 (right) dsRNA. **C.** Plot showing fractional fluorescence recovery of aggregates formed by either AGO2-L or AGO2-S in DCV infected cells. (*P value < 0.05; **P value < 0.01; ***P value < 0.001). Graphs are the result of at least two independent experiments.

AGO2-L (Fig. 7C). Additionally, FHV-B2-GFP did not colocalize with AGO2-S in DCV-infected cells (Fig. S5). Therefore, the aggregates formed by AGO2-L and AGO2-S upon infection appears to correspond to different structures.

Overall, these results suggest that the GRR domain grants AGO2-L increased efficiency to localize in the vicinity of a processed vdsRNA. This makes AGO2-L the preferential target for vsiRNA duplex loading. Further, the TRiC/CCT complex participates in antiviral immunity by regulating the dynamics of intracellular localization of AGO2-L.

Fig. 8

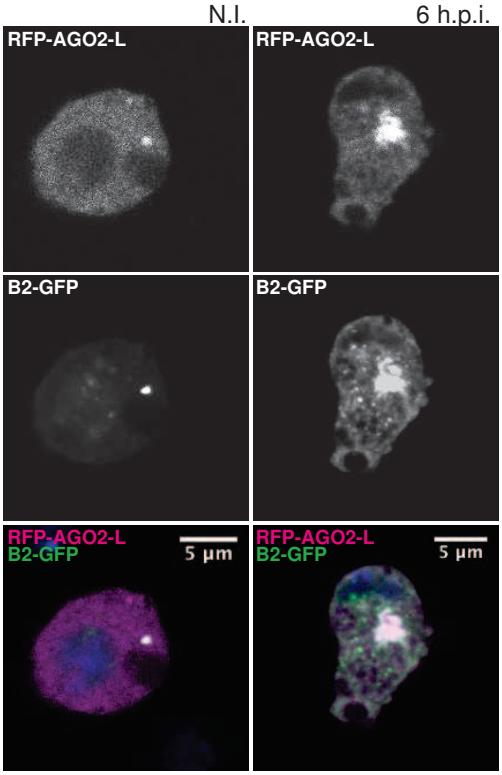
N.I.
6 h.p.i.
RFP-AGO2-L
RFP-AGO2-L
B2-GFP
B2-GFP
RFP-AGO2-L
B2-GFP
5 µm
RFP-AGO2-L
B2-GFP
5 µm

Fig. 8 AGO2-L colocalizes with the dsRNA binding protein B2 in DCV infected cells.

Representative pictures of S2 cells, either non-infected or 6 hours post DCV infection, co-transfected with RFP-AGO2-L and FHV-B2-GFP. Pictures representative of two independent experiments.

III Discussion

1. The TRiC/CCT complex dynamically regulates AGO2 antiviral activity

We used a broad proteomic approach to identify novel host factors interacting with Dcr-2, R2D2, and AGO2 and involved in the control of viral replication in *Drosophila*. The GO term analysis of the recovered interactants revealed prevalence of factors involved in translation and protein folding. The subsequent RNAi screen identified the TRiC/CCT complex as an important player in antiviral immunity. The TRiC/CCT complex has been involved in the folding of several crucial cellular components such as cytoskeletal proteins (Yaffe et al. 1992; Vinh & Drubin 1994), telomerase (Freund et al. 2014) and, more generally, large multidomain proteins and aggregation-prone proteins (Rüßmann et al. 2012; Yam et al. 2008; Tam et al. 2006). The interaction of the subunit CCT1 with AGO2 observed by immunoprecipitation and the effect of the whole complex on viral replication suggest two possible mode of action for the TRiC/CCT complex. First, it may exert a function similar to other chaperone proteins already shown to interact with AGO2. Indeed, the Hsc70/Hsp90 machinery has been reported to be essential for an efficient loading of the small RNA duplex produced by Dcr-2 (Iwasaki et al. 2010). Second, the long GRR domain of AGO2 may put into play the role of the TRiC/CCT complex in folding Gln-rich proteins (Tam et al. 2006). Given the low-complexity and aggregation-prone nature of this region, the TRiC/CCT complex might be necessary to prevent aggregation of AGO2-L, thus limiting the availability of the protein for the control of viruses.

Since depletion of different subunits of the TRiC/CCT complex have no effect on the silencing of an exogenous long dsRNA, we can exclude a role similar to the one described by the group of Y. Tomari (Iwasaki et al. 2010). Our data also indicate that the effect of the TRiC/CCT complex on AGO2 does not depend on its folding activity. Indeed,

knockdown of CCT1 does not impact the amount of either AGO2-L or AGO2-S. Rather, we found that the TRiC/CCT complex regulates the cellular distribution of AGO2 in a GRR dependent manner. Furthermore, our FRAP experiment confirmed that the granules formed by AGO2-L in the cytoplasm of S2 cells are not mere aggregates but dynamic structures under the control of the TRiC/CCT complex.

Taken together, these results suggest a novel role for the TriC/CCT chaperonin complex in antiviral RNAi.

2. The GRR domain is essential for AGO2 efficient antiviral response

The structure and function of the domains of AGO2 important for its catalytic activity have been characterized in detail (Jinek & Doudna 2009; MacRae 2008; Kwak & Tomari 2012). The N, MID, PAZ and PIWI domains are remarkably conserved throughout evolution, therefore, most of the inter-species variability of AGO2 proteins comes from non-catalytic regions (Obbard et al. 2006). In this regard, arthropods are remarkable, as the amino-terminal region of AGO2 in this group of animals is extremely large (up to 40% of the entire peptide sequence), variable in length and of low complexity (Hain et al. 2010). Recently the group of D. Obbard showed that the GRR domain of several insect species, while extremely variable in length, has a similar amino acid composition, enriched in Gln and Gly residues (Palmer & Obbard 2016). The same study also showed a slight association of some GRR haplotypes with better survival to DCV infection. Our results, which still have to be confirmed in vivo, now suggest that of the two AGO2 isoforms expressed by *D. melanogaster*, the one containing the GRR domain (AGO2-L) is the most active to control viral infection. Our analysis of the small RNAs bound to the two AGO2 isoforms further revealed that vsiRNA preferentially associates with AGO2-L.

Endo-siRNAs also associates mainly with AGO2-L in non-infected cells, but are predominantly found in AGO2-S following viral infection, suggesting they are outcompeted by vsiRNAs.

AGO2-L and AGO2-S differ exclusively by the presence of the GRR domain. Both AGO2 isoforms contain all the domains necessary for the catalytic activity. Therefore, it does not come as a surprise that *in vitro* data (Liu et al. 2009) showed that an AGO2 protein lacking the GRR domain is perfectly capable of performing loading, passenger strand ejection and target cleavage. I confirmed these results *in vivo*, since AGO2-S is fully capable of silencing a luciferase target gene in cells treated with dsRNA. My findings therefore raise the question of why the GRR domain is needed in the context of an antiviral response.

3. Phase separated cellular bodies and antiviral RNA silencing

Several studies (Lin et al. 2015; Nott et al. 2015; Elbaum-Garfinkle et al. 2015; Molliex et al. 2015; Jain et al. 2016) reported the ability of proteins containing Intrinsically Disordered Regions (IDRs) to form phase-separated liquid droplets in the cytoplasm. Interestingly, a high number of RNA-binding proteins contain IDRs (Kato et al. 2012; Lin et al. 2015; Jain et al. 2016). More and more evidence points to IRDs in RNA-binding proteins and to RNA itself as the driving force that initiate the formations of non membranous cytoplasmic structure such as P-bodies and stress granules (Kato et al. 2012; Molliex et al. 2015). A recent model proposed that, following an event such as inhibition of translation initiation, the amount of untranslated RNA bound to different RNA-binding proteins, increases. The increased local concentration of IRDs and RNA triggers the phase separation, thus initiating the formation of a stress granule (Jain et al. 2016). Of special interest, in the same work, the authors reported that the TRiC/CCT

complex plays a role in preventing the phase separation. Further, the authors also noted that the mammalian and yeast homologs of *Pontin* and *Reptin* (Ruvbl1 and 2), two genes that affected viral replication in our RNAi screen and whose products were identified in our interactome analysis, also play a role in preventing disassembly of phase separated droplets.

In the context of viral infection, an excess of viral RNA is produced in cellular compartments known as viral factories (Jose et al. 2009; Kopek et al. 2007). This excess of RNA, including replicating dsRNA as well as RNA-binding proteins from the host, could form phase-separated droplets where it can be sensed and processed by Dcr-2, and loaded onto AGO2. Since phase-separated droplets can effectively recruit proteins containing IDRs (Lin et al. 2015), AGO2-L, but not AGO2-S, would preferentially be loaded with the vsiRNAs. Once loaded, AGO2-L has to dissociate to bind and cleave the target single stranded viral RNA, possibly at the level of translation (Iwasaki et al. 2009). My results indicate that the TRiC/CCT complex participates in this dissociation step and to the dynamic relocalization of AGO2-L.

Because immunity related genes are generally fast-evolving genes, it has been speculated that the high variability of the GRR domain could be related to an evolutionary arms race between viral suppressor mechanisms and host proteins (Hain et al. 2010). However, it has also been proposed that the variability of the GRR domain could be the result of low selective constraint on this region (Palmer & Obbard 2016). Our data provide an explanation for the antiviral function of the GRR domain. The Gln repeats in the N-terminal domain give AGO2-L the ability to efficiently localize in proximity of processed vdsRNA. As long as the structure of this region remains intrinsically disordered it does not require any specific amino acid sequence. Therefore,

Fig. 9

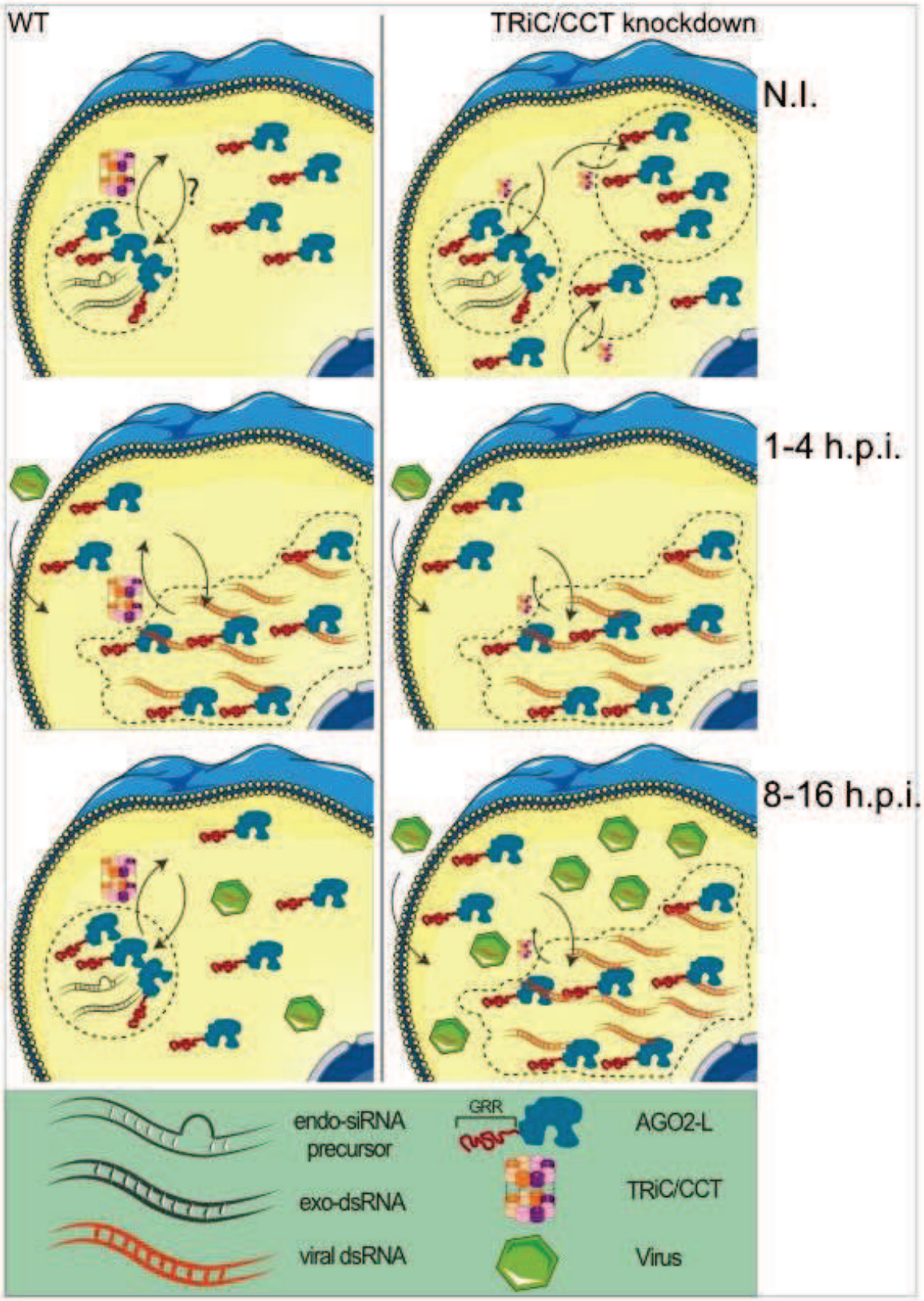

Fig. 9 A model for the involvement of the TriC/CCT complex in the regulation of AGO2 activity.

we propose that the high variability of the GRR domain is the result of low selective constraint rather than a pathogen driven selection.

4. A model for the antiviral action of AGO2 in the cellular context

In summary, the results I obtained during my PhD lead me to propose the following model for the antiviral role of AGO2 in infected cells. In non-infected (Fig. 9, top) condition, AGO2 localizes to granular structures together with dsRNA and presumably other RNA forms (Fig. 7B). The disruption of the TRiC/CCT complex alters the dynamics of the cytoplasmic diffused and granular AGO2 leading to the formation of larger and more numerous granules, as shown in Fig. 4A. Upon viral infection (Fig. 9, middle), cells with a functional TRiC/CCT complex and cells where the complex is disrupted behave in a similar fashion forming large AGO2 aggregates. At this stage, AGO2 occupies the same cellular compartment as the replicating virus, thus facilitating the loading of vsiRNA. Following vsiRNA loading, the TRiC/CCT complex mediates the dissociation (Fig. 9, bottom) of AGO2 molecules from the aggregates allowing binding and cleavage of their target. If the TRiC/CCT complex is disrupted, AGO2 remains stuck in the aggregate thus impairing an efficient silencing.

This model can now be tested. An obvious experiment that comes to mind involves monitoring by live imaging of the replication of different viruses. If our hypothesis is correct, the aggregates formed by AGO2-L would locate to different compartments depending on the place where the virus replicates. For example, we would expect to see a recruitment of AGO2-L to mitochondria in FHV infected cells (Ertel et al. 2017). It would also be interesting to study the impact of silencing *Pontin* and *Reptin* on the AGO2-L aggregates, as these two proteins were reported to have opposite effects compared to the TriC/CCT complex on the formation of SGs (Jain et al. 2016). Finally,

our data on the dynamics of AGO2 in infected cells raise fascinating questions regarding the mechanism involved in the active relocalization of the protein during infections. To address this question, it will be important to take into account two key facts brought forward by this thesis, namely that (i) the two isoforms of AGO2 have different functions and one should focus on AGO2-L in the context of viral infection; and (ii) much can be learned by studying the interactome at different stages of the viral infection, e.g. in the case of DCV infection 4hpi when the aggregates form and 12hpi when they resolve.

IV Matherials and methods

Molecular cloning

cDNAs from the Dcr-2, AGO2 and r2d2 genes were amplified by standard PCR and inserted into a pDONR221 vector (Invitrogen) using the Gateway® cloning technology (see Primers table). The PCR fragments were recombined (BP reaction) with pDONR221 to obtain pDONR221-Dcr-2, pDONR221-AGO2 and pDONR221-r2d2 and sequenced. pDONR221 clones were recombined (LR reaction) with pDEST vectors (pAGW, pARW (Drosophila Genomics Resource Center)) to obtain the final expression clones. The plasmid containing the shRNA targeting the PIWI domain of the AGO2 gene (TRiP.HMS00108) was constructed by annealing the two oligos pre-designed by the TRiP project (http://www.flyrnai.org/TRiP-TTR.html) (Ni et al., 2011) (see Table) and flanked by SpeI and EcoRI restriction sites and ligating them between the corresponding sites of the Drosophila pMT-V5His vector (Invitrogen).

The AGO2 variants (AGO2-L/S-shR) resistant to the shRNA were constructed by site directed mutagenesis using the QuikChange® Site-Directed Mutagenesis Kit (Agilent). A wild-type AGO2 cDNA clone (ORF from DmAGO2 cloned in pDONR221) was used as a template for the PCR using the mismatched primers listed in the Primers Table. The DONOR clones were verified by sequencing, and then recombined using the Gateway LR reaction to pAGW or pARW plasmids to express with the Actin5C promoter N-terminally GFP tagged versions of AGO2. The same DONOR clones were used to generate plasmids ready to inject in fly embryos (Genetic Services), for transgenesis based on the phiC31 system. The resulting vectors express RACK1 with an N-terminal HA tag, from the HSP promoter.

dsRNAs

Primers harboring the T7 polymerase sequence were designed. The primers (Table primers) were then used to generate template DNA for each gene of interest by PCR on complementary DNA (cDNA). Template size ranged from 300 to 600 nucleotides. The templates were verified on agarose gels for correct sizes. *In vitro* T7 polymerase transcription was then used to generate dsRNAs, which was then quality-controlled on agarose gel. dsRNAs were then used to reverse-soak S2 cells. Cells were kept with the dsRNA in media without serum for 1 hour. Complete medium was then added and cells were incubated for 4 days at 25°C to achieve efficient silencing.

Cell lines and transfections

Stable cell lines were generated by limiting dilution method. The plasmid carrying the gene of interest and a plasmid carrying a puromycin resistance gene were co-transfected in Drosophila S2 cells (Invitrogen) using the $CaPO_4$ precipitation method. Two day after transfection the selection agent (Puromycin, Sigma) was added to the culture media. Following two to three weeks of selective pressure, clones giving moderate and stable expression profiles were selected and characterized by western blot for the expression of the tagged proteins.

Luciferase assay

Cells were reverse soaked with dsRNA targeting Tcp-1, CCTγ, AGO2 or GFP. Plasmids

expressing Firefly luciferase and Renilla luciferase were co-transfected in S2 cells with a 1:5 ratio, respectively. The following day, cells were reverse soaked with dsRNA carrying the sequence of Renilla luciferase. 48-hour later cells were lysed and luciferase activity was measured with the Promega dual-luciferase assay, using a Berthold Luminometer.

To assess the silencing activity in shAGO2 stable cell lines, the two luciferase plasmids were co-transfected with either AGO2-L-shR or AGO2-S-shR using Effectene® transfection reagent (Qiagen). Extraction and luciferase activity mesure was carried out as described above.

Immunostaining

48 hours following transfection with fluorescently tagged constructs, S2 cells were fixed in 2% PFA. If immunostaining was required, fixed cells were incubated in a PBS-TritonX-BSA solution for 1h followed by incubation with primary antibody overnight. The following day fluorophore conjugated secondary antibody was added and the microscope slides were mounted with Vectashield® mounting media.

Virus infection and titration

Virus infection on S2 cells was performed as follows: the virus stock was diluted to the appropriate Multiplicity Of Infection (MOI) in culture media and added on the cells. Cells were incubated 1 hour at 4 °C (with gentle shaking every 10 min) to allow binding of the virus to the cells but not endocytosis synchronizing the infection. The virus-media solution was then removed, replaced by fresh culture media and incubated at 25 °C. Different MOIs were used depending on the virus: DCV MOI=1, FHV MOI=0,5, VSV MOI=10. After 16 hours of infection for DCV, 48 hours for FHV and 72 hours for VSV cells were lysed for RNA or viral particles extraction. RNA was purified using the NucleoSpin®RNA (Macherey-Nagel) extraction kit, quantified and used for retro-transcription (RT) reaction followed by qPCR.

The viral particles were extracted from the infected cells with multiple cycles of freeze-thaw in a dry ice bath. The viral suspension was then titrated in a series of 1:10 dilutions.

DCV viral particles dilutions were then used to re-infect KC167 cells in 96 well plates, 72 hours after the cells were fixed in 4% PFA and immunostained with an antibody targeting the DCV capsid protein. The $TCID_{50}$ was then measured using four wells of the 96 well plates for each dilution; a well was considered positive for the infection if at least 10 single cells were stained by the antibody.

VSV viral particles dilutions were used to re-infect Vero R cells in a 24 well plate, 48 hours after cells were stained with crystal violet and the lithic plaques were quantified.

Protein analysis and immunoprecipitation

Cells were lysed in Protein Extraction Buffer (30 mM Tris-HCl, pH7.5, 150 mM NaCl, 2 mM MgCl2, 1% NP40 2x Complete Protease Inhibitor Cocktail EDTA free from Roche). Lysates were kept on ice for 30 min then centrifuged at 13,000 rpm for 30 min at 4°C.

Supernatants were quantified with Bradford reagent, mixed with LDS sample buffer (LifeTechnologies) and run on SDS-PAGE. Separated proteins were then transferred on nitrocellulose membrane and blotted with the appropriate antibody.

For NATIVE-PAGE, cells were lysed in a detergent-free buffer following the manufacturer protocol: https://tools.thermofisher.com/content/sfs/manuals/MAN0007893_NativePAGE_BisTris_Gels.pdf.

GFP or RFP tagged proteins were immunoprecipitated using the GFP/RFP-Trap®-coupled agarose beads from Chromotek, following the protocol provided by the manufacturer.

Northern blotting

GFP tagged AGO2-L/s were immunoprecipitated and the associated small RNAs wer extracted using Trizol reagent (Euromedex). Purified small RNAs were run on a highly resolutive, denaturing polyacrylamide gel (15% bis/tris acrylamide, 8% Urea, 1x TBE). Separated small RNAs were then blotted on a neutrally charged nylon membrane (Hybond™, GE-Healthcare), chemically crosslinked with a Methilimidazole solution (Sigma) and hybridized with DCV or esi-2.1 overnight in PertfectHyb™ buffer. The following day the membrane was washed in washing buffer (2%SDS, 2%SSC) and exposed on Autoradiography films (Hyperfilm™, GE-Healthcare) for 24-72 hours before being developed.

Proteins contained in the organic fraction of the Trizol reagent were precipitated by addition of -20 °C 100% acetone and run on SDS-PAGE.

FRAP and live imaging

S2 cells were transfected with GFP/RFP tagged proteins. 48 hours after cells were diluted to ~1 mil/ml and transferred to ibiTreat multi-chambered slides for live imaging pre-coated with concanavilin-A (100 µg/ml) for optimal cell adhesion. For overnight tracking of the infection, cells were infected as described above with the timecourse starting 0-30 min after adding the fresh media.

Using a 100x oil immersion objective a region corresponding to the size of the granule/aggregate was bleached for 50-200 ns (depending on the size) using a laser intensity of 100% at 488 nm (GFP). Recovery was recorded for 400 timepoints (50 ms interval, 20 s total) or 600 time points (1 s interval, 10 minutes total) after bleaching. Analysis of the recovery curve was carried out as previously described (Patel et al. 2015). Half time recovery was calculated with the macro http://imagej.net/Analyze_FRAP_movies_with_a_Jython_script using Fiji/ImageJ. The relative fluorescence intensity at each time point was calculated using Fiji/ImageJ and plotted over the time course of the movie, using Prism (graphpad).

Table 1. Primers and oligos

Ref	Gene	Sequence	
OJL2549	CCT1 fw T7	taatacgactcactatagggCTGGCTCAGCTGCAGGAC	dsRNA
OJL2550	CCT1 rv T7	taatacgactcactatagggCACGGGGATCTGTGATTTTC	
OJL3054	CCT3 fw T7	taatacgactcactatagggGGACATGAACGTGAAGAACAT	
OJL3055	CCT3 rv T7	taatacgactcactatagggTCCTTCTTCCAGAGAAGCCAA	
OJL3058	CCT2 fw T7	taatacgactcactatagggTGGGCATCACCGAGTCGTTCG	
OJL3059	CCT2 rv T7	taatacgactcactatagggTCGCAGCACTCATCCTCGAAT	
OJL3062	CCT6 fw T7	taatacgactcactatagggTGGGCGTCTACGACAACTACA	
OJL3063	CCT6 rv T7	taatacgactcactatagggGAATACTTGCAGCCGCAACCA	
OJL3070	CCT5 fw T7	taatacgactcactatagggCGCCCAGTGCGCCATCAAGCA	
OJL3071	CCT5 rv T7	taatacgactcactatagggGGCTCAAACGGGCAGGTGAGA	
OJL3076	CCT8 fw T7	taatacgactcactatagggGAAGGCAAAGCTCTTCGATCT	
OJL3077	CCT8 rv T7	taatacgactcactatagggAATACAAGAAACTGTGTGCAT	
OJL3177	CCT7 fw T7	taatacgactcactatagggCCGTCCAAATTGTCGAACAG	
OJL3178	CCT7 rv T7	taatacgactcactatagggAGCTCCAATTCGATGTTGAG	
OJL3181	CCT4 fw T7	taatacgactcactatagggAAACAGATGTCCACTCCCAT	
OJL3182	CCT4 rv T7	taatacgactcactatagggACTGGATAAGACCGATCTTG	
OJL1569	AGO2 fw	taatacgactcactatagggcgctacacgatcgaaatcaa	
OJL1642	AGO2 rv	taatacgactcactatagggtatacccttggagcgctttg	
OJL2330	CCT1 fw	CTCCGCTCCTACCACAACTC	qPCR
OJL2331	CCT1 rv	GATCCAGACCGGTCCACTTA	
OJL3114	CCT3 fw	ATACTCGTGTTGAGTCAAAA	
OJL3115	CCT3 rv	TGTTCTCCAACTGCACTTTG	
OJL3102	CCT2 fw	AAGCTGCACCCACAGATCAT	
OJL3103	CCT2 rv	CTCCAGTGCCACCTGGGTGG	
OJL3175	CCT6 fw	CCTGATCAACCAGAAGGGCA	
OJL3176	CCT6 rv	ATGCCCTCCTTGGCCAGGGC	
OJL3112	CCT5 fw	ATTTAGGATCAGTCGTTCGT	
OJL3113	CCT5 rv	CAAGATTTAATTCCCGAGTT	
OJL3104	CCT8 fw	CTATCGCAATGTGGAGAAGG	
OJL3105	CCT8 rv	TACTGCTTCGACATGATCGA	
OJL3173	CCT7 fw	CACAGCTAGTGTCGGGTGTG	
OJL3174	CCT7 rv	GGCCATTTCAAAGCCGGCAT	
OJL3110	CCT4 fw	CAAGAGCGCCTCCACCTCGT	
OJL3111	CCT4 rv	GCCAGCAGGCTGCTCTGCTG	
OJL1545	AGO2 fw	TGAGAACACAGGCAATCTTGA	
OJL1546	AGO2 rv	CATGTGGCACAGGTTGTAGG	
OJL3453	Sh AGO2 TRiP fwd	ctagcagtAACGACATCGAACAAGTTCAAtagttatattca agcataTTGAACTTGTTCGATGTCGTTgcg	shAGO2
OJL3454	Sh AGO2 TRiP rv	aattcgcAACGACATCGAACAAGTTCAAtatgcttgaatat aactaTTGAACTTGTTCGATGTCGTTactg	shAGO2
OJL3754	AGO2 SH-RES rv	gttccggggtccacgttgttaaatttgttgctggtcgttac gtcgccgctggg	mut
OJL3755	AGO2 SH-RES fw	cccagcggcgacgtaacgaccagcaacaaatttaacaacgt ggaccccggaac	mut

Table 2. Antibodies

Target	Animal	Ref.
anti-Tcp1 alpha	rat	[91a] (abcam)
Anti-GFP monoclonal	mouse	11814460001 (ROCHE)
Rabbit polyclonal to Ago2	rabbit	eIF2C2 ab5072 (abcam)
Anti Actin, clone C4	mouse	MAB1501R (MILLIPORE)
Anti-R2D2 antibody	rabbit	ab14750 (abcam)
anti-rat HRP	goat	A9037-1ML (Sigma)
AntiRabbit IgG HRP	goat	3918-8816-31 (rockland)
Mouse IgG, HRP Linked Whole AB	goat	M365FK (Fisher Scient.)

V Supplementary figures

Fig. S1

A

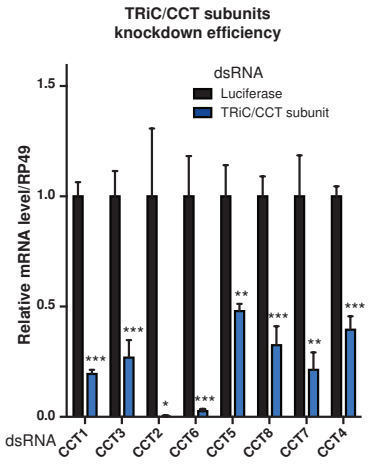

Fig. S1

A. Knockdown efficiency of the single TRiC/CCT subunit quantified by RT-qPCR on total RNA extract formS2 cells. **B.** Knockdown efficiency of CCT1, CCT3 and AGO2, respectively. Plots representative of two and three independent experiments, respectively.

B

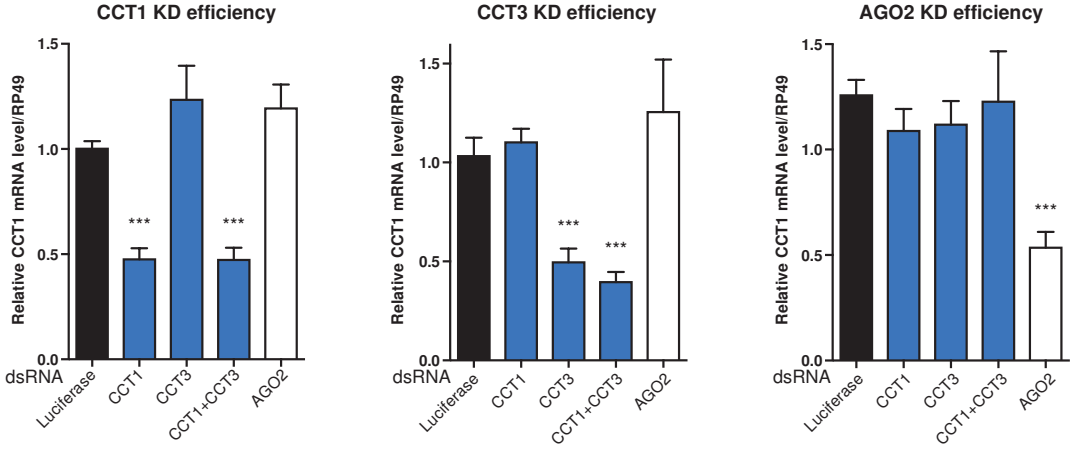

Fig. S2

A

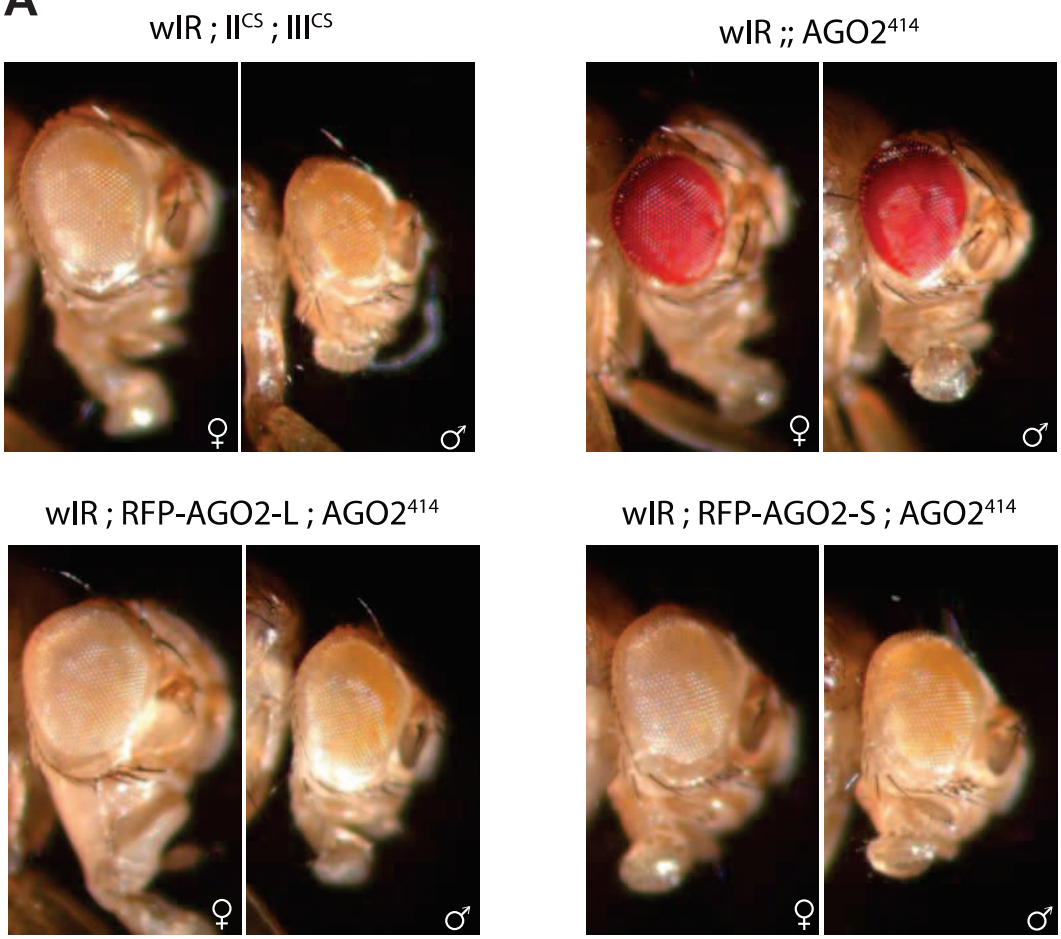

Fig. S2
Representative pictures of flies expressing the wIR transgene (Pham et al. 2004) either WT or carrying the AGO2414 mutation. Mutant flies were then rescued with constructs containing either RFP-AGO2-L or RFP-AGO2-S.

Fig. S3

A

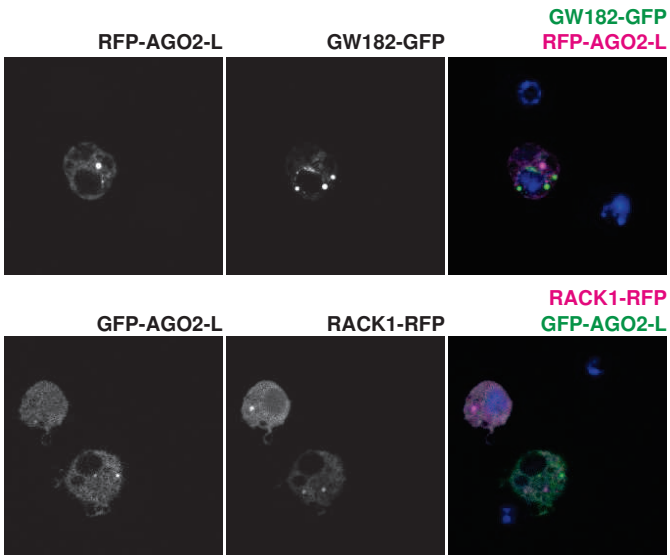

Fig. S3
A. (Top) Representative pictures of S2 cells co-transfected with GW182-GFP and RFP-AGO2-L **(Bottom)** Representative pictures of S2 cells co-transfected with RACK1-RFP and GFP-AGO2-L. Cells were treated with 20 mM H2O2 to induce the formation of stress granules. Representative of Two independent experiments. **B.** Bar chart showing the average t1/2 relative to figure 4C.

B

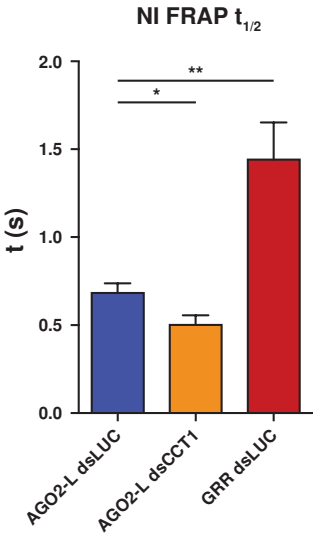

Fig. S4

A

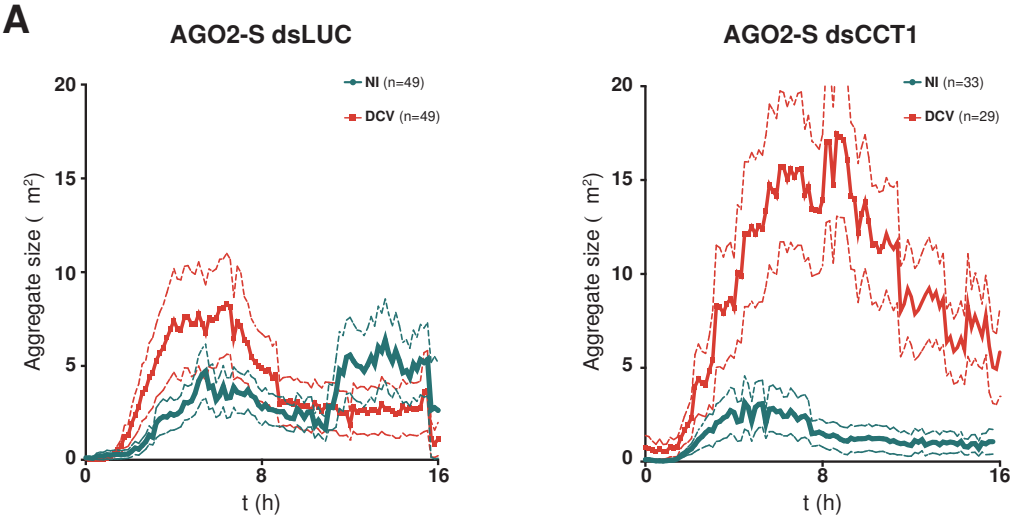

B

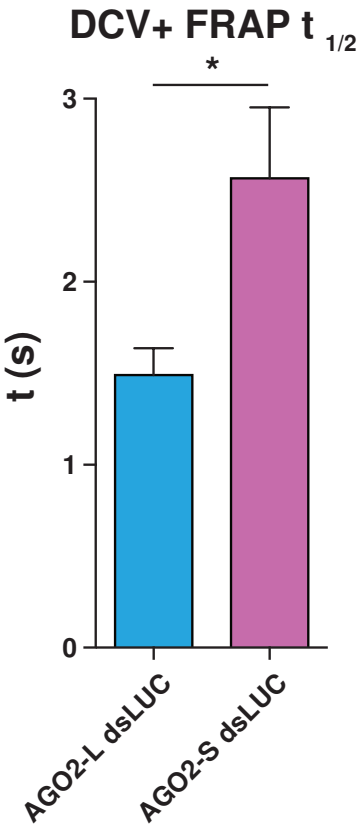

Fig. S4
A. Size tracking of the aggregates formed by AGO2-S in cells mock-treated or infected with DCV. Control **(left)** or CCT1 **(right)** dsRNA**. B.** Bar chart showing the average t1/2 relative to figure 7D.

Fig. S5

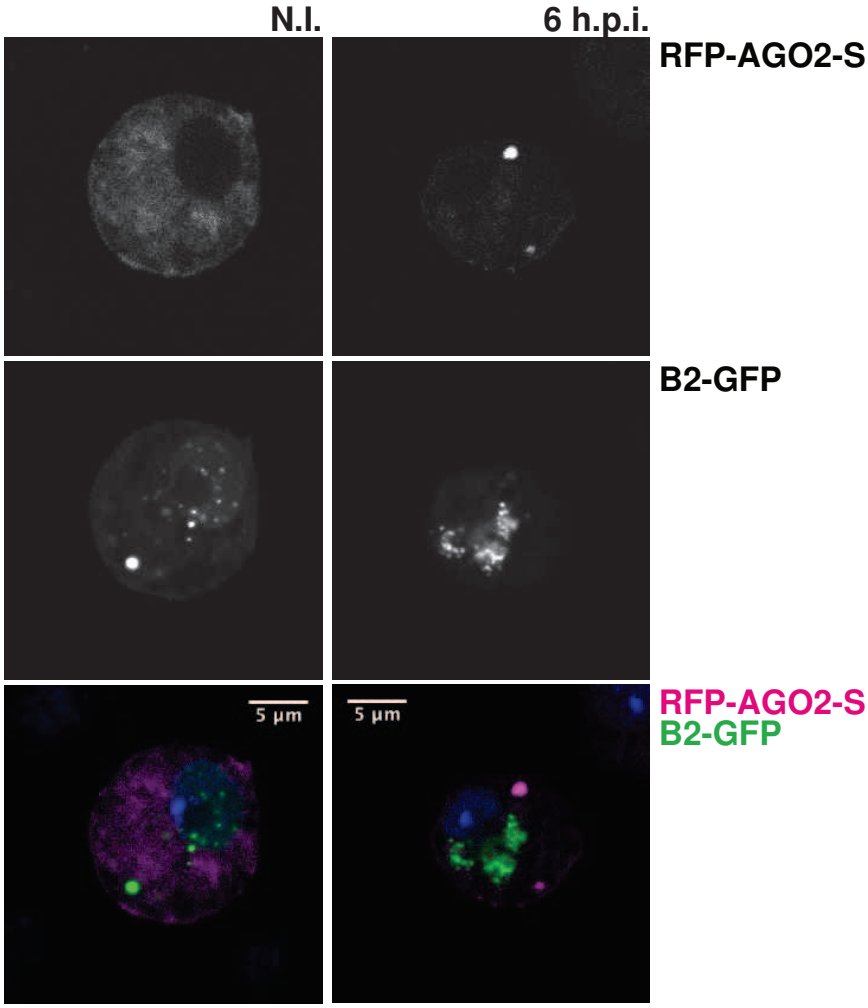

Fig. S5
Representative pictures of S2 cells, either non-infected or 6 hours post DCV infection, co-transfected with RFP-AGO2-S and FHV-B2-GFP. Pictures representative of one experiment.

VI Bibliography

Aliyari, R. et al., 2008. Mechanism of Induction and Suppression of Antiviral Immunity Directed by Virus-Derived Small RNAs in Drosophila. *Cell Host and Microbe*, 4(4), pp.387–397.
Ameres, S.L. et al., 2011. Target RNA-directed tailing and trimming purifies the sorting of endo-siRNAs between the two Drosophila Argonaute proteins. , 2, pp.54–63.
Aravin, A.A. et al., 2001. Double-stranded RNA-mediated silencing of genomic tandem repeats and transposable elements in the D. melanogaster germline. *Current Biology*, 11(13), pp.1017–1027.
Aravin, A., Lagos-Quintana, M. & Yalcin, A., 2003. The Small RNA Profile during *Drosophila melanogaster* Development. *Developmental cell*, 5, pp.337–350. Available at: http://www.ncbi.nlm.nih.gov/pubmed/12919683\nhttp://www.sciencedirect.com/science/article/pii/S1534580703002284.
Avadhanula, V. et al., 2009. A novel system for the launch of alphavirus RNA synthesis reveals a role for the Imd pathway in arthropod antiviral response. *PLoS Pathogens*, 5(9).
Avila, A. et al., 2002. The Drosophila Atypical Protein Kinase C-Ref(2)P Complex Constitutes a Conserved Module for Signaling in the Toll Pathway. *Molecular and Cellular Biology*, 22(24), pp.8787–8795. Available at: http://mcb.asm.org/cgi/doi/10.1128/MCB.22.24.8787-8795.2002.
Bohmert, K. et al., 1998. AGO1 defines a novel locus of Arabidopsis controlling leaf development. *EMBO Journal*, 17(1), pp.170–180.
Brackney, D.E. et al., 2010. C6/36 Aedes albopictus cells have a dysfunctional antiviral RNA interference response. *PLoS Neglected Tropical Diseases*, 4(10), pp.24–27.
Bradshaw, C.J.A. et al., 2016. Massive yet grossly underestimated global costs of invasive insects. *Nature Communications*, 7, p.12986. Available at: http://www.nature.com/doifinder/10.1038/ncomms12986.
Brennecke, J. et al., 2007. Discrete Small RNA-Generating Loci as Master Regulators of Transposon Activity in Drosophila. *Cell*, 128(6), pp.1089–1103.
Bronkhorst, A.W. et al., 2012. The DNA virus Invertebrate iridescent virus 6 is a target of the Drosophila RNAi machinery. *Proceedings of the National Academy of Sciences*, 109(51), pp.E3604–E3613.
Bronkhorst, A.W., Miesen, P. & van Rij, R.P., 2013. Small RNAs tackle large viruses: RNA interference-based antiviral defense against DNA viruses in insects. *Fly*, 7(4), pp.216–223.
Cao, C. et al., 2016. A Polymorphism in the Processing Body Component Ge-1 Controls Resistance to a Naturally Occurring Rhabdovirus in Drosophila. *PLoS Pathogens*, 12(1), pp.1–21.
Carthew, R.W. & Sontheimer, E.J., 2009. Origins and Mechanisms of miRNAs and siRNAs. *Cell*, 136(4), pp.642–655. Available at: http://dx.doi.org/10.1016/j.cell.2009.01.035.
Cenik, E.S. et al., 2011. Phosphate and R2D2 Restrict the Substrate Specificity of Dicer-2, an ATP-Driven Ribonuclease. *Molecular Cell*, 42(2), pp.172–184. Available at: http://dx.doi.org/10.1016/j.molcel.2011.03.002.
Chahar, H.S., Chen, S. & Manjunath, N., 2013. P-body components LSM1, GW182, DDX3, DDX6 and XRN1 are recruited to WNV replication sites and positively regulate viral replication. *Virology*, 436(1), pp.1–7. Available at: http://dx.doi.org/10.1016/j.virol.2012.09.041.
Chandradoss, S.D. et al., 2015. A Dynamic Search Process Underlies MicroRNA Targeting. *Cell*, 162(1), pp.96–107. Available at: http://dx.doi.org/10.1016/j.cell.2015.06.032.
Chao, J. a et al., 2005. Dual modes of RNA-silencing suppression by Flock House virus protein B2. *Nature structural & molecular biology*, 12(11), pp.952–957.
Cherry, S. et al., 2006. COPI activity coupled with fatty acid biosynthesis is required for viral replication. *PLoS Pathogens*, 2(10), pp.0900–0912.

Chung, W.J. et al., 2008. Endogenous RNA Interference Provides a Somatic Defense against Drosophila Transposons. *Current Biology*, 18(11), pp.795–802.
Contamine, D., Petitjean, A.M. & Ashburner, M., 1989. Genetic resistance to viral infection: the molecular cloning of a Drosophila gene that restricts infection by the rhabdovirus sigma. *Genetics*, 123(3), pp.525–533.
Coste, F. et al., 2012. Crystal structure of diedel, a marker of the immune response of drosophila melanogaster. *PLoS ONE*, 7(3), pp.1–8.
Cox, D.N. et al., 1998. A novel class of evolutionarily conserved genes defined by. *Genes & Development*, 12(23), pp.3715–3727.
Czech, B. et al., 2008. An endogenous small interfering RNA pathway in Drosophila. *Nature*, 453(7196), pp.798–802. Available at: http://www.ncbi.nlm.nih.gov/entrez/query.fcgi?cmd=Retrieve&db=PubMed&dopt=Citation&list_uids=18463631.
Czech, B. & Hannon, G.J., 2016. One Loop to Rule Them All: The Ping-Pong Cycle and piRNA-Guided Silencing. *Trends in Biochemical Sciences*, 41(4), pp.324–337. Available at: http://dx.doi.org/10.1016/j.tibs.2015.12.008.
Deddouche, S. et al., 2008. The DExD/H-box helicase Dicer-2 mediates the induction of antiviral activity in drosophila. *Nature immunology*, 9(12), pp.1425–1432.
Ding, S.-W., 2010. RNA-based antiviral immunity. *Nature reviews. Immunology*, 10(9), pp.632–644. Available at: http://dx.doi.org/10.1038/nri2824.
Ding, S.W. & Voinnet, O., 2007. Antiviral Immunity Directed by Small RNAs. *Cell*, 130(3), pp.413–426.
Dorner, S. et al., 2006. A genomewide screen for components of the RNAi pathway in Drosophila cultured cells. *Proceedings of the National Academy of Sciences of the United States of America*, 103(32), pp.11880–11885.
Dostert, C. et al., 2005. The Jak-STAT signaling pathway is required but not sufficient for the antiviral response of drosophila. *Nature immunology*, 6(9), pp.946–953.
Elbaum-Garfinkle, S. et al., 2015. The disordered P granule protein LAF-1 drives phase separation into droplets with tunable viscosity and dynamics. *Proceedings of the National Academy of Sciences of the United States of America*, 112(23), pp.7189–94. Available at: http://www.ncbi.nlm.nih.gov/pubmed/26015579.
Ertel, K.J. et al., 2017. Cryo-electron tomography reveals novel features of a viral rna replication compartment. *eLife*, 6, pp.1–24.
Filipowicz, W. & Sonenberg, N., 2015. The long unfinished march towards understanding microRNA-mediated repression. *Rna*, pp.519–524. Available at: http://rnajournal.cshlp.org/content/21/4/519.short.
Förstemann, K. et al., 2007. Drosophila microRNAs Are Sorted into Functionally Distinct Argonaute Complexes after Production by Dicer-1. *Cell*, 130(2), pp.287–297.
Freund, A. et al., 2014. Proteostatic control of telomerase function through TRiC-mediated folding of TCAB1. *Cell*, 159(6), pp.1389–1403. Available at: http://dx.doi.org/10.1016/j.cell.2014.10.059.
Fukuyama, H. et al., 2012. On-bead tryptic proteolysis: An attractive procedure for LC-MS/MS analysis of the Drosophila caspase 8 protein complex during immune response against bacteria. *Journal of Proteomics*, 75(15), pp.4610–4619. Available at: http://dx.doi.org/10.1016/j.jprot.2012.03.003.
Galiana-Arnoux, D. et al., 2006. Essential function in vivo for Dicer-2 in host defense against RNA viruses in drosophila. *Nature immunology*, 7(6), pp.590–7. Available at: http://www.ncbi.nlm.nih.gov/pubmed/16554838.
Gammon, D.B. & Mello, C.C., 2015. RNA interference-mediated antiviral defense in insects. *Current Opinion in Insect Science*, (8), pp.111–120.
Gerbasi, V.R. et al., 2011. Blanks, a nuclear siRNA/dsRNA-binding complex component, is required for Drosophila spermiogenesis. *Proceedings of the National Academy of Sciences of the United States of America*, 108(8), pp.3204–3209.
Ghildiyal, M. & Zamore, P.D., 2009. Small silencing RNAs: an expanding universe. *Nat Rev*

Genet, 10(2), pp.94–108. Available at: http://www.ncbi.nlm.nih.gov/pubmed/19148191.
Gibbings, D.J. et al., 2009. Multivesicular bodies associate with components of miRNA effector complexes and modulate miRNA activity. *Nature Cell Biology*, 11(9), pp.1143–1149. Available at: http://www.nature.com/doifinder/10.1038/ncb1929.
Gibbings, D.J. et al., 2009. Multivesicular bodies associate with components of miRNA effector complexes and modulate miRNA activity. *Nature cell biology*, 11(9), pp.1143–1149.
Goic, B. et al., 2016. Virus-derived DNA drives mosquito vector tolerance to arboviral infection. *Nature Communications*, 7, p.12410. Available at: http://www.nature.com/doifinder/10.1038/ncomms12410.
Goto, A. et al., 2003. Silencing of Toll pathway components by direct injection of double-stranded RNA into Drosophila adult flies. *Nucleic Acids Research*, 31(22), pp.6619–6623.
Grimson, A. et al., 2008. Early origins and evolution of microRNAs and Piwi-interacting RNAs in animals. *Nature*, 455(7217), pp.1193–1197. Available at: http://www.nature.com/doifinder/10.1038/nature07415.
Gubler, D.J., 2001. Human arbovirus infections worldwide. *Annals of the New York Academy of Sciences*, 951, pp.13–24.
Gubler, D.J., 1998. Resurgent vector-borne diseases as a global health problem. *Emerging infectious diseases*, 4(3), pp.442–50. Available at: http://www.ncbi.nlm.nih.gov/pubmed/9716967%5Cnhttp://www.pubmedcentral.nih.gov/articlerender.fcgi?artid=PMC2640300.
Gunawardane, L.S. et al., 2007. A slicer-mediated mechanism for repeat-associated siRNA 5' end formation in Drosophila. *Science*, 315(5818), pp.1587–1590. Available at: http://science.sciencemag.org/content/sci/315/5818/1587.full.pdf.
Guo, H.S. & Ding, S.W., 2002. A viral protein inhibits the long range signaling activity of the gene silencing signal. *The EMBO Journal*, 21(3), pp.398–407. Available at: http://emboj.embopress.org/cgi/doi/10.1093/emboj/21.3.398.
Hain, D. et al., 2010. Natural Variation of the Amino-Terminal Glutamine-Rich Domain in Drosophila Argonaute2 Is Not Associated with Developmental Defects. *PLoS ONE*, 5(12), pp.1–14.
Han, B.W. et al., 2015. piRNA-guided transposon cleavage initiates Zucchini-dependent, phased piRNA production. , 348(6236).
Harris, D.A. et al., 2011. Cargo sorting to lysosome-related organelles regulates siRNA-mediated gene silencing. *Journal of Cell Biology*, 194(1), pp.77–87.
Hartig, J.V. et al., 2009. Endo-siRNAs depend on a new isoform of loquacious and target artificially introduced, high-copy sequences. *The EMBO journal*, 28(19), pp.2932–44. Available at: http://emboj.embopress.org.emedien.ub.uni-muenchen.de/content/28/19/2932.abstract.
Hauptmann, J. et al., 2013. Turning catalytically inactive human Argonaute proteins into active slicer enzymes. *Nature structural & molecular biology*, 20(7), pp.814–7. Available at: http://www.ncbi.nlm.nih.gov/pubmed/23665583.
Hedges, L.M. & Johnson, K.N., 2008. Induction of host defence responses by Drosophila C virus. *Journal of General Virology*, 89(6), pp.1497–1501.
Hess, A.M. et al., 2011. Small RNA profiling of Dengue virus-mosquito interactions implicates the PIWI RNA pathway in anti-viral defense. *BMC Microbiology*, 11(1), p.45. Available at: http://bmcmicrobiol.biomedcentral.com/articles/10.1186/1471-2180-11-45.
Hopkins, K.C. et al., 2013. A genome-wide RNAi screen reveals that mRNA decapping restricts bunyaviral replication by limiting the pools of dcp2-accessible targets for cap-snatching. *Genes and Development*, 27(13), pp.1511–1525.
Horwich, M.D. et al., 2007. The Drosophila RNA Methyltransferase, DmHen1, Modifies Germline piRNAs and Single-Stranded siRNAs in RISC. *Current Biology*, 17(14),

pp.1265–1272.
Iwasaki, S. et al., 2015. Defining fundamental steps in the assembly of the Drosophila RNAi enzyme complex. *Nature*, 2. Available at: http://www.nature.com/doifinder/10.1038/nature14254.
Iwasaki, S. et al., 2010. Hsc70/Hsp90 chaperone machinery mediates ATP-dependent RISC loading of small RNA duplexes. *Molecular Cell*, 39(2), pp.292–299. Available at: http://dx.doi.org/10.1016/j.molcel.2010.05.015.
Iwasaki, S., Kawamata, T. & Tomari, Y., 2009. Drosophila Argonaute1 and Argonaute2 Employ Distinct Mechanisms for Translational Repression. *Molecular Cell*, 34(1), pp.58–67. Available at: http://dx.doi.org/10.1016/j.molcel.2009.02.010.
Jain, S. et al., 2016. ATPase-Modulated Stress Granules Contain a Diverse Proteome and Substructure. *Cell*, 164(3), pp.487–498. Available at: http://dx.doi.org/10.1016/j.cell.2015.12.038.
Jiang, F. et al., 2005. Dicer-1 and R3D1-L catalyze microRNA maturation in Drosophila. *Genes and Development*, 19(14), pp.1674–1679.
Jinek, M. & Doudna, J.A., 2009. A three-dimensional view of the molecular machinery of RNA interference. *Nature*, 457(7228), pp.405–412. Available at: http://www.nature.com/doifinder/10.1038/nature07755.
Jonas, S. & Izaurralde, E., 2015. Towards a molecular understanding of microRNA-mediated gene silencing. *Nature reviews. Genetics*, 16(7), pp.421–433. Available at: http://www.nature.com/nrg/journal/v16/n7/full/nrg3965.html?WT.ec_id=NRG-201507.
Jose, J., Snyder, J. & Kuhn, R., 2009. A structural and functional perspective of alphavirus replication and assembly. *Future Microbiol*, 4, p.30. Available at: file:///D:/INFORMACION/Downloads/nihms-145820.pdf.
Jupatanakul, N. et al., 2017. Engineered Aedes aegypti JAK/STAT Pathway-Mediated Immunity to Dengue Virus. *PLoS Neglected Tropical Diseases*, 11(1), pp.1–24.
Kalmykova, A.I., Klenov, M.S. & Gvozdev, V.A., 2005. Argonaute protein PIWI controls mobilization of retrotransposons in the Drosophila male germline. *Nucleic Acids Research*, 33(6), pp.2052–2059.
Kato, M. et al., 2012. Cell-free formation of RNA granules: Low complexity sequence domains form dynamic fibers within hydrogels. *Cell*, 149(4), pp.753–767. Available at: http://dx.doi.org/10.1016/j.cell.2012.04.017.
Kawamata, T., Seitz, H. & Tomari, Y., 2009. Structural determinants of miRNAs for RISC loading and slicer-independent unwinding. *Nature structural & molecular biology*, 16(9), pp.953–960. Available at: http://dx.doi.org/10.1038/nsmb.1630.
Kawamura, Y. et al., 2008. Drosophila endogenous small RNAs bind to Argonaute 2 in somatic cells. *Nature*, 453(June), pp.793–797.
Kemp, C. et al., 2013. Broad RNA interference-mediated antiviral immunity and virus-specific inducible responses in Drosophila. *J Immunol*, 190(2), pp.650–658. Available at: http://www.jimmunol.org/content/190/2/650.full.pdf.
Kemp, C. & Imler, J.L., 2009. Antiviral immunity in drosophila. *Current Opinion in Immunology*, 21(1), pp.3–9.
Khong, A. & Jan, E., 2011. Modulation of stress granules and P bodies during dicistrovirus infection. *Journal of virology*, 85(4), pp.1439–1451.
Kim, V.N., Han, J. & Siomi, M.C., 2009. Biogenesis of small RNAs in animals. *Nat Rev Mol Cell Biol*, 10(2), pp.126–139. Available at: http://www.ncbi.nlm.nih.gov/pubmed/19165215.
Kitamura, A. et al., 2006. Cytosolic chaperonin prevents polyglutamine toxicity with altering the aggregation state. *Nature cell biology*, 8(10), pp.1163–1170.
Kopek, B.G. et al., 2007. Three-dimensional analysis of a viral RNA replication complex reveals a virus-induced mini-organelle. *PLoS Biology*, 5(9), pp.2022–2034.
Ktistakis, N.T. & Tooze, S.A., 2016. Digesting the Expanding Mechanisms of Autophagy. *Trends in Cell Biology*, 26(8), pp.624–635. Available at:

http://dx.doi.org/10.1016/j.tcb.2016.03.006.
Kwak, P.B. & Tomari, Y., 2012. The N domain of Argonaute drives duplex unwinding during RISC assembly. *Nature structural & molecular biology*, 19(2), pp.145–51. Available at: http://dx.doi.org/10.1038/nsmb.2232.
Lambrechts, L. & Scott, T.W., 2009. Mode of transmission and the evolution of arbovirus virulence in mosquito vectors. *Proceedings of the Royal Society B: Biological Sciences*, 276(1660), pp.1369–1378. Available at: http://rspb.royalsocietypublishing.org/cgi/doi/10.1098/rspb.2008.1709.
Lamiable, O., Arnold, J., et al., 2016. Analysis of the contribution of hemocytes and autophagy to *Drosophila* antiviral immunity. *Journal of Virology*, 90(March), p.JVI.00238-16. Available at: http://jvi.asm.org/lookup/doi/10.1128/JVI.00238-16.
Lamiable, O., Kellenberger, C., et al., 2016. Cytokine Diedel and a viral homologue suppress the IMD pathway in *Drosophila*. *Proceedings of the National Academy of Sciences*, 113(3), p.201516122. Available at: http://www.pnas.org/lookup/doi/10.1073/pnas.1516122113.
Lee, Y.S., Pressman, S., Andress, A.P., et al., 2009. Silencing by small RNAs is linked to endosomal trafficking. *Nature Cell Biology*, 11(9), pp.1150–1156. Available at: http://www.nature.com/doifinder/10.1038/ncb1930.
Lee, Y.S., Pressman, S., Andress, A.P., et al., 2009. Silencing by small RNAs is linked to endosomal trafficking. *Nature cell biology*, 11(9), pp.1150–1156.
Leger, P. et al., 2013. Dicer-2- and Piwi-Mediated RNA Interference in Rift Valley Fever Virus-Infected Mosquito Cells. *Journal of Virology*, 87(3), pp.1631–1648. Available at: http://jvi.asm.org/cgi/doi/10.1128/JVI.02795-12.
Lewis, S.H., Salmela, H. & Obbard, D.J., 2016. Duplication and diversification of Dipteran Argonaute genes, and the evolutionary divergence of Piwi and Aubergine. *Genome Biol Evol*, 8(3), p.evw018-. Available at: http://gbe.oxfordjournals.org/content/early/2016/02/11/gbe.evw018.short?rss=1.
Lim, A.K. & Kai, T., 2007. to repress selfish genetic elements in Drosophila melanogaster. , 104(16), pp.6714–6719.
Lin, H. & Spradling, A., 1997. A novel group of pumilio mutations affects the asymmetric division of germline stem cells in the Drosophila ovary. *Development (Cambridge, England)*, 124(12), pp.2463–2476.
Lin, Y. et al., 2015. Formation and Maturation of Phase-Separated Liquid Droplets by RNA-Binding Proteins. *Molecular Cell*, 60(2), pp.208–219. Available at: http://dx.doi.org/10.1016/j.molcel.2015.08.018.
Liu, Q. et al., 2003. R2D2, a bridge between the initiation and effector steps of the Drosophila RNAi pathway. *Science (New York, N.Y.)*, 301(5641), pp.1921–1925.
Liu, X. et al., 2006. Dicer-2 and R2D2 coordinately bind siRNA to promote assembly of the siRISC complexes. *RNA (New York, N.Y.)*, 12(8), pp.1514–1520.
Liu, Y. et al., 2009. C3PO, an endoribonuclease that promotes RNAi by facilitating RISC activation. *Science (New York, N.Y.)*, 325(5941), pp.750–753.
Lopez, T., Dalton, K. & Frydman, J., 2015. The mechanism and function of group II chaperonins. *Journal of Molecular Biology*. Available at: http://linkinghub.elsevier.com/retrieve/pii/S0022283615002673.
MacRae, N.T.S. and I.J., 2008. The Crystal Structure of Human Argonaute2. *Science (New York, N.Y.)*, 321(5888), pp.572–5. Available at: http://www.ncbi.nlm.nih.gov/pubmed/18653896.
Magwire, M.M. et al., 2012. Genome-Wide Association Studies Reveal a Simple Genetic Basis of Resistance to Naturally Coevolving Viruses in Drosophila melanogaster. *PLoS Genetics*, 8(11).
Marques, J.T. et al., 2013. Functional Specialization of the Small Interfering RNA Pathway in Response to Virus Infection. *PLoS Pathogens*, 9(8).

Marques, J.T. et al., 2010. Loqs and R2D2 act sequentially in the siRNA pathway in Drosophila. *Nature structural & molecular biology*, 17(1), pp.24–30. Available at: http://dx.doi.org/10.1038/nsmb.1735.
Marques, J.T. & Imler, J.L., 2016. The diversity of insect antiviral immunity: Insights from viruses. *Current Opinion in Microbiology*, 32, pp.71–76.
Martins, N.E. et al., 2014. Host adaptation to viruses relies on few genes with different cross-resistance properties. *Proceedings of the National Academy of Sciences*, 111(16), pp.5938–5943. Available at: http://www.pnas.org/cgi/doi/10.1073/pnas.1400378111.
Meister, G., 2013. Argonaute proteins: functional insights and emerging roles. *Nature reviews. Genetics*, 14(7), pp.447–59. Available at: http://www.ncbi.nlm.nih.gov/pubmed/23732335.
Merkling, S.H., Bronkhorst, A.W., et al., 2015. The Epigenetic Regulator G9a Mediates Tolerance to RNA Virus Infection in Drosophila. *PLoS Pathogens*, 11(4), pp.1–25.
Merkling, S.H., Overheul, G.J., et al., 2015. The heat shock response restricts virus infection in Drosophila. *Scientific Reports*, 5, p.12758. Available at: http://www.nature.com/doifinder/10.1038/srep12758.
Messina, J.P. et al., 2014. Global spread of dengue virus types: Mapping the 70 year history. *Trends in Microbiology*, 22(3), pp.138–146. Available at: http://dx.doi.org/10.1016/j.tim.2013.12.011.
van Mierlo, J., van Cleef, K. & van Rij, R., 2011. Defense and Counterdefense in the RNAi-Based Antiviral Immune System in Insects. *Methods*, 721(8), pp.67–75. Available at: http://www.springerlink.com/index/10.1007/978-1-61779-037-9.
van Mierlo, J.T. et al., 2012. Convergent Evolution of Argonaute-2 Slicer Antagonism in Two Distinct Insect RNA Viruses. *PLoS Pathogens*, 8(8).
van Mierlo, J.T. et al., 2014. Novel Drosophila Viruses Encode Host-Specific Suppressors of RNAi. *PLoS Pathogens*, 10(7).
Miesen, P. et al., 2016. Small RNA Profiling in Dengue Virus 2-Infected Aedes Mosquito Cells Reveals Viral piRNAs and Novel Host miRNAs. *PLoS Neglected Tropical Diseases*, 10(2), pp.1–22.
Miesen, P., Girardi, E. & Van Rij, R.P., 2015. Distinct sets of PIWI proteins produce arbovirus and transposon-derived piRNAs in Aedes aegypti mosquito cells. *Nucleic Acids Research*, 43(13), pp.6545–6556.
Misof, B. et al., 2014. Phylogenomics resolves the timing and pattern of insect evolution. *Science*, 346(6210), pp.763–768. Available at: http://www.sciencemag.org/content/346/6210/763/suppl/DC1\nhttp://www.sciencemag.org/content/346/6210/763.full.html\nhttp://www.ncbi.nlm.nih.gov/Traces/wgs/?val=GAYP0.
Miyoshi, K. et al., 2010. Molecular mechanisms that funnel RNA precursors into endogenous small-interfering RNA and microRNA biogenesis pathways in Drosophila. *RNA (New York, N.Y.)*, 16(3), pp.506–15. Available at: http://www.pubmedcentral.nih.gov/articlerender.fcgi?artid=2822916&tool=pmcentrez&rendertype=abstract.
Mohn, F., Handler, D. & Brennecke, J., 2015. Noncoding RNA. piRNA-guided slicing specifies transcripts for Zucchini-dependent, phased piRNA biogenesis. *Science*, 348(6236), pp.812–817. Available at: http://science.sciencemag.org/content/sci/348/6236/812.full.pdf.
Molliex, A. et al., 2015. Phase Separation by Low Complexity Domains Promotes Stress Granule Assembly and Drives Pathological Fibrillization. *Cell*, 163(1), pp.123–133. Available at: http://dx.doi.org/10.1016/j.cell.2015.09.015.
Mueller, S. et al., 2010. RNAi-mediated immunity provides strong protection against the negative-strand RNA vesicular stomatitis virus in Drosophila. *Proceedings of the National Academy of Sciences of the United States of America*, 107(45), pp.19390–5. Available at:

http://www.pubmedcentral.nih.gov/articlerender.fcgi?artid=2984213&tool=pmcentrez&rendertype=abstract.
Nakanishi, K., 2016. Anatomy of RISC: how do small RNAs and chaperones activate Argonaute proteins? *Wiley Interdisciplinary Reviews: RNA*. Available at: http://doi.wiley.com/10.1002/wrna.1356.
Nayak, A. et al., 2010. Cricket paralysis virus antagonizes Argonaute 2 to modulate antiviral defense in Drosophila. *Nature structural & molecular biology*, 17(5), pp.547–54. Available at: http://dx.doi.org/10.1038/nsmb.1810.
Nishida, K.M. et al., 2013. Roles of R2D2, a Cytoplasmic D2 Body Component, in the Endogenous siRNA Pathway in Drosophila. *Molecular Cell*, 49(4), pp.680–691. Available at: http://dx.doi.org/10.1016/j.molcel.2012.12.024.
Nott, T.J. et al., 2015. Phase Transition of a Disordered Nuage Protein Generates Environmentally Responsive Membraneless Organelles. *Molecular Cell*, 57(5), pp.936–947. Available at: http://dx.doi.org/10.1016/j.molcel.2015.01.013.
Obbard, D.J. et al., 2006. Natural selection drives extremely rapid evolution in antiviral RNAi genes. *Current Biology*, 16(6), pp.580–585.
Obbard, D.J. et al., 2009. The evolution of RNAi as a defence against viruses and transposable elements. *Philosophical transactions of the Royal Society of London. Series B, Biological sciences*, 364(1513), pp.99–115. Available at: http://www.ncbi.nlm.nih.gov/pubmed/18926973.
Okamura, K. et al., 2011. R2D2 organizes small regulatory RNA pathways in *Drosophila*. *Molecular and Cellular Biology*, 31(4), pp.884–896.
Okamura, K., Chung, W.J., et al., 2008. The Drosophila hairpin RNA pathway generates endogenous short interfering RNAs. *Nature*, 453(7196), pp.803–806. Available at: http://www.ncbi.nlm.nih.gov/entrez/query.fcgi?cmd=Retrieve&db=PubMed&dopt=Citation&list_uids=18463630.
Okamura, K., Balla, S., et al., 2008. Two distinct mechanisms generate endogenous siRNAs from bidirectional transcription in Drosophila melanogaster. *Nat Struct Mol Biol*, 15(6), pp.581–590. Available at: http://www.ncbi.nlm.nih.gov/entrez/query.fcgi?cmd=Retrieve&db=PubMed&dopt=Citation&list_uids=18500351.
Okamura, K. & Lai, E.C., 2008. Endogenous small interfering RNAs in animals. *Nature reviews. Molecular cell biology*, 9(9), pp.673–8. Available at: http://www.pubmedcentral.nih.gov/articlerender.fcgi?artid=2729316&tool=pmcentrez&rendertype=abstract.
Olovnikov, I. et al., 2013. Bacterial Argonaute Samples the Transcriptome to Identify Foreign DNA. *Molecular Cell*, 51(5), pp.594–605. Available at: http://dx.doi.org/10.1016/j.molcel.2013.08.014.
Palmer, W.H. & Obbard, D.J., 2016. Variation and Evolution in the Glutamine-Rich Repeat Region of Drosophila Argonaute-2. *G3: Genes|Genomes|Genetics*, 6(8), pp.2563–2572. Available at: http://g3journal.org/cgi/doi/10.1534/g3.116.031880.
Pan American Health Organization / World Health Organization. Zika Epidemiological Update, 25 May 2017, 2017. Zika - Epidemiological Update. , (May).
Paradkar, P.N. et al., 2014. Dicer-2-Dependent Activation of Culex Vago Occurs via the TRAF-Rel2 Signaling Pathway. *PLoS Neglected Tropical Diseases*, 8(4).
Paradkar, P.N. et al., 2012. Secreted Vago restricts West Nile virus infection in Culex mosquito cells by activating the Jak-STAT pathway. *Proceedings of the National Academy of Sciences*, pp.1–6.
Patel, A. et al., 2015. A Liquid-to-Solid Phase Transition of the ALS Protein FUS Accelerated by Disease Mutation. *Cell*, 162(5), pp.1066–1077. Available at: http://dx.doi.org/10.1016/j.cell.2015.07.047.
Petit, M. et al., 2016. piRNA pathway is not required for antiviral defense in *Drosophila melanogaster*. *Proceedings of the National Academy of Sciences*, 113(29), pp.E4218–

E4227. Available at:
http://www.pnas.org/lookup/doi/10.1073/pnas.1607952113.
Pham, J.W. et al., 2004. A Dicer-2-dependent 80S complex cleaves targeted mRNAs during RNAi in Drosophila. *Cell*, 117(1), pp.83–94.
Van Rij, R.P. et al., 2006. The RNA silencing endonuclease Argonaute 2 mediates specific antiviral immunity in Drosophila melanogaster. *Genes and Development*, 20(21), pp.2985–2995.
Rüßmann, F. et al., 2012. Folding of large multidomain proteins by partial encapsulation in the chaperonin TRiC/CCT. *Proceedings of the National Academy of Sciences of the United States of America*, 109(52), pp.21208–15. Available at:
http://www.pubmedcentral.nih.gov/articlerender.fcgi?artid=3535605&tool=pmcentrez&rendertype=abstract.
Sabin, L.R., Delás, M.J. & Hannon, G.J., 2013. Dogma Derailed: The Many Influences of RNA on the Genome. *Molecular Cell*, 49(5), pp.783–794.
Saito, K. et al., 2007. Pimet, the \textit{Drosophila} homolog of HEN1, mediates \textit{2′}-O-methylation of Piwi- interacting RNAs at their 3′ ends. *Genes Dev*, 21(13), pp.1603–1608.
Saito, K. et al., 2005. Processing of pre-microRNAs by the Dicer-1-Loquacious complex in drosophila cells. *PLoS Biology*, 3(7), pp.1202–1212.
Saleh, M.-C. et al., 2009. Antiviral immunity in Drosophila requires systemic RNA interference spread. *Nature*, 458(7236), pp.346–350. Available at:
http://www.nature.com/doifinder/10.1038/nature07712.
Shelly, S. et al., 2009. Autophagy Is an Essential Component of Drosophila Immunity against Vesicular Stomatitis Virus. *Immunity*, 30(4), pp.588–598. Available at:
http://dx.doi.org/10.1016/j.immuni.2009.02.009.
Sienski, G., Dönertas, D. & Brennecke, J., 2012. Transcriptional silencing of transposons by Piwi and maelstrom and its impact on chromatin state and gene expression. *Cell*, 151(5), pp.964–980.
Siomi, M.C. et al., 2011. PIWI-interacting small RNAs: the vanguard of genome defence. *Nature Reviews Molecular Cell Biology*, 12(4), pp.246–258. Available at:
http://www.nature.com/doifinder/10.1038/nrm3089.
Siomi, M.C., Saito, K. & Siomi, H., 2008. How selfish retrotransposons are silenced in Drosophila germline and somatic cells. *FEBS Letters*, 582(17), pp.2473–2478.
Song, J.-J., 2004. Crystal Structure of Argonaute and Its Implications for RISC Slicer Activity. *Science*, 305(5689), pp.1434–1437. Available at:
http://www.sciencemag.org/cgi/doi/10.1126/science.1102514.
Souza-Neto, J.A., Sim, S. & Dimopoulos, G., 2009. An evolutionary conserved function of the JAK-STAT pathway in anti-dengue defense. *Proceedings of the National Academy of Sciences*, 106(42), pp.17841–17846. Available at:
http://www.pnas.org/cgi/doi/10.1073/pnas.0905006106.
Tabara, H. et al., 1998. RNAi in C . elegans : Soaking in the Genome Sequence. , 282(5388), pp.430–431.
Tabara, H. et al., 1999. The rde-1 gene, RNA interference, and transposon silencing in C. elegans. *Cell*, 99(2), pp.123–132.
Tam, S. et al., 2006. The chaperonin TRiC controls polyglutamine aggregation and toxicity through subunit-specific interactions. *Nature cell biology*, 8(10), pp.1155–1162.
Thomson, T. & Lin, H., 2009. The Biogenesis and Function PIWI Proteins and piRNAs: Progress and Prospect. *Cell*, 2006, pp.355–376.
Tomari, Y. et al., 2004. A protein sensor for siRNA asymmetry. *Science (New York, N.Y.)*, 306(5700), pp.1377–80. Available at:
http://www.ncbi.nlm.nih.gov/pubmed/15550672.
Tomari, Y., Du, T. & Zamore, P.D., 2007. Sorting of Drosophila Small Silencing RNAs. *Cell*, 130(2), pp.299–308.

Vagin, V. V et al., 2006. A Distinct Small RNA Pathway Silences Selfish Genetic Elements in the Germline. *Science*, 313(July), pp.320–324.
Vagin, V. V et al., 2004. The RNA interference proteins and vasa locus are involved in the silencing of retrotransposons in the female germline of Drosophila melanogaster. *RNA biology*, 1(1), pp.54–8. Available at: http://www.ncbi.nlm.nih.gov/pubmed/15118411\nhttp://www.ncbi.nlm.nih.gov/pubmed/17194931\nhttp://www.ncbi.nlm.nih.gov/pubmed/17194939.
Vinh, D.B. & Drubin, D.G., 1994. A yeast TCP-1-like protein is required for actin function in vivo. *Proceedings of the National Academy of Sciences of the United States of America*, 91(September), pp.9116–9120.
Vodovar, N. et al., 2012. Arbovirus-derived piRNAs exhibit a ping-pong signature in mosquito cells. *PLoS ONE*, 7(1).
Vodovar, N. et al., 2011. In silico reconstruction of viral genomes from small RNAs improves virus-derived small interfering RNA profiling. *Journal of virology*, 85(21), pp.11016–21. Available at: http://jvi.asm.org/content/85/21/11016.long.
Voinnet, O. & Baulcombe, D.C., 1997. Systemic signalling in gene silencing. *Nature*, 389(6651), p.553.
Wang, X.-H. et al., 2006. RNA interference directs innate immunity against viruses in adult Drosophila. *Science (New York, N.Y.)*, 312(5772), pp.452–4. Available at: http://www.pubmedcentral.nih.gov/articlerender.fcgi?artid=1509097&tool=pmcentrez&rendertype=abstract.
Weaver, S.C. & Reisen, W.K., 2010. Present and future arboviral threats. *Antiviral Research*, 85(2), pp.328–345.
Willkomm, S. et al., 2015. A prokaryotic twist on argonaute function. *Life (Basel, Switzerland)*, 5(1), pp.538–53. Available at: http://www.pubmedcentral.nih.gov/articlerender.fcgi?artid=4390867&tool=pmcentrez&rendertype=abstract.
World Health Organization, 2014. A global brief on vector-borne diseases. *World Health Organization*, p.9. Available at: http://apps.who.int/iris/bitstream/10665/111008/1/WHO_DCO_WHD_2014.1_eng.pdf.
Wu, Q. et al., 2010. Virus discovery by deep sequencing and assembly of virus-derived small silencing RNAs. *Proceedings of the National Academy of Sciences of the United States of America*, 107(4), pp.1606–1611.
Wyers, F. et al., 1993. Immunological cross-reactions and interactions between the Drosophila melanogaster ref(2)P protein and sigma rhabdovirus proteins. *Journal of virology*, 67(6), pp.3208–16. Available at: http://www.ncbi.nlm.nih.gov/pubmed/7684462\nhttp://www.pubmedcentral.nih.gov/articlerender.fcgi?artid=PMC237660.
Yaffe, M.B. et al., 1992. TCP1 complex is a molecular chaperone in tubulin biogenesis. *Nature*, 358(6383), pp.245–248. Available at: http://www.ncbi.nlm.nih.gov/pubmed/1630491\nhttp://www.nature.com/doifinder/10.1038/358245a0.
Yam, A.Y. et al., 2008. Defining the TRiC/CCT interactome links chaperonin function to stabilization of newly made proteins with complex topologies. *Nature structural & molecular biology*, 15(12), pp.1255–62. Available at: http://dx.doi.org/10.1038/nsmb.1515\nhttp://www.ncbi.nlm.nih.gov/pubmed/19011634\nhttp://www.pubmedcentral.nih.gov/articlerender.fcgi?artid=PMC2658641.
Yasunaga, A. et al., 2014. Genome-wide RNAi screen identifies broadly-acting host factors that inhibit arbovirus infection. *PLoS pathogens*, 10(2), p.e1003914. Available at: http://journals.plos.org/plospathogens/article?id=10.1371/journal.ppat.1003914 [Accessed June 3, 2015].

Zhou, R. et al., 2009. Processing of Drosophila endo-siRNAs depends on a specific Loquacious isoform. *RNA (New York, N.Y.)*, 15(10), pp.1886–1895.

VII Résumé en français

1. Introduction

Les insectes, avec plus de 70% d'espèces répertoriées, forment le groupe d'animaux le plus important et le plus diversifié (Misof et al., 2014). Cela comprend les ravageurs de cultures et les parasites domestiques ainsi que les vecteurs de maladies. Les changements climatiques et l'urbanisation tropicale toujours croissante favorisent la propagation d'espèces d'insectes non indigènes représentant un fardeau économique majeur pour les années à venir. En plus du coût sociétal majeur découlant de la perte de cultures, des stocks alimentaires et du bétail, les insectes envahissants représentent également une menace majeure pour la santé humaine. Avec des coûts de santé associés supérieurs à 6,9 milliards de dollars par an (estimation de 2014) (Bradshaw et al., 2016), la propagation d'arbovirus arthropodes (arthropode-borne viruses) à travers des vecteurs d'insectes est l'une des principales causes de décès au cours des trois derniers siècles (Gubler, 1998). Le terme arbovirus se réfère à un groupe de virus non taxonomique. Tout en pouvant potentiellement causer des maladies graves chez les vertébrés, les arbovirus sont transmis par les moustiques et sont exposés à son système immunitaire (Lambrechts & Scott 2009). Le moustique devient infecté de manière persistante et peut transmettre un virus avec chaque repas sanguin suggérant que les moustiques vecteurs possèdent les moyens de monter efficacement une réponse antivirale capable de contrôler le virus. Il est donc nécessaire d'étudier la réponse immunitaire antivirale chez les insectes et la mouche drosophile représente un modèle de choix pour ceci.

2. Résultats

Des lignées cellulaires stables exprimant Dicer-2, R2D2 et Ago2 étiquetés N- ou C-terminale ont été construits et validés. Ces cellules ont été infectées par 3 virus DCV (8h

Fig. 1

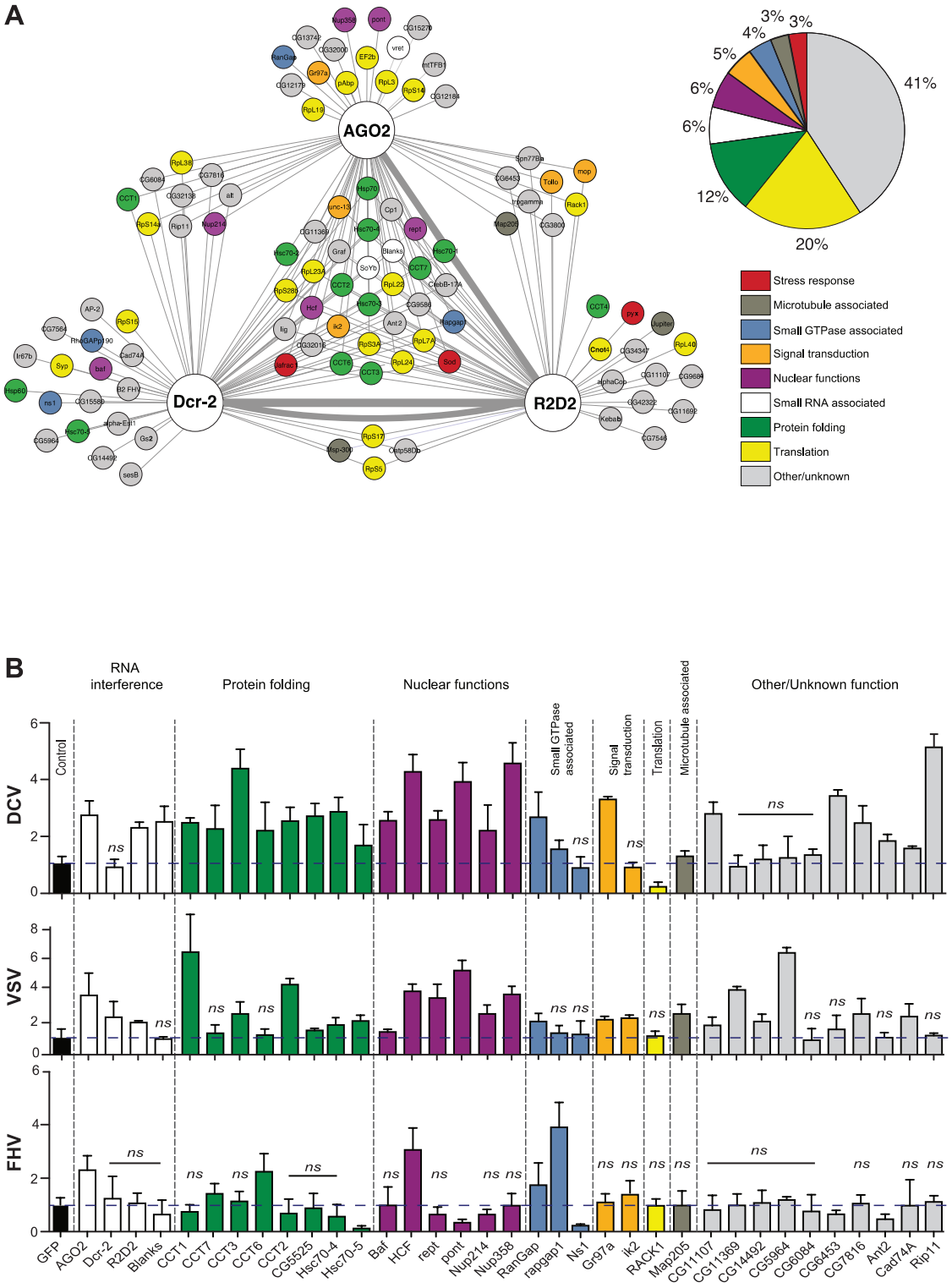

Fig. 1. Définition d'un interactome de la voie antivirale des siRNAs

A. Représentation schématique des protéines interagissant identifiées. Les protéines amorces Dcr-2, R2D2 et AGO2 sont représentées par des cercles élargis. Chaque protéine est colorée en fonction de sa fonction moléculaire. **B**. Résultats des cibles du crible RNAi qui montrent une différence supérieure à deux fois en terme de charge

virale pour au moins un des virus et qui n'ont pas montré de défaut de prolifération ou de viabilité suite au knockdown. ns : non significatif. Lorsqu'une barre ne montre pas de signe *ns*, cela signifie que la différence est statistiquement signifiante (Valeur de $P < 0.05$).

Fig. 2

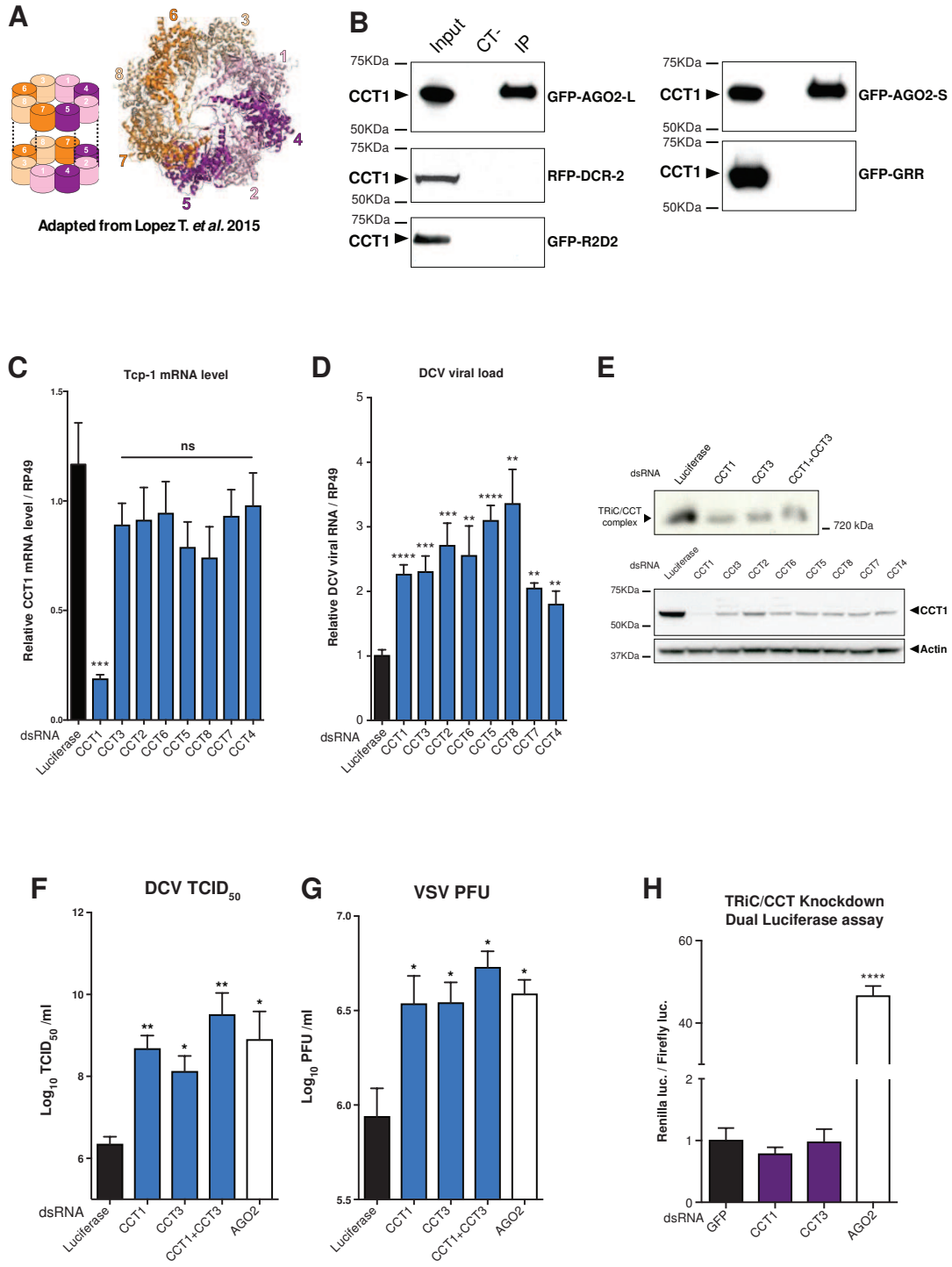
A
Adapted from Lopez T. et al. 2015
B
Input
CT-
IP
75KDa
50KDa
CCT1
GFP-AGO2-L
RFP-DCR-2
GFP-R2D2
GFP-AGO2-S
GFP-GRR
C
Tcp-1 mRNA level
Relative CCT1 mRNA level / RP49
ns
dsRNA
Luciferase
CCT1
CCT3
CCT2
CCT6
CCT5
CCT8
CCT7
CCT4
D
DCV viral load
Relative DCV viral RNA / RP49
E
TRiC/CCT complex
720 kDa
37KDa
Actin
F
DCV TCID50
Log10 TCID50 /ml
CCT1+CCT3
AGO2
G
VSV PFU
Log10 PFU /ml
H
TRiC/CCT Knockdown
Dual Luciferase assay
Renilla luc. / Firefly luc.
GFP

Fig. 2 Le complex TRiC/CCT et AGO2 restreint l'infection virale dans les cellules S2

A. Représentation schématique de la structure et de l'organisation des sous-unités du complexe TRiC/CCT (Lopez et al. 2015). B. Immunoprecipitation des protéines AGO2-L, AGO2-S, GRR, Dcr-2 ou R2D2 taguées suivie d'une analyse par immunoblot avec des anticorps anti-CCT1. Des billes d'agarose non couplées ont été utilisées comme contrôle négatif (ligne centrale). C. Expression de CCT1 déterminée par qRT-PCR dans des cellules où les gènes indiqués ont été éteins. D. Abondance relative d'ARN de DCV contrôlé par qRT-PCR dans des cellules traitées avec un ARNdb contrôle ou des ARNdb ciblant les sous-unités du complexe TRiC/CCT. E. (haut) Gel PAGE natif suivi d'un immunoblot contre la sous-unité CCT1 montrant l'abondance du complexe TRiC/CCT dans sa conformation native. (bas) Immunoblot contre CCT1 montrant l'abondance de la protéine suite au knockdown de chaque sous-unité du complet TRiC/CCT. F, G. Titres viraux de DCV (TCID50) et VSV (test de plaque) respectivement, dans des cellules où les gènes indiqués ont été éteins. H. Activité luciférase dans des cellules traitées avec un ARNdb ciblant la luciférase et éteintes pour les gènes indiqués (*Valeur de $P<0.05$; ** Valeur de $P <0.01$; *** Valeur de $P <0.001$; **** Valeur de $P < 0.0001$). les graphiques des panels C, D, F-H sont le résultat de deux (C, D, H) ou trois (F,G) expériences indépendantes, chacune contenant au moins deux réplicas biologiques. Les gels sont le résultat d'au moins deux expériences indépendantes.

ou 16hpi), FHV (16hpi) ou VSV (48hpi). Les protéines d'appât ont été récupérées par purification par affinité et analysées par spectrométrie de masse (Fig. 1). 103 protéines interactives couvrant une large gamme de fonctions moléculaires ont été identifiées dans les 42 conditions totales. Leur fonction a ensuite été testée par un crible ARN interférence. 71 gènes, pour lesquels un traitement par ARN double brin (db) n'a eu aucun effet sur la viabilité ou la prolifération des cellules, ont été testés pour leur effet sur la réplication de trois virus appartenant à différentes familles Dicistroviridae (DCV), Rhabdoviridae (VSV) et Nodaviridae (FHV). L'inhibition de 34 gènes a entraîné une augmentation ou une diminution de deux fois ou plus dans la réplication d'au moins un des trois virus testés. En particulier l'élimination de l'un des six composants du complexe TRiC / CCT identifiés par spectrométrie de masse a conduit à une réplication virale accrue d'au moins un des trois virus testés. Dans l'ensemble, ces résultats suggèrent que le complexe TRiC / CCT interagit avec les composants de base de la voie d'ARNsi et que cette interaction est pertinente pour l'immunité antivirale. Nous avons donc décidé d'étudier plus avant le rôle du complexe TRiC / CCT. Nous avons inhibé l'expression des huit sous-unités du complexe TRiC / CCT et analysé l'impact sur la réplication DCV (Fig. 2). Toutes les sous-unités ont affecté la réplication de DCV sans aucune indication d'effet compensatoire, en accord avec un rapport précédent (Kitamura et al., 2006). La surveillance du titre infectieux pour DCV et VSV a confirmé que le complexe TRiC / CCT empêche la réplication virale, comme AGO2. De manière surprenante cependant, l'inhibition de Tcp-1 (ou CCTγ) n'a pas abouti à une dé-répression d'un gène rapporteur de luciférase dans des cellules traitées avec un ARNdb long ciblant ce gène.

Nous avons ensuite analysé si le complexe TRiC / CCT affectait l'expression ou la stabilité d'AGO2 (Fig. 3). L'analyse par immunoblot des extraits de cellules S2 a révélé

Fig. 3

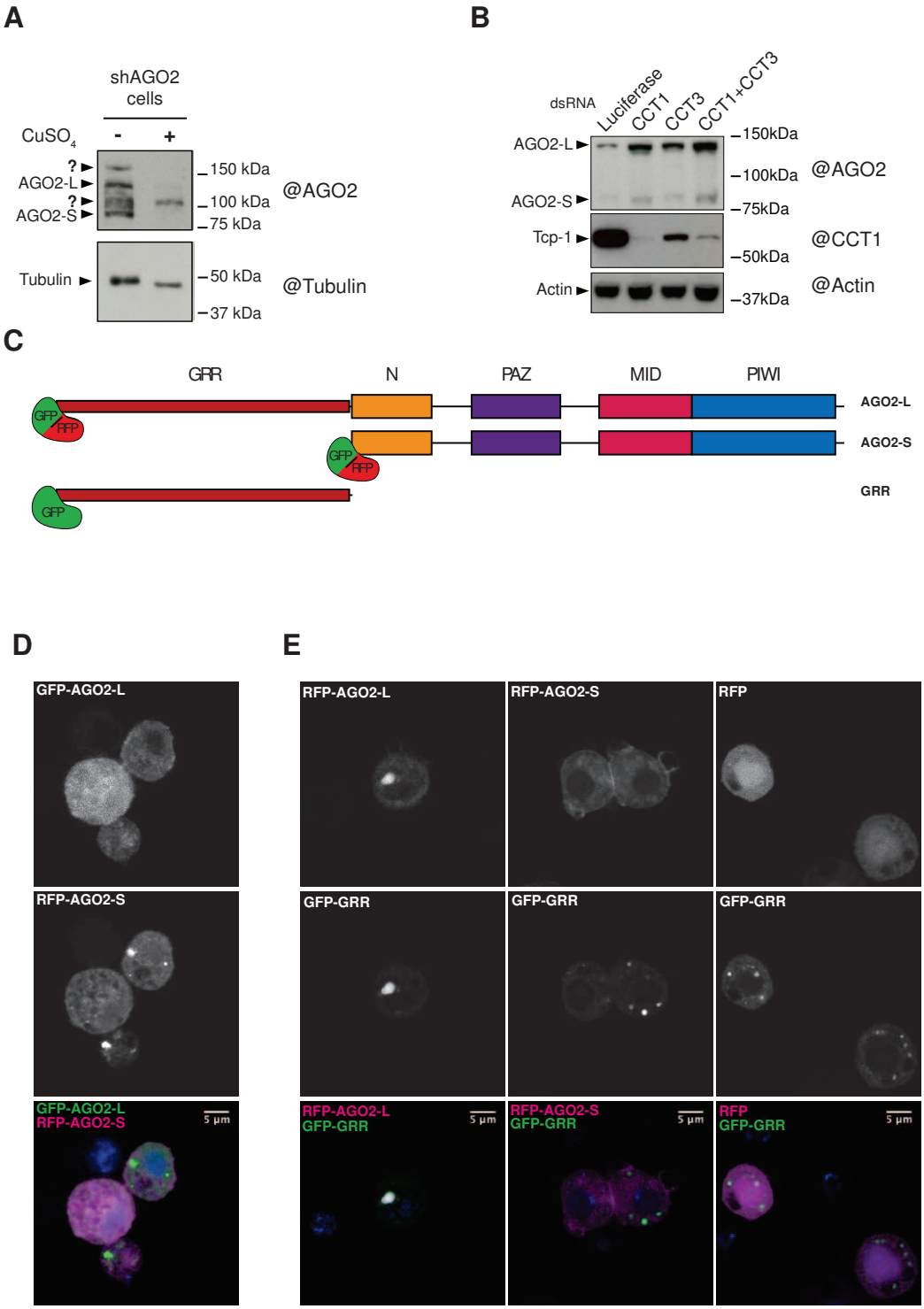
A
shAGO2 cells
CuSO4
-
+
?
AGO2-L
?
AGO2-S
150 kDa
100 kDa
75 kDa
@AGO2
Tubulin
50 kDa
37 kDa
@Tubulin
B
dsRNA
Luciferase
CCT1
CCT3
CCT1+CCT3
AGO2-L
AGO2-S
150kDa
100kDa
75kDa
@AGO2
Tcp-1
50kDa
@CCT1
Actin
37kDa
@Actin
C
GRR
N
PAZ
MID
PIWI
GFP
RFP
AGO2-L
AGO2-S
GRR
D
GFP-AGO2-L
RFP-AGO2-S
GFP-AGO2-L
RFP-AGO2-S
5 μm
E
RFP-AGO2-L
RFP-AGO2-S
RFP
GFP-GRR
GFP-GRR
GFP-GRR
RFP-AGO2-L
GFP-GRR
RFP-AGO2-S
GFP-GRR
RFP
GFP-GRR

Fig. 3 Les cellules S2 expriment deux isoformes de AGO2 et leur stabilité n'est pas affectée par le complexe TRiC/CCT.

A. Immunoblot contre AGO2 montrant les deux isoformes présents dans les cellules S2. Une lignée de cellule stable exprimant un shRNA ciblant AGO2 sous le contrôle d'un promoteur inductible au cuivre a été utilisée pour valider la spécificité des bandes. Un anticorps anti-Tubuline a été utilisé comme contrôle de charge. Les deux bandes marquées avec « ? » ne sont pas détectées de manière consistante et ne correspondent pas à la taille prédite des isoformes de AGO2. B. Immunoblot contre AGO2 dans des cellules S2 traitées avec un ARNdb contrôle, un ARNdb ciblant CCT1 et/ou CCT3. Un anticorps anti-actine a été utilisé comme contrôle de charge. C. Représentation schématique des construits des formes recombinantes de AGO2 taguées GFP/RFP. D. Images représentatives de cellules S2 transfectées de manière transitoire avec GFP-AGO2-L et RFP-AGO2-S. Les gels sont le résultat d'une(B), ou trois (A) expériences indépendantes.

Fig. 4

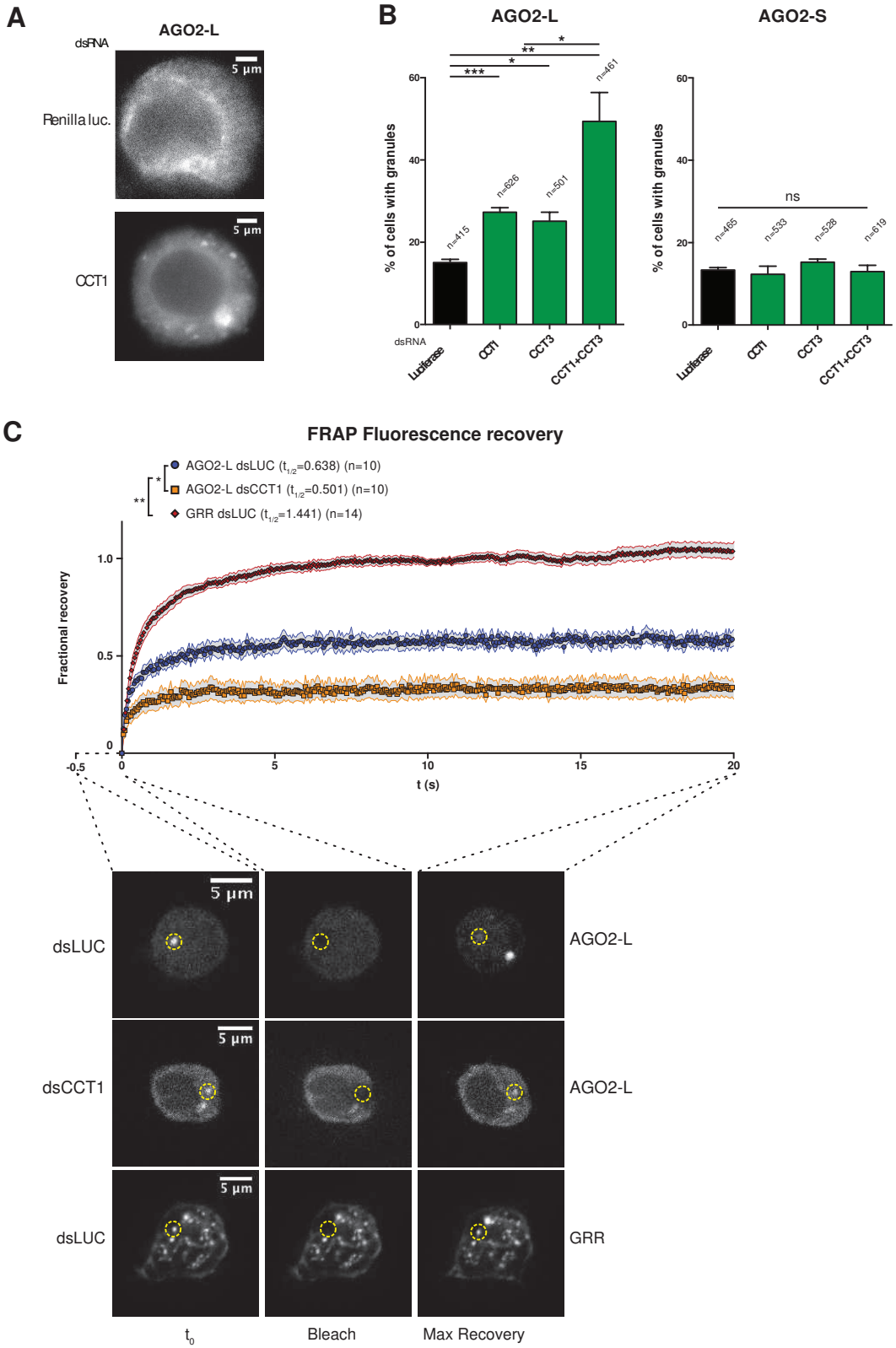
A
AGO2-L
dsRNA
Renilla luc.
CCT1
5 µm
B
AGO2-L
AGO2-S
% of cells with granules
dsRNA
Luciferase
CCT1
CCT3
CCT1+CCT3
n=415
n=626
n=501
n=461
n=465
n=533
n=528
n=619
ns
C
FRAP Fluorescence recovery
AGO2-L dsLUC (t1/2=0.638) (n=10)
AGO2-L dsCCT1 (t1/2=0.501) (n=10)
GRR dsLUC (t1/2=1.441) (n=14)
Fractional recovery
t (s)
dsLUC
dsCCT1
AGO2-L
GRR
t0
Bleach
Max Recovery

Fig. 4 Le complexe TRiC/CCT contrôle la dynamique des granules d'AGO2-L

A. Images représentatives de cellules S2 exprimant de manière stable GFP-AGO2-L dans une condition contrôle ou dans une condition où CCT1 est éteint. B. Diagramme à barres montrant le pourcentage de cellules contenant des granules dans des cellules stables exprimant soit GFP-AGO2-L ou GFP-AGO2-S. Les cellules ont été traitées avec un ARNdb contrôle, un ARNdb ciblant CCT1 et/ou CCT3. C. (haut) Graphique montrant la récupération fractionnée de fluorescence de granules GFP-AGO-L décolorés dans des cellules traitées soit avec un ARNdb contrôle ou un ARNdb ciblant CCT1. La valeur « 1 » représente l'intensité de fluorescence avant la décoloration par la lumière. (bas) Images représentatives des différentes conditions avant (t0) immédiatement après décoloration par la lumière (Bleach) et après une récupération maximale de fluorescence (Max Recovery). (*Valeur de $P<0.05$; ** Valeur de $P<0.01$; *** Valeur de $P<0.001$). Les graphiques des panels B et C sont le résultat de trois (F,G) expériences indépentantes.

Fig. 5

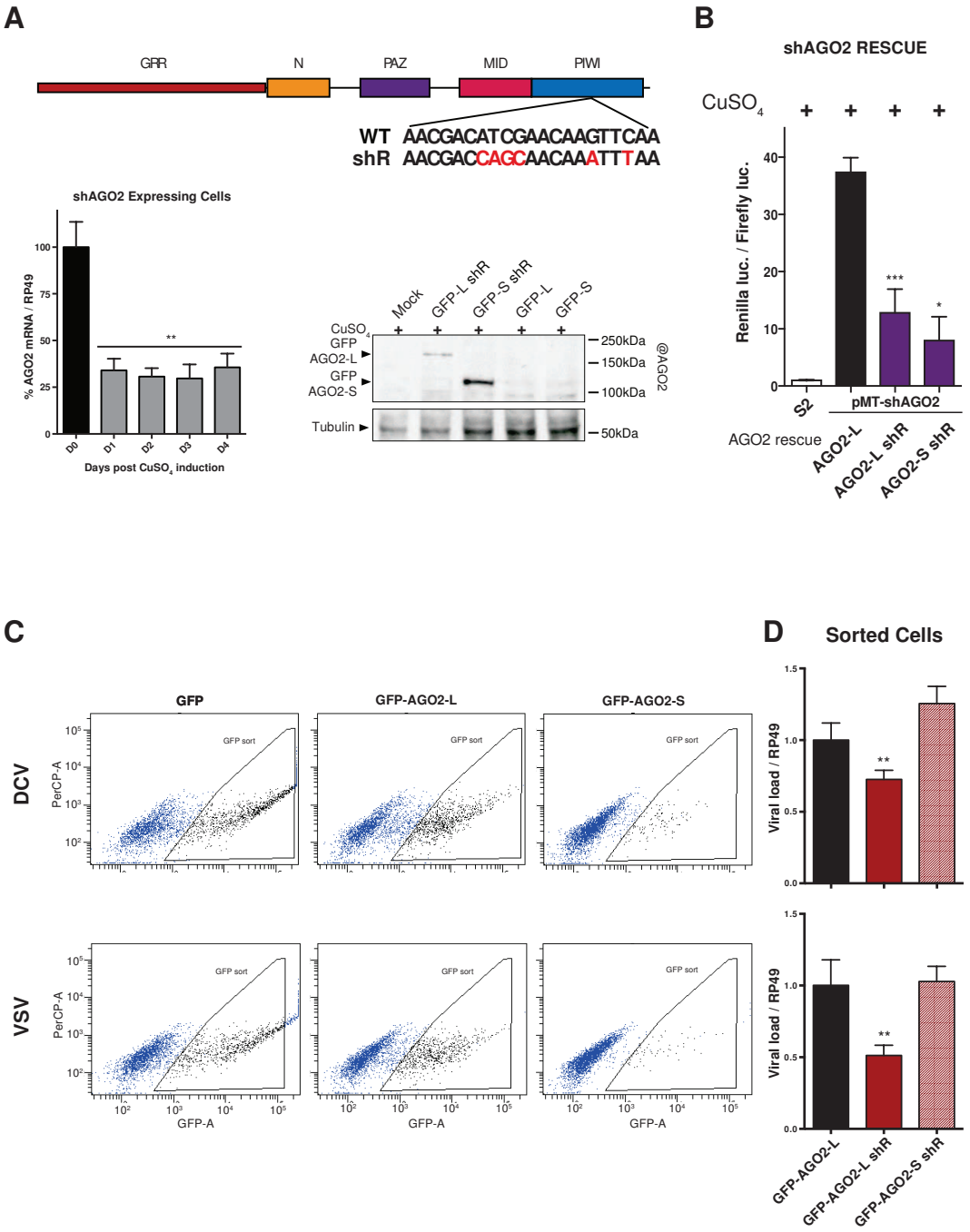
A
GRR
N
PAZ
MID
PIWI
WT AACGACATCGAACAAGTTCAA
shR AACGACCAGCAACAAATTTAA
shAGO2 Expressing Cells
% AGO2 mRNA / RP49
Days post CuSO4 induction
D0
D1
D2
D3
D4
Mock
GFP-L shR
GFP-S shR
GFP-L
GFP-S
CuSO4
GFP
AGO2-L
GFP
AGO2-S
Tubulin
250kDa
150kDa
100kDa
50kDa
@AGO2
B
shAGO2 RESCUE
CuSO4
Renilla luc. / Firefly luc.
S2
pMT-shAGO2
AGO2 rescue
AGO2-L
AGO2-L shR
AGO2-S shR
C
GFP
GFP-AGO2-L
GFP-AGO2-S
DCV
VSV
PerCP-A
GFP-A
GFP sort
D
Sorted Cells
Viral load / RP49
GFP-AGO2-L
GFP-AGO2-L shR
GFP-AGO2-S shR

Fig. 5 Le domaine N-terminal GRR est essentiel pour l'activité antivirale de AGO2

A. (haut) Représentation schématique de AGO2 mettant en avant la région du domaine PIWI ciblé par le shRNA et les mutations ponctuelles (en rouge) insérées pour créer des construits résistants au shRNA. (bas) Validation du knockdown de AGO2 dans des cellules stables exprimant le shRNA sous le contrôle d'un promoteur metallothionein inductible au cuivre (à gauche) et sauvetage des mutants shR par immunoblot contre AGO2 (à droite). B. Activité luciférase dans des cellules traitées avec un ARNdb ciblant la luciférase et co-transfectées avec un vecteur luciférase, un vecteur diminuant AGO2 (pMT-shAGO2) et le plasmide de sauvetage AGO2 indiqué. Des cellules S2 en présence de cuivre ont été utilisées comme contrôle positif pour la diminution de l'expression d'AGO2. GFP-AGO2-L non résistant au shRNA a été utilisé comme contrôle négatif. C. Graphique montrant les délimitations utilisées pour trier les cellules S2 GFP positives par cytométrie de flux. D. Charge viral en ARN déterminée par qRT-PCR sur les cellules infectées soit par DCV (haut) soit par VSV (bas). (*Valeur de $P<0.05$; ** Valeur de $P<0.01$; *** Valeur de $P<0.001$). Les graphiques des panels A, B et D sont le résultat de deux (A, D) ou trois (B) expériences indépentantes, chacune contenant au moins deux réplicats biologiques.

deux bandes de 132 kDa et 90 kDa correspondant aux deux isoformes d'AGO2 précédemment décrites (ci-après dénommées AGO2-L et AGO2-S). L'inhibition de deux sous-unités différentes du complexe TRiC / CCT n'affecte la stabilité d'aucune des isoformes. Nous avons ensuite étudié si l'inhibition du complexe TRiC / CCT entraînait une localisation altérée d'AGO2 dans les cellules. Nous avons construit des versions GFP ou RFP recombinantes des isoformes longues et courtes d'AGO2 pour surveiller leur distribution intracellulaire. Transitoirement transfectées, Ago2-L-S et Ago2 ne colocalisent pas dans des cellules de drosophile S2. En effet, AGO2-L forme des granules tandis que AGO2-S reste diffus dans le cytoplasme. Le domaine GRR forme des granules, plus grands et plus nombreux que AGO2-L, ce qui suggère qu'ils pourraient être des agrégats.

Pour approfondir les différences entre AGO2-L et AGO2-S, nous avons établi des lignées cellulaires stables exprimant des versions GFP étiquetées des deux protéines (Fig. 4). Après avoir éliminé Tcp-1 ou CCTγ, nous avons observé une augmentation du nombre de cellules contenant des granules d'AGO2-L. La technique FRAP (Fluorescence Recovery Après Photobleaching) a été utilisé pour blanchir un seul granule et observer sa reprise de fluorescence au fil du temps. Nous avons observé que les granules formés par AGO2-L se rétablissent beaucoup plus rapidement que les granules composés uniquement du domaine GRR, ce qui indique qu'ils ne sont pas de simples agrégats de protéines mais correspondent à des structures dynamiques. En outre, l'inhibition de Tcp-1 a entraîné une récupération de fluorescence plus rapide. Nous concluons que les granules formés par AGO2-L sont des agrégats dynamiques et non simplement un agrégat de protéines mal repliées, et que le complexe TRiC / CCT contrôle la dynamique de ces granules, ce qui affecte la fonction antivirale d'AGO2.

Fig. 6

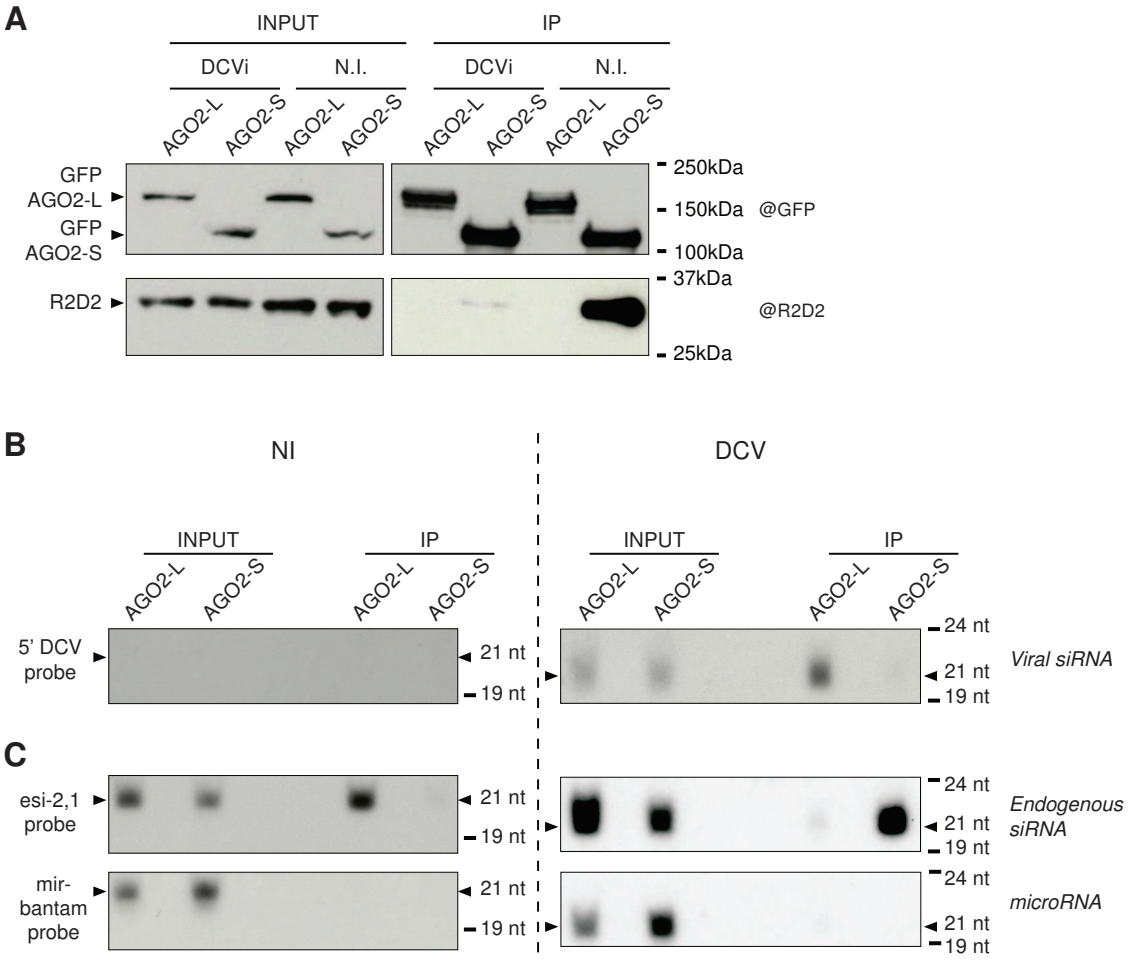
A
INPUT
IP
DCVi
N.I.
DCVi
N.I.
AGO2-L
AGO2-S
AGO2-L
AGO2-S
AGO2-L
AGO2-S
AGO2-L
AGO2-S
GFP
AGO2-L
GFP
AGO2-S
R2D2
250kDa
150kDa
100kDa
37kDa
25kDa
@GFP
@R2D2
B
NI
DCV
INPUT
IP
INPUT
IP
AGO2-L
AGO2-S
AGO2-L
AGO2-S
AGO2-L
AGO2-S
AGO2-L
AGO2-S
5' DCV
probe
21 nt
19 nt
24 nt
21 nt
19 nt
Viral siRNA
C
esi-2,1
probe
21 nt
19 nt
24 nt
21 nt
19 nt
Endogenous
siRNA
mir-
bantam
probe
21 nt
19 nt
24 nt
21 nt
19 nt
microRNA

Fig. 6 Les deux isoformes de AGO2 différent par leur interaction avec R2D2 et les petits ARNs.

A. Immunoblot de la fraction protéique résultant des immunoprécipitations de AGO2-L et AGO2-S. La membrane a été utilisée avec soit un anticorps anti-GFP (top) soit un anticorps anti-R2D2 (bas). B. Northern blot des petits ARNs isolés des immunoprécipitations de AGO2-L et AGO2-S depuis des cellules infectées ou non avec DCV. La membrane a été incubée avec des sondes ciblant les 500 premières bases du génome de DCV. C. La même membrane a été lavée et réutilisée avec une sonde oligo ciblant le endo-siRNA esi-2,1. Les blots sont représentatifs d'au moins deux expériences indépendantes.

Fig. 7

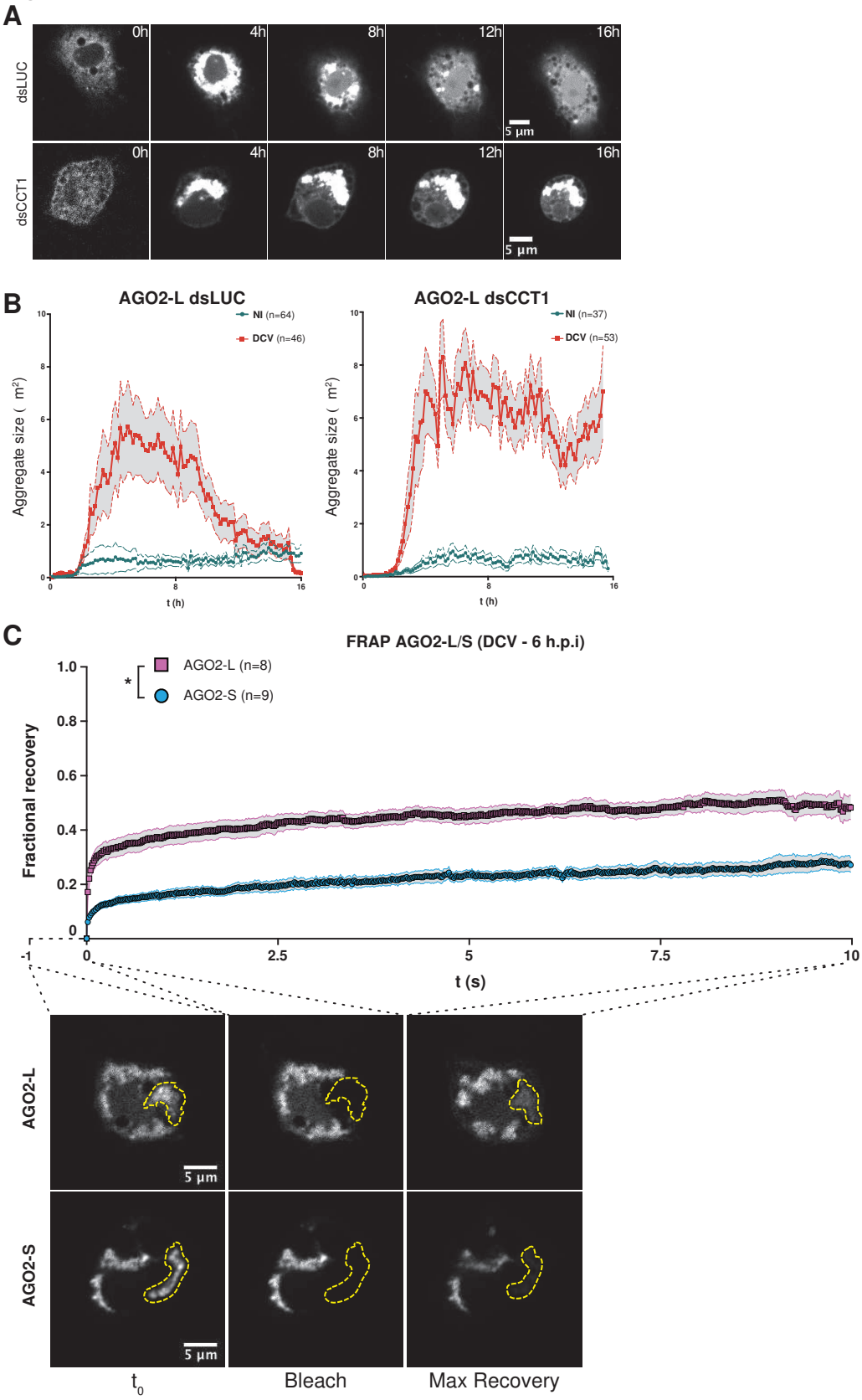
A
dsLUC
dsCCT1
0h
4h
8h
12h
16h
5 µm
B
AGO2-L dsLUC
AGO2-L dsCCT1
NI (n=64)
DCV (n=46)
NI (n=37)
DCV (n=53)
Aggregate size (m²)
t (h)
C
FRAP AGO2-L/S (DCV - 6 h.p.i)
AGO2-L (n=8)
AGO2-S (n=9)
*
Fractional recovery
t (s)
AGO2-L
AGO2-S
t0
Bleach
Max Recovery

Fig. 7 L'infection virale induit la formation d'agrégats transitoires péri nucléaires de AGO2.

Des cellules S2 traitées avec soit un ARNdb contrôle ou un ARNdb ciblant CCT1 ont été transfectées avec des versions RFP taguées de AGO2-L et AGO2-S . Les cellules ont ensuite été infectées ou non avec DCV et observées à magnification 100X pendant 16 heures avec une image prise toutes les 10 minutes. A. Images représentatives d'une cellule infectée par DCV pendant 16 heures (images à 0, 4, 8, 12, 16 heures) traitée avec soit un ARNdb contrôle (haut) ou ciblant CCT1 (bas). B. Suivi de la taille des agrégats formés par AGO2-L dans des cellules infectées ou non. ARNdb contrôle (gauche) ou ciblant CCT1 (droit). C. Graphique montrant la récupération fractionnée de fluorescence des agrégats formés soit par AGO2-L soit AGO2-S dans des cellules infectées par DCV. (*Valeur de $P<0.05$; ** Valeur de $P <0.01$; *** Valeur de $P <0.001$). Les graphiques sont le résultat d'au moins deux expériences indépendantes.

Les cellules S2 transfectées de manière transitoire avec AGO2-L ou AGO2-S ont été triées pour une expression GFP et la réplication virale a été surveillée par qRT-PCR (Fig. 5). Les cellules AGO2-L, mais pas AGO2-S complétées, contiennent moins d'ARN DCV ou VSV. Nous concluons que le domaine GRR joue un rôle important dans la fonction antivirale de l'AGO2, bien qu'il ne soit pas nécessaire pour l'ARNi contre des séquences endogènes ou des ARNdb transfectés. Ceci est conforme à l'observation selon laquelle le complexe TRiC / CCT n'est pas nécessaire pour inhiber un gène rapporteur de luciférase par un ARNdb long. Nous avons cherché ensuite à comprendre ce qui différencie AGO2-L d'AGO2-S dans le contexte de l'infection virale. Nous avons infecté les lignées cellulaires stables exprimant GFP-AGO2-L ou GFP-AGO2-S, lysé les cellules, effectué une immunoprécipitation à l'aide de l'étiquette GFP, extrait les petits ARN associés et effectué un sondage Northern Blot pour de petits ARN issus de DCV ou des loci endogènes de siRNA (Esi-2) (Fig. 6). D'une manière frappante, les ARNsi dérivés du DCV sont associés à AGO2-L. D'autre part, les endo-siRNAs s'associent principalement à AGO2-L dans les cellules non infectées, mais sont principalement détectés dans l'immunoprécipité AGO2-S lors d'une infection virale.

Pour comprendre comment le complexe TRiC / CCT a un impact sur AGO2 pendant l'infection virale, nous avons surveillé la distribution de GFP-AGO2-L et GFP-AGO2-S dans les cellules S2 infectées par DCV où Tcp-1 a été abattu. Dans les cellules non infectées ou dans les cellules infectées traitées avec le dsRNA témoin, les granules AGO2-L sont extrêmement dynamiques au cours de la durée de l'infection (Fig. 7). Dans de rares cas, AGO2-L forme des agrégats transitoires. Dans les cellules traitées avec dsTcp-1, les agrégats perinucléaires formés par AGO2-L apparaissent dans la grande majorité des cellules. Étonnamment, il en va de même pour AGO2-S. Nous avons co-exprimé RFP-AGO2-L et B2-GFP. B2 est connu pour lier l'ARNdb, qui est présent dans les sites de

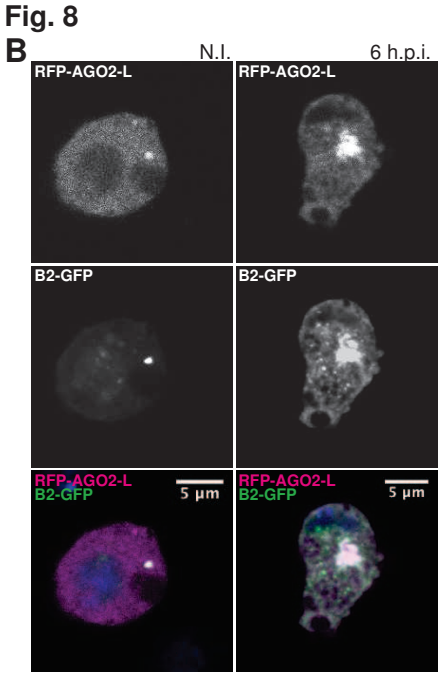

Fig. 8 AGO2-L colocalise avec la protéine de liaison à l'ARNdb B2 dans des cellules infectées par DCV.

Images représentatives de cellules S2, non infectées ou 6 heures après infection par DCV, co-transfectées avec RFP-AGO2-L et FHV-B2-GFP. Les images sont représentatives de deux expériences indépendantes.

réplication virale. AGO2-L colocalise avec B2-GFP et on peut donc supposer que les agrégats que nous observons correspondent à l'emplacement où AGO2 est chargé avec le duplex vsiRNA (Fig. 8). Nous avons surveillé la taille des agrégats périnucléaires au cours de la durée de l'infection. Les agrégats formés à la fois par AGO2-L et AGO2-S semblent être beaucoup plus grands et plus stables dans les cellules où Tcp-1 a été inhibé. La dynamique similaire d'AGO2-L et d'AGO2-S n'explique pas le phénotype que nous avons observé concernant la réplication virale et le chargement de vsiRNA. Le blanchiment d'une partie des agrégats formés par AGO2-L et AGO2-S a montré que les agrégats formés par AGO2-L se rétablissent beaucoup plus rapidement que les agrégats formés par AGO2-S. Nous pouvons conclure que la vitesse de localisation d'AGO2 vers les sites de réplication virale est essentielle pour une réponse antivirale efficace.

3. Discussion

L'interaction de la sous-unité Tcp-1 avec AGO2 observée par immunoprécipitation et l'effet de l'ensemble du complexe sur la réplication virale suggèrent deux modes d'action possibles pour le complexe TRiC / CCT. Tout d'abord, elle peut exercer une fonction similaire à celle d'autres protéines chaperons qui a déjà montré qu'il interagissait avec AGO2 (Iwasaki et al., 2010). Deuxièmement, le long domaine GRR d'AGO2 met en jeu le rôle du complexe TRiC / CCT dans le repliement de protéines riches en Gln (Tam et al., 2006). Nos données excluent un rôle similaire à celui décrit par le groupe de Y. Tomari car le knockdown de Tcp-1 n'affecte pas la quantité d'AGO2-L ou AGO2-S, indiquant que le complexe TriC / CCT n'est pas impliqué dans le repliement de ces protéines. Nous avons montré que le complexe TRiC / CCT régule la distribution cellulaire d'AGO2 de manière dépendante de GRR. De plus, notre expérience FRAP a confirmé que les granules formés par AGO2-L dans le cytoplasme des cellules S2 ne sont pas des simples

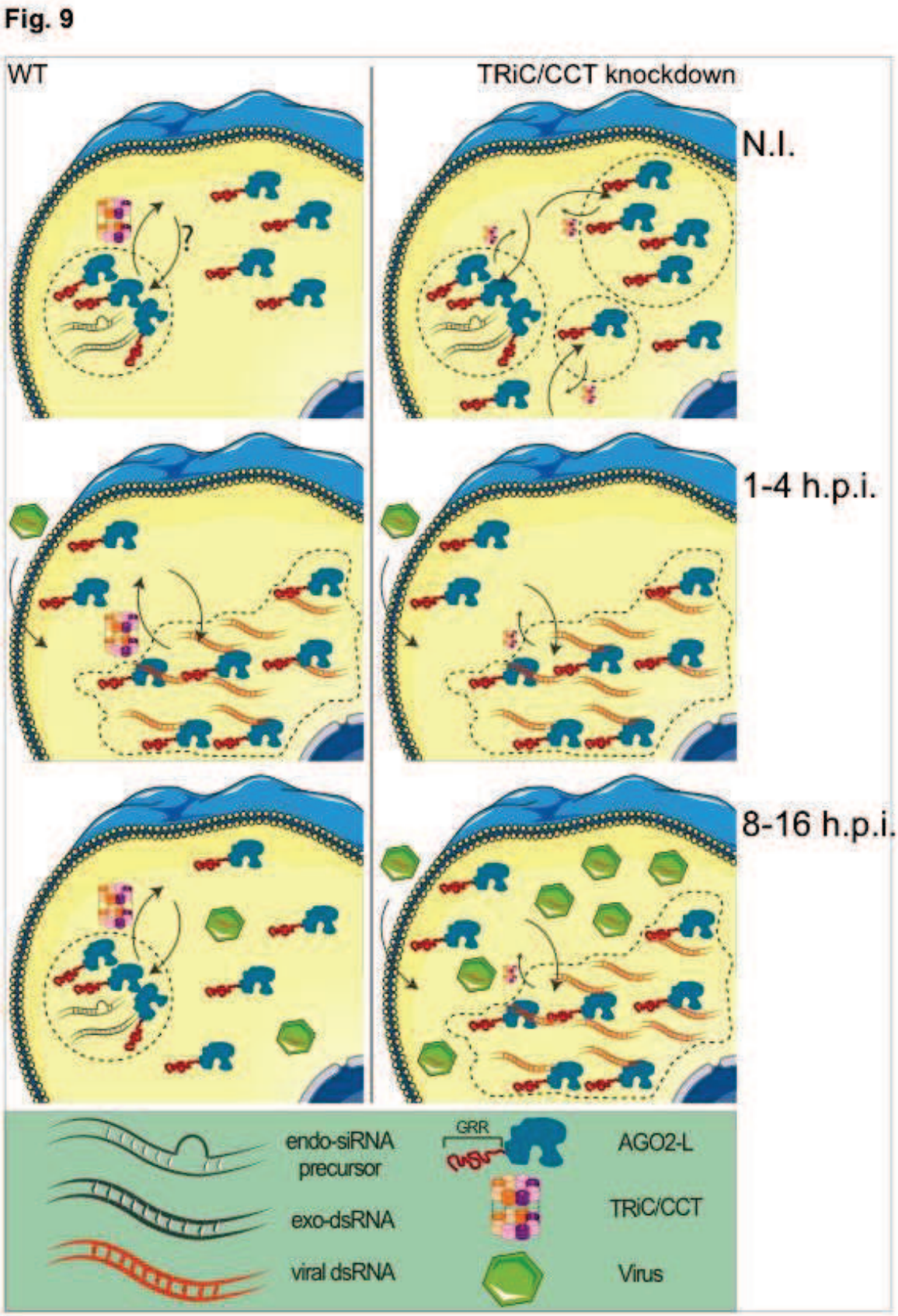

Fig. 9 Un modèle d'implication du complex TRiC/CCT dans la régulation de l'activité de AGO2.

agrégats mais des structures dynamiques sous le contrôle du complexe TRiC / CCT. Ensemble, ces résultats suggèrent un rôle nouveau pour un complexe chaperon dans l'ARNi antiviral.

Mes résultats soulèvent la question de savoir pourquoi le GRR semble être nécessaire dans le contexte d'une réponse antivirale. Plusieurs études (Lin et al. 2015; Nott et al. 2015; Elbaum-Garfinkle et al., 2015; Molliex et al., 2015; Jain et al., 2016) ont rapporté la capacité des protéines contenant des régions à intrusion intrinsèque (IDR) à former une phase - gouttelettes liquides séparées dans le cytoplasme. Un modèle récent a proposé que, suite à un événement tel que l'inhibition de l'initiation de la traduction, la quantité d'ARN non traduit liée à différentes protéines liées à l'ARN augmente. La concentration locale accrue des IRD et de l'ARN déclenche la séparation des phases, initiant ainsi la formation d'un granulé de stress (Jain et al., 2016). Dans le contexte de l'infection virale, un excès d'ARN viral est produit dans des compartiments cellulaires connus sous le nom d'usines virales (Jose et al., 2009; Kopek et al., 2007). Cet excès d'ARN, y compris le dsRNA réplicant, pourrait former des gouttelettes séparées par phases où il peut être détecté et traité par Dcr-2 et chargé sur AGO2. Puisque les gouttelettes séparées en phase peuvent effectivement recruter des protéines contenant des IDR (Lin et al. 2015), AGO2-L, mais pas AGO2-S, serait préférentiellement chargé avec les vsiRNA (Fig. 9). Une fois chargé, AGO2-L doit se dissocier pour lier et cliver l'ARN viral à brin simple, probablement au niveau de la traduction. Mes résultats indiquent que le complexe TRiC / CCT participe à cette étape de dissociation et à la relocalisation dynamique d'AGO2-L.

Francesco BERGAMI

L'extension N-terminale riche en glutamine de la protéine de Drosophile AGO2 joue un rôle critique dans l'ARN interférence antivirale d'une manière dépendante du complexe TRiC / CCT

Résumé

L'analyse par spectrométrie de masse des les protéines qu'interagies avec Dicer-2, R2D2 a identifié sis sur huit composent du complexe chaperon TRiC / CCT. L'élimination de l'un des six composants du complexe TRiC / CCT identifiés par spectrométrie de masse a conduit à une réplication virale accrue d'au moins un des trois virus testés.

L'ensemble des mes résultats suggèrent un rôle nouveau pour le complexe TRiC / CCT dans l'ARNi antiviral. Mes résultats soulèvent la question de savoir pourquoi le GRR d'AGO2 semble être nécessaire dans le contexte d'une réponse antivirale. Mes résultats indiquent que le complexe TRiC / CCT participe à l'étape de dissociation et à la relocalisation dynamique d'AGO2-L pendant l'infection virale.

Résumé en anglais

The mass spectrometry analysis of the complexes associating with Dicer-2, R2D2, and AGO2 identified six out of the eight subunits forming the TRiC/CCT complex. Knockdown of one of the six subunits identified is sufficient to increase the replication of DCV (DrosophilaC Virus). My results identify an interaction between the TRiC/CCT complex and the antiviral RNA interference. This interaction raises the question of how the GRR region of AGO2 is necessary for the antiviral response. My results suggest that the TRiC/CCT complex is involved in the dynamic dissociation and relocalization of AGO2 during viral infection.